The Green Solar Collector: optimization of microalgal areal productivity

Promotoren

Prof. dr. ir. R.H. Wijffels

Hoogleraar in de Bioprocestechnologie, Wageningen Universiteit

Prof. dr. ir. J. Tramper

Hoogleraar in de Bioprocestechnologie, Wageningen Universiteit

Co-promotor

Dr. ir. M.G.J. Janssen

Senior onderzoeker, leerstoelgroep Bioprocestechnologie, Wageningen Universiteit

Promotiecommissie

Dr. C. Vilchez

Universidad de Huelva, Spanje

Prof. dr. J.P.M. Sanders

Wageningen Universiteit

Prof. dr. ir. M.J. Groeneveld

Universiteit Twente

Prof. dr. L.E.M. Vet

Nederlands Instituut voor Ecologie

Dit onderzoek is uitgevoerd binnen de onderzoeksschool VLAG.

The Green Solar Collector: optimization of microalgal areal productivity

Jan-Willem Feye Zijffers

Proefschrift
ter verkrijging van de graad van doctor
op gezag van de rector magnificus
van Wageningen Universiteit,
Prof. dr. M.J. Kropff,
in het openbaar te verdedigen
op maandag 12 januari 2009
des namiddags te vier uur in de aula

Jan-Willem Feye Zijffers
The Green Solar Collector: optimization of microalgal areal productivity
Thesis Wageningen University, the Netherlands, 2009 – with summary in Dutch and English

ISBN: 978-90-8585-301-5

voor Maartje

Contents

Chapter 1

Introduction

Microalgae are an interesting source of biofuel components and products, such as vitamins, carotenoids and polyunsaturated fatty acids, because of the high areal productivities that can be obtained when compared to agricultural crops (Apt and Behrens 1999; Chisti 2007; Spolaore et al. 2006). To maximize the areal productivity of biomass or specific biomass components, all available sunlight must be captured and used as efficiently as possible in photosynthesis. A cultivation system that successfully combines these two aspects does not exist yet. Biomass yields on light energy close to the maximal obtainable yield have been reported based on the amount of light energy entering the cultivation system. However, the areal yield was low because a large part of the available sunlight was not captured inside the cultivation system. Other systems were designed to efficiently capture available sunlight, but as a result of the design growth conditions could not be maintained optimal for the microalgae, because the microalgae were exposed to the (over-) saturating sunlight intensity and the efficiency of light use decreased. This thesis focuses on the efficient production of microalgal biomass on sunlight through the design of a reactor that efficiently captures available sunlight and through the optimization of cultivation conditions and light input, leading to efficient light use by the microalgae.

Outline of this thesis

Chapter two discusses the design of a photobioreactor for area efficient cultivation of microalgae. This photobioreactor, called the Green Solar Collector (GSC), is designed to completely cover the ground surface to fully capture available irradiance. Direct sunlight is captured by Fresnel lenses on top of the reactor that focus the sunlight on top of light guides. The sunlight refracts into the guides and propagates downwards into the reactor via internal reflection inside the light

guides. Diffuse light is able to illuminate the algae through the transparent reactor cover. The design of the reactor is explained based on four efficiency determining aspects:

1. Capture of light
2. Transport of light
3. Distribution of light
4. Efficient conversion of light energy into biomass

Chapter three focuses on the capture and distribution of light out of the bottom part of the light guide. This part, called the distributor, has a triangular shape and its surface is either smooth or sandblasted. Reflection and refraction of light from focus to distribution is traced and the uniformity of light distribution out of the distributor is discussed. Based on the ray tracing results suggestions for the distributor geometry and for the optimal location of the GSC are made.

Chapter four shows the results of the cultivation of two microalgae, i.e. *Dunaliella tertiolecta* and *Chlorella sorokiniana*. They were cultivated in panel photobioreactors with an light path of 1.25 cm and 2.15 cm under artificial light and controlled conditions. Using the D-stat cultivation technique, the dilution rate through the reactor was gradually decreased, increasing the biomass concentration. The biomass concentration also decreased with increasing light path and decreasing volumetric light input. The biomass yield on light energy was similar for the two microalgae and light path lengths. The yield decreased at high biomass concentrations and low growth rates. The biomass yield on light energy could be explained by a constant true biomass yield on light energy and a constant maintenance requirement per gram of biomass.

Chapter five shows the results of cultivating the alga *Chlorella sorokiniana* at different levels of turbulence in a 1.25 cm light path reactor. Results of D-stat cultivations showed an increase in biomass yield on light energy at high biomass concentrations at an increased superficial gas velocity. At a higher superficial gas velocity the yield decreased again. Assuming a constant biomass maintenance

requirement, a true biomass yield was obtained that approached the theoretical maximum. However, high maintenance requirements limit the observed yield.

Chapter six discusses the potential for high areal microalgal biomass production based on literature results and results published in this thesis. Ideally, the composing parts of the GSC should be integrated and tested under outdoor conditions. However, we were unable to run such an integrated system for long periods of time. The variable Dutch weather conditions did not permit a full investigation into the actual performance, because consecutive days of full sunlight directly before and after the summer solstice were not obtained.

Nevertheless, a couple of batch cultivation experiments were carried out in the Netherlands and allow some preliminary conclusions to be drawn, as discussed below.

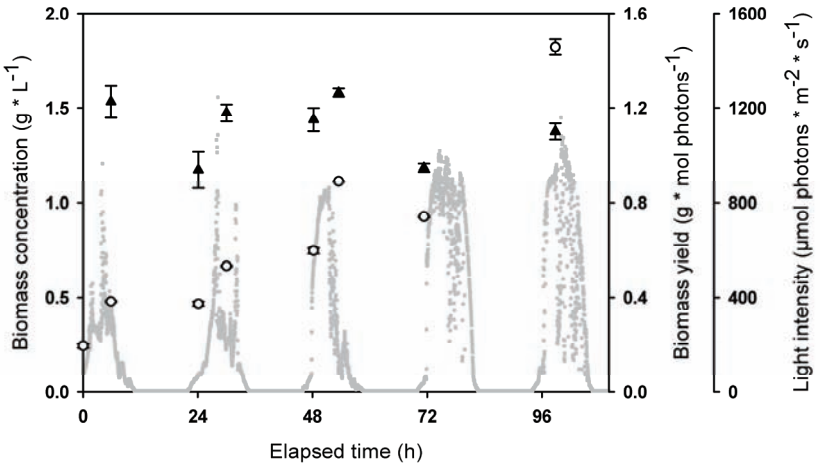

Figure 1. Chlorella sorokiniana biomass concentration (○) and yield on light energy (▲) during batch cultivation in the GSC. Light intensity (■) is corrected for reflection losses in passing the lens and refracting into the light guide.

Figure 1 and 2 show results of two batch cultivations in the GSC. The efficiency of light use was based on the amount of sunlight captured into the GSC and the biomass increase relative to the point of inoculation. The results show that it was

possible to grow microalgae under outdoor conditions in the GSC. The yield obtained during a *Chlorella sorokiniana* cultivation was higher than during a *Dunaliella tertiolecta* cultivation, however, the final biomass concentration in the *D. tertiolecta* cultivation was higher. The results of the cultivations are difficult to compare because the sunlight intensities present during the *D. tertiolecta* cultivation were higher than during the *C. sorokiniana* cultivation. The *C. sorokiniana* yield was 67% of the theoretical maximum yield and the *D. tertiolecta* yield was 40% of the theoretical maximum yield.

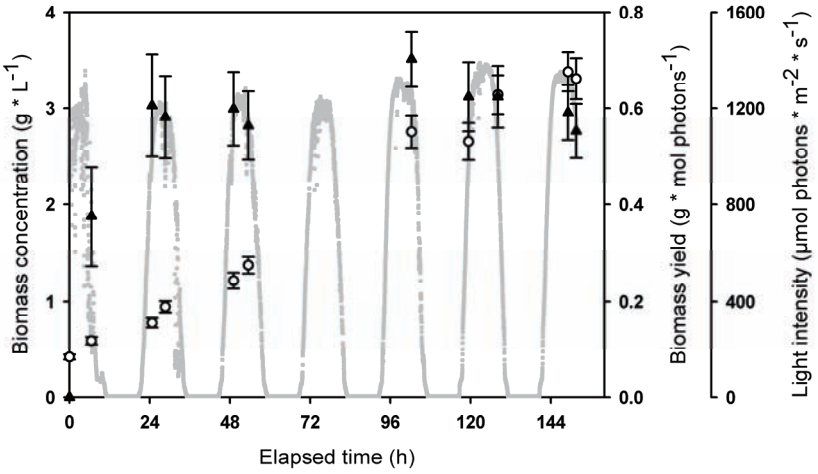

Figure 2. Dunaliella tertiolecta biomass concentration (○) and yield on light energy (▲) during batch cultivation in the GSC. Light intensity (■) is corrected for reflection losses in passing the lens and refracting into the light guide.

In this thesis the potential for light energy efficient cultivation based on efficient capture of sunlight and efficient use of light energy is investigated and discussed. The actual performance of the Green Solar Collector should be tested at locations close to the equator with constant high levels of direct sunlight.

References

Apt KE, Behrens PW. 1999. Commercial developments in microalgal biotechnology. Journal of Phycology 35(2):215-226.

Chisti Y. 2007. Biodiesel from microalgae. Biotechnology Advances 25(3):294-306.

Spolaore P, Joannis-Cassan C, Duran E, Isambert A. 2006. Commercial applications of microalgae. Journal of Bioscience and Bioengineering 101(2):87-96.

Chapter 2

Design process of an area efficient photobioreactor

Abstract

This article describes the design process of the Green Solar Collector (GSC), an area efficient photobioreactor for the outdoor cultivation of microalgae. The overall goal has been to design a system in which all incident sunlight on the area covered by the reactor is delivered to the algae at such intensities that the light energy can be efficiently used for biomass formation. A statement of goals is formulated and constraints are specified to which the GSC needs to comply. Specifications are generated for a prototype which form and function achieve the stated goals and satisfy the specified constraints. This results in a design in which sunlight is captured into vertical plastic light guides. Sunlight reflects internally in the guide and eventually scatters out of the light guide into flat-panel photobioreactor compartments. Sunlight is focused on top of the light guides by dual-axis positioning of linear Fresnel lenses. The shape and material of the light guide is such that light is maintained in the guides when surrounded by air. The bottom part of a light guide is sandblasted to obtain a more uniform distribution of light inside the bioreactor compartment and is triangular-shaped to ensure the efflux of all light out of the guide. Dimensions of the guide are such that light enters the flat-panel photobioreactor compartment at intensities that can be efficiently used by the biomass present. The integration of light capturing, transportation, distribution, and usage is such that high biomass productivities per area can be achieved.

This chapter has been published as: Zijffers JWF, Janssen M, Tramper J, Wijffels RH. 2008. Design process of an area efficient photobioreactor. Marine Biotechnology 10(4):404-415.

Introduction

Ideally, a photobioreactor for production of biomass should catch all sunlight available at the allocated spot, and transport, channel, and distribute it in such a way into the cultivation vessel that all caught light energy is used for biomass formation. Biomass productivities per area in reported photobioreactors are limited by suboptimal circumstances in the reactor, limiting biological efficiency, or by a suboptimal design limiting light supply into the reactor. High yields can only be achieved by linking photobioreactor design to the biological processes inside. The efficiency of the photobioreactor is determined by the integration of: light capturing, light transportation, light distribution, and light usage.

This article describes the design process of the Green Solar Collector (GSC), a light and area efficient photobioreactor for the cultivation of microalgae on sunlight. Light efficient production of algal biomass has been reported in experiments using single flat-panel photobioreactors (Qiang et al. 1998a; Qiang et al. 1998b). These reactors have a large light capturing reactor surface per reactor volume and therefore optimal illumination of the biomass can be achieved. However, area efficient production is difficult to achieve using flat-panel reactors. The tilt angle, the direction the panel faces, i.e. facing east–west or north–south, and the number of panels per area all influence the total productivity per unit ground surface. Shading always influences irradiance levels on the surface of flat-panel reactors that are close together (Pulz et al. 1995), which is required if use of all sunlight per ground area is desired. Creating flat-panel reactor compartments through internal illumination by light channeling and distributing elements (light guides) in a larger vessel (Figure 1), as presented by Janssen et al. (2003), can solve the problems in the delivery of sunlight and the use of all light on the reactor area.

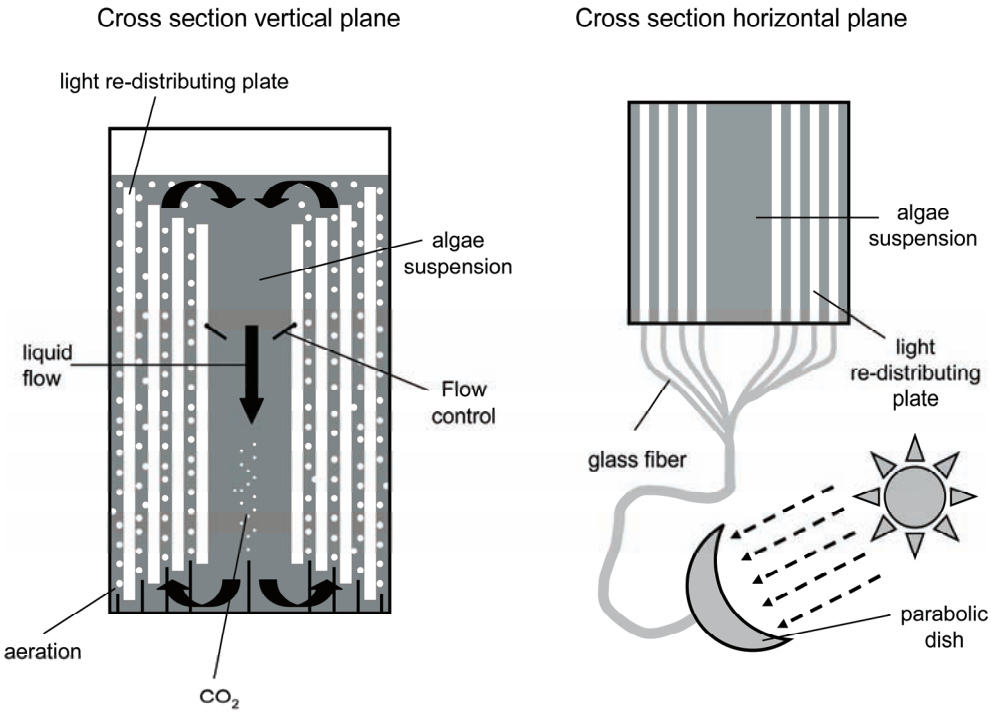

Figure 1. Design of a rectangular air-lift photobioreactor with light redistributing plates and external light collection (Janssen et al. 2003).

To combine a complete coverage of the ground surface and high productivity, sunlight is captured by lenses on top of the GSC (Figure 2) and is directed to the photobioreactor compartment through light guides. These light guides are flat, rectangular sheets of plastic, guiding the light downwards into the algal suspension. The light guides distribute the high intensity direct solar irradiance over a larger area inside the reactor to lower the sunlight intensity without losing light energy. The combination of decreased sunlight intensities, a short light path between the light guides inside the liquid phase of the photobioreactor, resembling a flat-panel photobioreactor, and intensive mixing of the liquid phase by rising air bubbles create an environment to achieve high photosynthetic yields. The goal of the GSC is to efficiently use light energy incident on the bioreactor surface for the production of algal biomass.

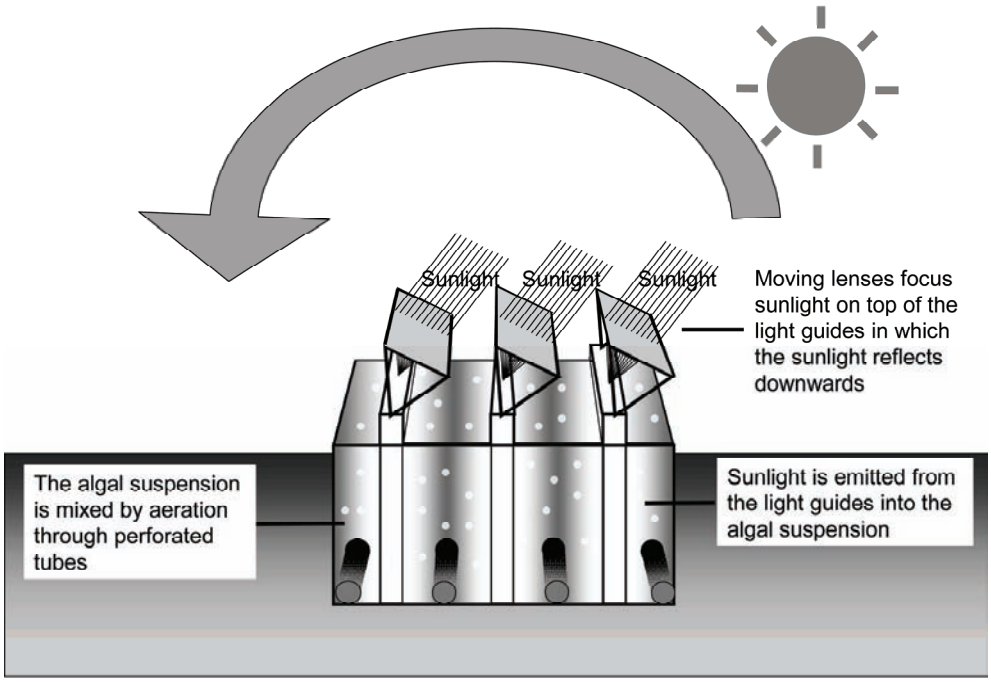

Figure 2. The Green Solar Collector

The following design goals were set for the Green Solar Collector:

1. All sunlight falling on top of the reactor must be concentrated into light guides.
2. All captured light must be fully channeled through the light guides towards the bioreactor compartment.
3. All channeled light must be homogeneously scattered from the light guides into the bioreactor compartment.
4. All scattered light must be efficiently used for the production of biomass.

To enlarge the economical feasibility of using the reactor the following additional constraints were set:

1. It must be easy to install; for instance on rooftops of industrial complexes where ample waste CO_2 is available.

2. It must be made of cheap and durable materials.
3. It must accommodate an easy to control and robust process.

These goals and constraints have yielded a prototype in which the four composing system elements, light capturing, light channeling, light scattering, and biomass production, are integrated as shown in Figure 2. The prototype is placed on top of one of our university buildings and the efficiency of light use will be evaluated by cultivation of microalgae.

The article has been split up in the design of all GSC elements through separately addressing each design goal in the order as stated. In the end, all are integrated and the design of the complete system is discussed.

1. Capturing sunlight

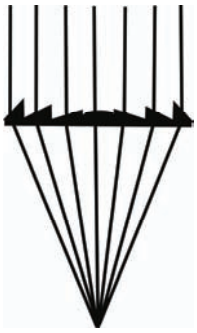

Figure 3. Focussing of light by a Fresnel lens.

All light energy falling on the top surface of the Green Solar Collector must be captured into light guides. Sunlight must be focused in a line on top of the flat, rectangular plastic light guides to have a good distribution of light energy over the light guide surface. Linear or cylindrical lenses can be used to focus sunlight into a straight line on top of these guides. Light falling on the cylindrical curved surface of convex cylindrical lenses refracts toward the center of the lens, forming a line at a certain distance from the lens. On linear Fresnel lenses the curved surface is replaced by parallel prisms on a flat surface; because of the difference in angle of

the prisms light is refracted towards the focal line (Figure 3). Fresnel lenses have the same energy concentrating effect as conventional convex linear or cylindrical lenses, but are less expensive and less heavy.

Parallel placement of linear Fresnel lenses enables the focusing of almost all sunlight falling on the reactor surface into a number of parallel lines. Rotation over an east-west and north-south axis, called dual-axis rotation, of a lens or a mirror as in the "Himawari" solar light collection device (Mori 1985) and the solar fiber-optic mini-dish concentrators (Feuermann et al. 2002; Gordon 2002) enables tracking of the sun. Correct dual-axis positioning of linear Fresnel lenses enables full focusing of sunlight on rectangular light guides during the entire year and an almost full capturing of sunlight as stated in design goal 1.

Positioning the lenses

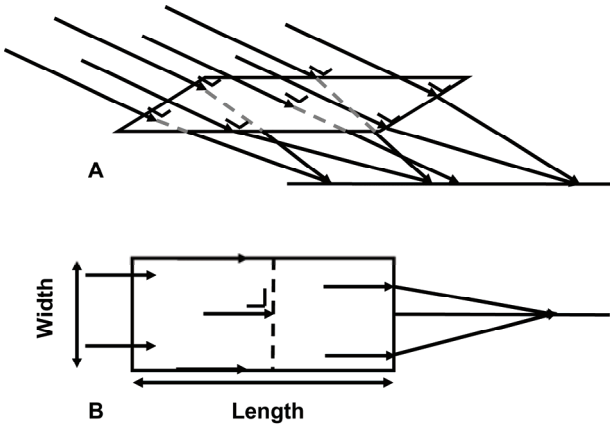

Figure 4. Focussing of light into a line by a linear lens. A: 3-dimensional side view. B: 2-dimensional view from the top.

A linear Fresnel lens focuses light into a line. Light does not need to enter perpendicularly from all directions as illustrated in Figure 4 to be focused into a line. Light only needs to enter perpendicularly with respect to the width of the lens, as can be seen in the top view illustration in Figure 4. A linear Fresnel lens focuses light within a 2-dimensional plane: parallel rays incident over the entire length and

perpendicular to width of the lens are focused into a line. The focal distance is fixed and depends on the lens (Figure 3). In case the light hits the lens surface non-perpendicularly in the length-direction, as in Figure 4, the line of focus is closer to the lens. The light refracts out of the lens with the same angle as it enters in the length-direction, whereas the focal length, the length of the lines leaving the lens in Figure 3 is fixed. Focusing light in a line, even when light enters non perpendicular, makes the lens ideal for focusing of light into the light guide. However, the distance between the lens and light guide needs to be adjustable to keep the line of focus on the light guide.

Two control strategies can be applied for positioning the lens. The sun can be tracked using a light sensor mounted on the lens to position the lens perpendicular to the sun or the position of the lens can be programmed. Both need precise dual-axis positioning of the lens. Tracking the sun using a sensor would require repositioning of the lenses when the sun is intermittently blocked by clouds. Programming the position of the lens is more efficient because the position of the sun on the horizon can be precisely calculated (Duffie and Beckman 1974), resulting in a correct position of the lens during the entire day.

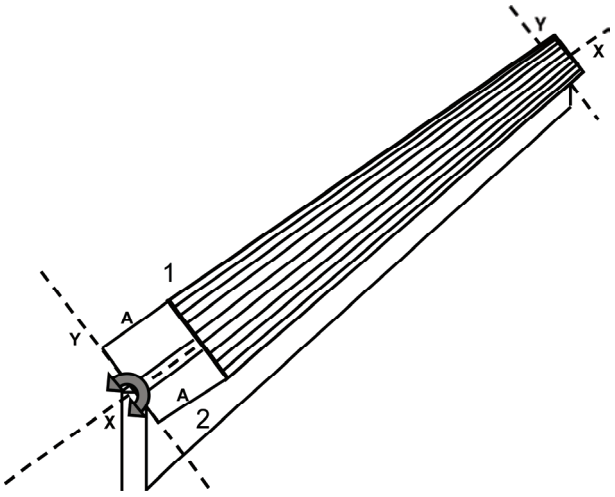

Figure 5. Rotation of the system holding the lens (1) over axis "X", being the top of the light guide (2). The system consists of legs "A" and axis "Y".

Rotation of the system holding the lens over the sheet, rotation over axis “X” in Figure 5, positions the width of the lens perpendicular to the sun. The distance between the lens and sheet is decreased by rotating the four legs holding the lens “A” over axis “Y”, as shown in Figure 6. The rotation can take place independent of the rotation over axis “X”. The rotation over axis “Y” is called the angle of hinge of the lens; the rotation over axis “X” is called the angle of rotation of the lens. The distance between lens and sheet is determined by the incoming angle of the sun; the diagonal parallel to the sun rays between the middle of the lens and the top of the light guide in the two dimensional plane of focus has to equal the focal length “F” of the lens. In other words, the legs “A”, positioning the lens (Figure 5 and 6), need to point towards the sun to have a correct positioning of the lens.

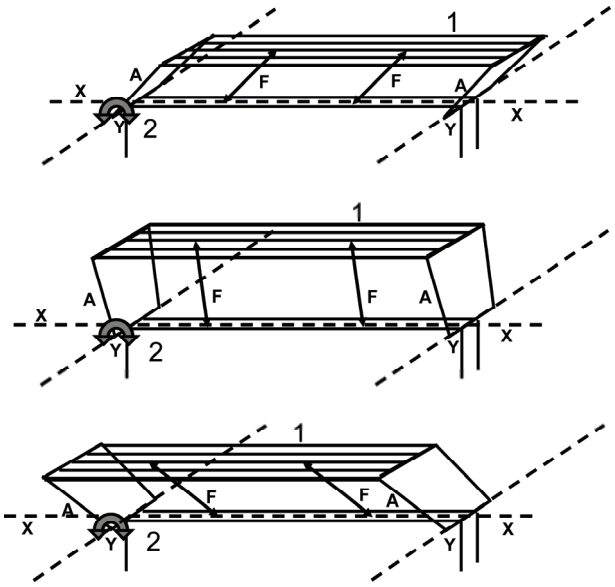

Figure 6. Different angles of hinge of the lens. Legs “A”, of the system holding the lens (1), rotate over axis “Y” to decrease the distance between lens (1) and light guide (2). The diagonal between the middle of the lens and light guide, equals the focal distance “F”.

Calculating the correct position of the lenses

The position of the sun on the horizon during the year can be calculated based on geographical location, date, and time (Duffie and Beckman 1974). The position of

the sun is expressed by two angles. The azimuth angle, the position of the sun on the horizon, e.g. commonly referred to as amount of degrees north, east, south, or west (Figure 7), and the angle of elevation, the angle of the altitude of the sun in the sky relative to a horizontal surface. The position of the lens is calculated based on these angles. The angle of rotation and the angle of hinge are calculated based on the elevation angle and the azimuth angle relative to the orientation of the reactor as described in more detail in Appendix 1.

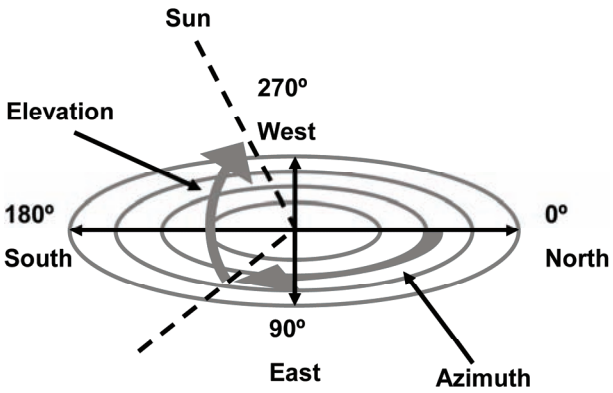

Figure 7. Azimuth and elevation angle of the sun.

The angle of rotation and hinge during a number of days, during the year in Wageningen, the Netherlands is illustrated in Figure 8 and 9. As an example the Green Solar Collector (GSC) is positioned in a north-south orientation, meaning the light guides stretch from north to south. However, the GSC can be placed in any orientation and maintain a good focussing of sunlight on the light guide. A 90° angle of rotation means that the lens is in a horizontal position, a 90° angle of hinge means that the legs "A" positioning the lens are upright. At a 0° and 180° rotation angle the lens is in a vertical position. At a 0° and 180° angle of hinge the lens is positioned downward on top of the light guide.

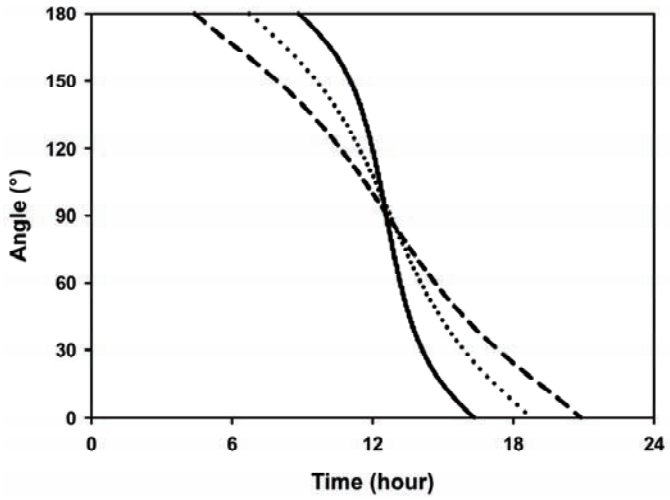

Figure 8. Angle of rotation in a north-south oriented GSC located in Wageningen, the Netherlands. ——— *21st of December* ..... *21st of March* – – – *21st of June*

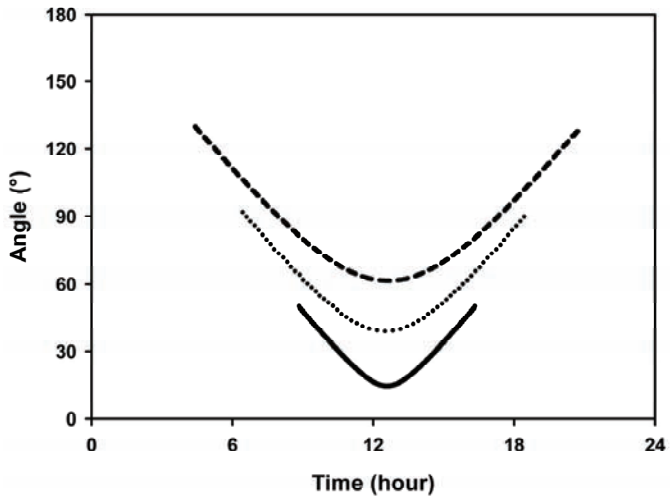

Figure 9. Angle of hinge in a north-south oriented GSC located in Wageningen, the Netherlands. ——— *21st of December* ..... *21st of March* – – – *21st of June*

The position of the lens precisely follows the trajectory of the sun, which can be seen in Figure 8 and 9. The sun rises in the east and the lens has to be rotated to a vertical position facing east. The angle of rotation at sunrise is 180° during the entire year. The angle of hinge at sunrise is determined by the azimuth angle

(Figure 7) at sunrise. During summer the sun rises in the northeast, which means the angle of hinge is larger than 90° to point the legs holding the lens to the north. The combination of the angle of hinge and rotation points the legs holding the lens towards the northeast. During the 21st of March the sun rises in the east, therefore the angle of hinge is 90° and the legs holding the lens are upright pointing to the east. During every day, the lens rotates to a horizontal position at solar noon, when the sun is located in the south. The angle of hinge at this time equals the elevation angle of the sun and again the legs holding the lens are pointing to the sun. During the afternoon the sun descends toward the west where it sets. The angle of hinge during the afternoon increases to follow the sun when it descends from the south towards the north. The rotation angle decreases to rotate the lens towards the west until it is vertical at sunset.
In a north-south oriented reactor the angle of hinge is the rotation over the east-west axis of the reactor to position the lens with respect to the north-south position of the sun. The rotation angle is a rotation over the north-south axis of the reactor to position the lens with respect to the east-west position of the sun. The angle of hinge and rotation can be adjusted to position the lenses in other reactor orientations.

2. Channeling of light to the bioreactor compartment

Transport and distribution of light is integrated in the light guide (Figure 2). Sunlight is transported efficiently by total internal reflection in the light guide. All light entering the guide is channeled to the bottom of the guide, where it is scattered into the algal suspension inside the bioreactor. In the design of the GSC, care had to be taken that light actually enters the light guide and that it reflects inside the light guide when surrounded by air and refracts out of the guide when surrounded by the algal suspension. Whether light reflects from or refracts into the light guide depends on the angle at which the light hits the top of the guide, the refractive index of the material of which the light guide is made, and the shape of the guide.

Material of the light guide

Whether light reflects from or refracts into the horizontal top of the light guide is calculated using Snell's law and Fresnel's formula (Sears 1974) (Appendix 2). Light coming from air always refracts into a clear material with a higher refractive index than air. At small angles, relative to the normal, the highest percentage of light refracts into this clear material, whereas at larger angles the amount of reflection increases, but still a certain percentage of light refracts into the material up to an angle of 89°.

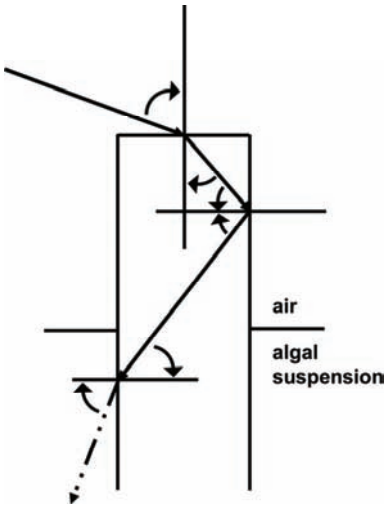

Figure 10. Light refracts into the light guide. Inside the light guide it reflects internally when surrounded by air and it refracts out of the guide when it is surrounded by the algal suspension.

Materials with refractive indices close to the refractive index of air cause light to refract out of the guide over its vertical sides, which is undesired on the upper part of the guide where it is not surrounded by the algal suspension (Figure 10). High refractive indices, on the other hand, cause a large amount of light to reflect at the light guide's point of entry. This is also undesired, because light would not refract into the guide and is not available for the algae. Thus, the refractive index of the guide had to be high enough to ensure total internal reflection when surrounded by

air (Ries et al. 1997), but not much higher to limit the reflection on top of the guide. Whether light reflects internally in the guide or refracts out of the guide at the vertical guide-air interface can again be calculated using Snell's law and Fresnel's formula (Appendix 2). A light guide, surrounded by air and accepting all possible angles on the top surface must have a refractive index higher than 1.415 (see Appendix 2). Polymethylmethacrylate (PMMA) a clear transparent plastic with the highest transmittance for visible light compared to other plastics is an ideal material for a light guide. It has the same transmittance as glass and it has a refractive index of 1.49 to 1.50 for visible light, which is larger than the required refractive index of 1.415. This ensures total internal reflection inside the light guide when it is surrounded by air, while limiting the reflection of light on top of the guide.

Reflection and refraction in the top of the light guide

As calculated in Appendix 2, total internal reflection occurs when light refracts towards the center of the light guide when entering into the top of the guide. Figure 11 shows that light does not refract towards the center in a guide with a round top surface. Because of the more perpendicular angles of the incoming light on the round top surface, light does not refract sufficiently and total internal reflection does not occur. More sunlight reflects from the guide's flat top surface than from a round top surface because light enters more perpendicularly on the round surface. However, loss of light energy due to refraction out of the guide because of a round top surface is larger than reflection on top of a flat top surface. Light must refract downward into the guide to be available to the algae. The top surface of the guide is therefore flat, because it is the best shape to capture and keep light in the guide.

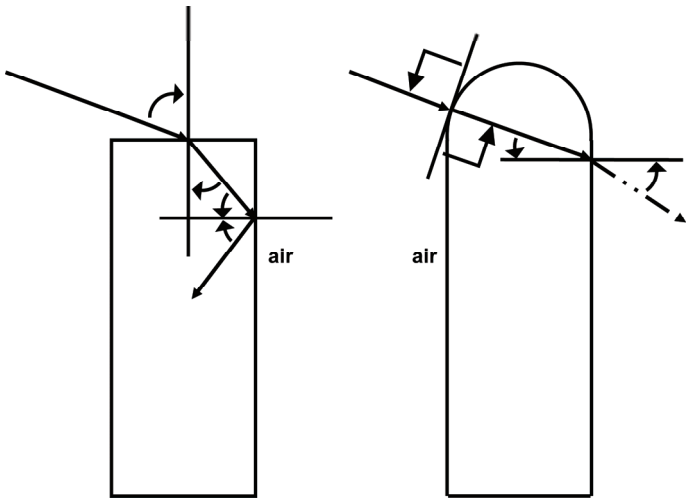

Figure 11. Influence of the shape of the top of the light guide on the reflection and refraction of light inside the light guide.

3. Scattering of light into the bioreactor compartment

The top part of the light guide is surrounded by air and light needs to reflect internally, but the bottom part is surrounded by the algal suspension and light needs to be scattered from the light guide into the suspension. As calculated in Appendix 2, the maximum angle for which total internal reflection occurs when surrounded by water is 26.8º from the vertical sides. Sunlight with an angle between 0º and 42.2º from the normal, entering on top of the light guide, would still reflect internally and eventually leave through the bottom of a rectangular guide. This is undesired since light has to leave the guide over its left and right surface in order to have a uniform scattering of light out of the light guide surface into the bioreactor compartment.

The only way to ensure that all light leaves the guide over its left and right surface is to change the incident angle of the light on the bottom part of the guide. A triangular shaped bottom part changes the angle at which the light reflects and results in the refraction of all light out of the bottom part of the guide. Figure 12 shows the refraction and reflection of light on top of and inside the guide. The light

guide needs to narrow towards the bottom to let all light refract out of the guide and the tip has to be surrounded by the algal suspension.

The uniformity of scattering of light out of the guide is still under investigation. Preliminary measurements showed that light does not reflect uniformly out of a guide with a smooth surface, while a surface treatment, such as sandblasting, showed a more uniform scattering of light out of the entire surface of the triangular bottom part. Calculations show (data not presented), that all light scatters out of the light guide for the smooth as well as the sandblasted surface.

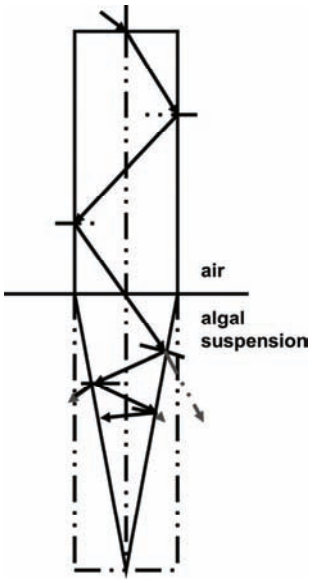

Figure 12. Reflection of light inside the light guide. Total internal reflection in the top part and total refraction out of the guide in the bottom part.

4. Efficient use of scattered light

The use of scattered light by the algae is maximized by creating compartments, numbered "3" in Figure 13, with short light paths and turbulent mixing, similar to the flat-panel compartments described by Qiang et al. (1998a; 1998b). In these flat-panel photobioreactor experiments up to 20% of the PAR (photosynthetic active

radiation; wavelength range of 400 nm to 700 nm) sunlight energy falling on the reactor surface was stored as biomass; approaching the theoretical maximum conversion efficiency of 21% of light within the PAR range (Bolton and Hall 1991).

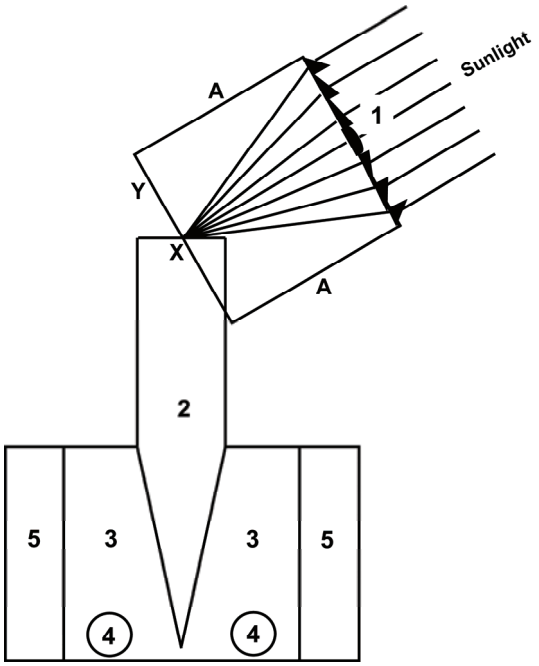

Figure 13. Schematic drawing of a cross section of the photobioreactor. The numbers indicate the following: 1: linear Fresnel lens, 2: light guide, 3: flat-panel reactor compartment, 4: perforated tube for aeration, 5: water jacket. The letters indicate the following: A: legs holding the lens, X: axis of rotation of the lens, Y: axis of rotation of the legs "A".

The short light path in a flat-panel photobioreactor, combined with turbulent mixing induced by aeration at the bottom causes a rapid circulation of the algae from the illuminated reactor wall to the dark interior of the reactor. It subjects the algae to intermittent illumination which is suggested to increase the efficiency of use of (over-) saturating light intensities (Richmond 1996). Well controllable flat-panel compartments with turbulent mixing by aeration also are comprised between the light guide and water jacket in the GSC. Although the width of the compartment in our reactor varies from top to bottom, on average it is similar to the width reported by Qiang et al. (1998a; 1998b).

The flat-panel compartment

Figure 13 shows the design of the GSC. The light guide separates the reactor into two flat-panel compartments between the left and right water jacket. The light guide resembles the transparent reactor wall of a panel reactor. Instead of being a light transparent barrier between the algal culture and the outside, it now separates two algal culture compartments and delivers light to both compartments. The rectangular light guide, the wall of the water jacket, and aeration at the bottom along the length of the reactor create an environment similar to a flat-panel photobioreactor.

Integrating the four reactor elements

Use of focused sunlight

Light is captured and distributed into the GSC during the entire day, but optimal conditions need to be provided for the algae. The most important is to provide a suitable light intensity in the GSC. In the flat-panel photobioreactor cultivation experiments described by Qiang et al. (1998a; 1998b) the highest volumetric productivity was not achieved in the reactor with the highest efficiency. An efficiency of 20% was achieved in a panel reactor not fully exposed to sunlight. It was positioned vertically; therefore reflection of light occurred on the reactor surface, decreasing the light intensity inside the panel reactor
In the GSC care is taken in supplying sunlight to the algae at the right intensity. If light is captured and transported with 100% efficiency, only the dimensions of the lens and light guide determine the light intensity in the bioreactor compartment; it then is determined by the ratio of the surface of the lens to the surface of the light guide in the algal culture.

Total design of the bioreactor

The GSC contains flat-panel bioreactor compartments of 18 mm (top) to 25 mm (bottom) wide and the maximum light intensity has to be approximately half of the

intensity of the sun to have an efficient use of light while having a high biomass productivity. Therefore, the illuminating surface of the light guide has to be the double of the light capturing surface of the lens to dilute the maximum sunlight intensity to the desired intensity. Because the length of the lens and light guide are equal, the height of the triangular shaped bottom part has to be equal to the width of the lens, because light refracts from both sides of the bottom part of the guide. The GSC is designed to cover large areas by having multiple light guides next to each other in a larger housing. The distance from one light guide to another is constructed by two flat-panel compartments, one water jacket, and the light guide itself. This distance is fixed at 60 mm. To be able to have an unhindered movement of neighboring lenses; a lens with a width of 52 mm and a focal distance of 51 mm is chosen. The width of the lens fixes the height of the bottom part of the light guide to 50 mm as explained above. The width of a flat-panel compartment is constraint by design limitations, but the length of the compartment is not and can stretch up to several meters. Taking into account the rectangular top part of the light guide and the lens, it results in a system that is maximal approximately 200 mm high and contains 36 liters of algal suspension per square meter.

Discussion

The real proof of efficient use of light is in determining the actual area biomass yield of the GSC. This will be determined by the integration of: light capturing, light transportation, light distribution, and light usage. In our design, sunlight is captured directly in the light guide to minimize loss of light energy. Previous attempts by others to capture sunlight with lenses and to transport light into a light guide through optical fibers proved less efficient and expensive. Gordon (2002) and Ogbonna et al. (1999) stated that low efficiencies in the delivery of light into the photobioreactor through optical fibers were obtained due to coupling problems between different light guiding fibers and loss of light in transport through the fibers. Costs and construction considerations for large scale optical fiber photobioreactor cultivation systems further limited the application of fibers (Gordon 2002). These considerations and the efficiency problems do not meet the Green Solar Collector's design goals and constraints. Focusing sunlight directly on

the light guide is more efficient, because light does not have to be transported over long distances. Light reflects internally without loss in intensity over the small distance where it needs to be transported.

The GSC's light guides increase the illuminated surface per reactor volume and therefore resemble the sheets described by Janssen et al. (2003). Multiple light guides next to each other increase the illuminated surface in larger bioreactors. Previously, scratched optical fibers were used to internally illuminate a photobioreactor and to increase the illuminated surface per reactor volume (An and Kim 2000; Matsunaga et al. 1991). Large numbers of optical fibers are needed to have an increased surface to volume ratio compared with non internal illuminated reactors. The construction and maintenance of large photobioreactor systems containing thousands of optical fibers will not meet the design constraints posed in the introduction; therefore a sheet of PMMA is used to internally illuminate the photobioreactor compartments in the GSC.

An effect such as shading, common in vertical plate or column reactors placed close together does not interfere with the light supply. The potential for achieving optimal conditions in our photobioreactor is present due to uniform illumination inside the reactor. Each lens focuses the same amount of sunlight into the light guide, due to the parallel placement of the lenses, creating a similar illumination pattern throughout large areas of the GSC. Process conditions are therefore similar throughout large GSC areas. Depending on the orientation of the reactor, the lenses shade each other somewhat at low altitudes of the sun. However, because the lenses are placed parallel, shading is the same on each lens, again leading to the same illumination in all flat-panel compartments.

The GSC has been constructed (Figure 14) and by visual observation it is clear that the lenses are able to focus sunlight on top of the light guide and that light refracts out of the guide into the algal suspension. The actual efficiency of light supply is still unknown, but can be estimated based on the reflection of light on the lens and light guide as shown earlier. Also the uniform illumination over both sides of the bottom part of the light guide is still being investigated.

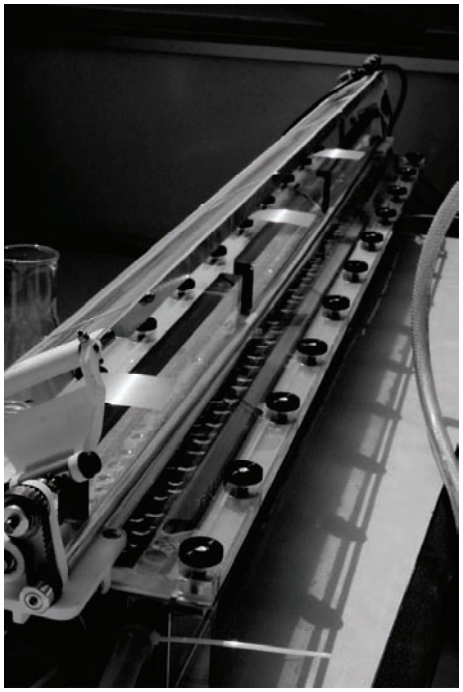

Figure 14. Picture of the GSC; the lens focuses light on top of the light guide (line of focus visible on top of the sheets of paper on the guide). Light refracts internally inside the guide and is scattered into the algal suspension.

Conclusions

The GSC complies with the stated goals and constraints. The lenses capture sunlight coming from all angles through dual-axis positioning of linear Fresnel lenses. Sunlight is focused on the light guides in which it propagates by internal reflection and ends up in the algal suspension in the flat-panel compartments. Almost all light falling on the GSC is intercepted by the lenses during the day, except when the lenses are in a horizontal position. At maximum, 8.7% of the direct sunlight passes in between the lenses and will strike the transparent reactor cover. The demand to capture all sunlight per ground area in the light guides is therefore almost completely met. Capturing all sunlight into the light guides was not possible, because some space is needed in between lenses to allow unhindered movement of the lenses. This fraction of direct sunlight as well as diffuse sunlight

can still enter the reactor compartment through the transparent top reactor cover and is not lost for the microalgae.

Table 1. Capturing efficiency of direct sunlight in the GSC in Wageningen, the Netherlands.

Day of the year	Light capturing efficiency
21st of December	27% - 32%
21st of March	57% - 61%
21st of June	76% - 67%
21st of September	57% - 61%

The capturing efficiencies of the GSC were calculated based on reflection on the lens and light guide during the day combined with reported direct irradiance values[1]. The capturing efficiency decreases in fall and winter due to the lower elevation angles of the sun (Table 1). The amount of reflection on top of the light guide increases significantly. The different capturing efficiencies presented in Table 1 are related to the chosen orientation of the GSC with respect to the sun (Appendix 1).

The efficiency of scattering from the light guide into the bioreactor compartment is estimated to be 100% based on the reflection and refraction of light. Therefore, high biomass productivities can be obtained during summer in the Netherlands. During winter the GSC is less efficient due to a lower capturing efficiency. At low latitudes, on the other hand, high productivities can be achieved during the entire year. At these locations the sun has a higher angle of elevation which reduces the reflection of sunlight on top the light guide. However, clear skies are still a prerequisite for high productivities.

The production costs of the GSC are expected to be higher than those of conventional outdoor photobioreactors, such as horizontal and vertical tubes or vertical panels. The production costs compared with fiber optic photobioreactors (Mori 1985), on the other hand, will be lower because of ease of construction and

[1] PVGIS: Geographical Assessment of Solar Energy Resource and Photovoltaic Technology (http://re.jrc.ec.europa.eu/pvgis/index.htm).

maintenance, and the use of cheap materials (PMMA). The most expensive part will be the system to position the lenses, but on large areas covered with multiple units all lenses have to be in the same position. The lens positioning system therefore can be integrated in one single system controlling multiple reactor units. Consequently, economy of scales can significantly reduce reactor costs.

A robust process can be run in the GSC because suitable light intensities are combined with turbulent mixing and control of pH and temperature. The GSC is constructed of durable plastics and is light in weight. The reactor can thus be easily placed on horizontal rooftops and can be an alternative to conventional thermal or photovoltaic solar collectors. A new type of solar collector had been created: “the Green Solar Collector”. The real proof of functionality of the designed reactor needs to come from cultivation experiments; conclusions can then be made on the overall efficiency of use of light in the Green Solar Collector.

Acknowledgements

This research was supported by Senternovem Neo (0268-03-04-03-002), Biopartner (807.04.220), BWP II (EET K 03028) and Solar-H (516510).
The system to position the lenses was constructed by TNO Industrial Technology, the Netherlands.

Appendix 1

The position of the lenses is calculated based on the elevation angle of the sun and the relative orientation of the reactor to the azimuth angle of the sun. Starting point is a north-south orientation of the reactor, which means that the lenses on top of the reactor stretch from north to south. If the orientation changes, if the reactor for instance stretches from east to west, or northwest to southeast, the azimuth angle has to be adjusted. Equation 1 and 2 yield the position of the lens based on the position of the sun (γ and α) and the orientation of the reactor (β).

$$\tan(rotation) = \tan\left(\frac{\sin(\gamma)}{\cos(\gamma) * \cos(\alpha - \beta)}\right)$$ Equation 1

$$\sin(hinge) = \sin\left(\sqrt{\left(\sin(\gamma)\right)^2 + \left(\cos(\gamma) * \cos(\alpha - \beta)\right)^2}\right)$$ Equation 2

α = recalculated azimuth angle of the sun on the horizon (Table 2 and Figure 7).
γ = angle of elevation of the sun in the sky (Figure 7).
β = orientation of the Green Solar Collector (Table 3).

Table 2. Redefining the azimuth angle into α to calculate the angle of hinge and rotation.

	Azimuth	α
North	0°	90°
Northeast	45°	45°
East	90°	0°
Southeast	135°	45°
South	180°	90°
Southwest	225°	45°
West	270°	0°
Northwest	315°	45°

Table 3. Factor β; correcting the orientation of the photobioreactor to calculate the angle of hinge and rotation.

Orientation	β
North - South	0°
Northeast - Southwest	45°
East - West	90°
Southeast- Northwest	45°

Table 2 shows the values for α to calculate the position of the lenses. The value for α is continuously changing with the azimuth angle of the sun. The value for β (Table 3) is fixed with the chosen orientation of the reactor.

A rotation angle of 0° or 180° means that the lens is in a vertical position on the left or right side of the light guide. An angle of hinge of 0° or 180° means that the lens is positioned on top of the light guide on the left or right side. At an angle of 90°, the lens is in an upward and/or horizontal position. Whether 0° or 180° is left or right for the angle of hinge or rotation is a matter of definition, because the path of the sun on the horizon is the same in the morning and the afternoon, where the solar noon functions as the mirror point.

The angle of rotation is calculated using Equation 1. The result is an angle between 0° and 90°. The angle of rotation on one side of the light guide is defined as this angle; the one on the other side as 180° minus this angle. The angle of hinge is calculated using Equation 2. The result is an angle between 0° and 90°. The angle of hinge in one direction is defined as this angle; the one in the other direction as 180° minus this angle.

Appendix 2

The angle of refraction of light propagating from one material into the other is calculated using Snell's law. The index of refraction (n) of each material and the angle of incidence (θ) determine what the angle of refraction or reflection is. When light refracts from a material (n_1) with a low refractive index into one (n_2) with a high refractive index the sine of the angle of refracted light (θ_2) is smaller than of the light entering (θ_1), so light will be refracted towards the normal. When the refractive index of the material from which light propagates (n_1) is higher, the sine of the angle of refracted light (θ_2) increases, therefore it is refracted away from the normal and at larger angles of incident light (θ_1) it will not refract into the material (n_2) at all. It then reflects on the interface.

$$\frac{n_1}{n_2} = \frac{\sin\theta_2}{\sin\theta_1}$$ Equation 3

Snell's law

Θ = angle from the normal

When light refracts into a material, a part of the light energy is lost due to reflection; this can be calculated using Fresnel's formula (Equation 4). The difference in angle of incidence and refracted light determines the amount of reflected light energy. A larger difference causes more reflection. Therefore, the larger the relative difference in refractive index of the materials, the higher the amount of reflection.

$$R = 100\% * \left[0.5 * \frac{\tan^2(\theta_1 - \theta_2)}{\tan^2(\theta_1 + \theta_2)} + 0.5 * \frac{\sin^2(\theta_1 - \theta_2)}{\sin^2(\theta_1 + \theta_2)} \right] \quad \text{Equation 4}$$

Fresnel's formula

Θ = angle from the normal

R= percentage of light energy that reflects from the surface

In the case of normal incident irradiance from the air, the reflection can be calculated using Equation 5.

$$R = 100\% * \left(\frac{n_2 - n_1}{n_1 + n_2} \right)^2 \quad \text{Equation 5}$$

When light refracts into a rectangular light guide, it can reflect internally on the vertical sides of the guide, depending on the shape and surrounding material. When light is not refracted towards the normal on the top of the guide, the resulting angle of incidence on the side of the guide is too high to ensure internal reflection.

An example:

Incident light at an angle of 45° (θ_1) hits a light guide (n_2 = 1.8) from air (n_1 = 1). It refracts into the guide at an angle of 23.1° (θ_2) and 9.4% of the light energy is lost due to reflection. The refracted light hits the vertical side of the guide at an angle of 90° - 23.1° = 66.9° (θ_1), relative to the normal. Using Snell's law (n_1 = 1.8; n_2 = 1), the angle of refraction on the side of the guide results in an angle larger than 90° (θ_2); meaning all light reflects inside the guide.

Incident light at an angle of 45° (θ_1) hits a light guide with a different material (n_2 = 1.2) from air (n_1 = 1). It refracts into the guide at an angle of 36.1° (θ_2) and 1.3% of the light energy is lost due to reflection. The refracted light hits the vertical side of the guide at an angle of 90° - 36.1° = 53.9° (θ_1), relative to the normal. Using Snell's law (n_1 = 1.2; n_2 = 1), the light refracts out of the guide at an angle of 75.8° (θ_2) and only 17.4% of the light energy is reflected on the interface. The major part of the light energy, 82.6%, is lost as a result of refraction out of the side of the light guide.

Whether light will reflect internally can also be determined by calculating the numerical aperture (NA). It is the sine of the angle of incident light on top of the light guide for which total internal reflection occurs and it determines the applicability of a material as a light guide (Gordon 2002). The angle for which total internal reflection occurs can be calculated using Equation 6 and 7.

$$NA = n_1 * \sin(\theta_{\max}) \qquad \text{Equation 6}$$

$$NA = \sqrt{(n_2^2 - n_1^2)} \qquad \text{Equation 7}$$

The refractive index only needs to be high enough to ensure total internal reflection in the rectangular light guide, when surrounded by air. Taking the maximum angle on the light guide (θ_{max} = 90°) and the refractive index of air (n_1 = 1), the NA of the light guide can be calculated using Equation 6. The refractive index of the light guide (n_2) needs to be 1.414 to have internal reflection of all captured light as can be calculated from Equation 7. At this or higher refractive indices, light at an angle of 90° refracts into the light guide at an angle of 45° or lower, while total internal reflection can already occur at angles of 45° or higher. At lower refractive indices, the angle of refraction will be larger than 45° and total internal reflection will only occur at angles lower than 45°, resulting in refraction of light out of the sides of the light guide.

The NA also can be calculated, when a PMMA (n_1 = 1.49) light guide is surrounded by water (n_2 = 1.33), using Equation 7. The maximum acceptance angle on top of

the light guide can be calculated using Equation 6 in which $n_1 = 1$, because light enters the guide from air. The maximum angle of incident light on top of the light guide for which total internal occurs (θ_{max}) is 42.2°. Incident light with angles smaller than 42.2° from the normal reflects internally when the light guide is surrounded by water.

References

An JY, Kim BW. 2000. Biological desulfurization in an optical-fiber photobioreactor using an automatic sunlight collection system. Journal of Biotechnology 80(1):35-44.

Bolton JR, Hall DO. 1991. The Maximum Efficiency of Photosynthesis. Photochemistry and Photobiology 53(4):545-548.

Duffie JA, Beckman WA. 1974. Solar engineering of thermal processes. New York: John Wiley & Sons. 386 p.

Feuermann D, Gordon JM, Huleihil M. 2002. Solar fiber-optic mini-dish-concentrators: First experimental results and field experience. Solar Energy 72(6):459-472.

Gordon JM. 2002. Tailoring optical systems to optimized photobioreactors. International Journal of Hydrogen Energy 27(11-12):1175-1184.

Janssen M, Tramper J, Mur LR, Wijffels RH. 2003. Enclosed outdoor photobioreactors: Light regime, photosynthetic efficiency, scale-up, and future prospects. Biotechnology and Bioengineering 81(2):193-210.

Matsunaga T, Takeyama H, Sudo H, Oyama N, Ariura S, Takano H, Hirano M, Burgess JG, Sode K, Nakamura N. 1991. Glutamate Production from Co2 by Marine Cyanobacterium Synechococcus Sp using a novel Biosolar Reactor employing Light-Diffusing Optical Fibers. Applied Biochemistry and Biotechnology 28-9:157-167.

Mori K. 1985. Photoautotrophic bioreactor using visible solar rays condensed by Fresnel lenses and transmitted through optical fibers. Biotechnology Bioengineering Symposium vol. 15(15):331-345.

Ogbonna JC, Soejima T, Tanaka H. 1999. An integrated solar and artificial light system for internal illumination of photobioreactors. Journal of Biotechnology 70(1-3):289-297.

Pulz O, Gerbsch N, Buchholz R. 1995. Light energy supply in plate-type and light diffusing optical-fiber bioreactors. Journal of Applied Phycology 7(2):145-149.

Qiang H, Faiman D, Richmond A. 1998a. Optimal tilt angles of enclosed reactors for growing photoautotrophic microorganisms outdoors. Journal of Fermentation and Bioengineering 85(2):230-236.

Qiang H, Zarmi Y, Richmond A. 1998b. Combined effects of light intensity, light-path and culture density on output rate of Spirulina platensis (Cyanobacteria). European Journal of Phycology 33(2):165-171.

Richmond A. 1996. Efficient utilization of high irradiance for production of photoautotropic cell mass: A survey. Journal of Applied Phycology 8(4-5):381-387.

Ries H, Segal A, Karni J. 1997. Extracting concentrated guided light. Applied Optics 36(13):2869-2874.

Sears FW. 1974. Optics, third edition. Reading, Massachusetts: Addison - Wesley publishing company. 390 p.

Chapter 3

Capturing sunlight into a photobioreactor; Ray tracing simulations of the propagation of light from capture to distribution into the reactor

Abstract

The Green Solar Collector (GSC), a photobioreactor designed for area efficient outdoor cultivation of microalgae uses Fresnel lenses and light guides to focus, transport, and distribute direct light into the algae suspension. Calculating the path of rays of light, so called ray tracing, is used to determine local light intensities inside the photobioreactor based on the focused rays of sunlight. Reflection and refraction of the propagating rays of sunlight from point of focus to refraction into the photobioreactor is calculated. Refraction out of smooth and sandblasted distributor surfaces is simulated. For the sandblasted surface a specific structure is assumed and corresponding reflection and refraction patterns are described by a 2-dimensional modeling approach. Results of the simulations are validated by measurements on real light guide surfaces. The validated model is used to determine the influence of the solar angle on the uniformity and efficiency of light distribution over the light distributor surface.

The simulations show that efficient capturing of sunlight and redistribution inside the algal biomass can be achieved in the Green Solar Collector at higher elevation angles of the sun, making the Green Solar Collector suitable for operation at low latitudes with a high level of direct irradiance.

This chapter has been published as: Zijffers JWF, Salim S, Janssen M, Tramper J, Wijffels RH. 2008. Capturing sunlight into a photobioreactor: Ray tracing simulations of the propagation of light from capture to distribution into the reactor. Chemical Engineering Journal 145(2):316-327.

Introduction

The volumetric biomass productivity of a microalgal culture in a photobioreactor is determined by the light input in the photobioreactor and the efficiency of light use for microalgal growth. Light intensity is an important parameter for the photosynthetic efficiency in photobioreactors. Exposure to full sunlight intensities limits the microalgae's light use efficiency, while prolonged exposure to darkness stops the microalgae's autotrophic processes. To efficiently cultivate microalgae, the exposure to light has to be carefully regulated and therefore it is important to know local light intensities inside a photobioreactor (Perner-Nochta and Posten 2007; Pruvost et al. 2002).

The Green Solar Collector (GSC) (Zijffers et al. 2008) was developed to obtain high area biomass yields by efficiently capturing, transporting, and redistributing available direct sunlight into the microalgal culture. It was designed to supply captured sunlight to the microalgae at reduced intensities. This in combination with a short light path and turbulent mixing is expected to result in high light use efficiency and high volumetric biomass productivity. To be able to run a light efficient cultivation an investigation into distribution of captured sunlight into the reactor compartment is necessary. A uniform distribution on the light distributor surface is needed to have a reduced and uniform light intensity inside the microalgal culture such that light can be efficiently used by the microalgae.

Extracting light uniformly from the lateral surfaces of optical fibers and light guides or distributor-like structures has been a problem in previous research (An and Kim 2000; Hirata et al. 1996; Pulz et al. 1995). The problem was either caused by getting the light into the illumination plate (An and Kim 2000) or getting the light out of the distributor over its lateral surface (Hirata et al. 1996; Pulz et al. 1995). Csögör et al. (1999) managed to improve the lateral distribution to a large extend by roughening the surface of the illuminating surface of the distributor. The short distance between the light source and the end of the distributor helped to achieve a more uniform illumination in the work performed by Csögör et al. (1999).

Sunlight is captured into the GSC through Polymethylmethacrylate (PMMA) Fresnel lenses that are able to rotate over two axes to follow the sun. The lenses can rotate over the light guide and the distance between the lens and light guide is adjustable to maintain the line of focus on top of the light guide as explained by Zijffers et al. (2008). Light focused on top of the light guides refracts into the light guides and internal reflection in the guides directs light into the bioreactor compartment. Internal reflection inside the guides and refraction out of the guides into the algal suspension is calculated based on the specific incident angles of sunlight rays on the interior surface of the light guide. Based on the relation between the light capturing surface of the lens and the light emitting surface of the light guide, the light intensity on the light distributor surface will be about half of the sunlight intensity. However, due to the changing position of the sun on the horizon and the position of the lens with respect to the sun, reflection, and refraction of light on the lens and light guide vary. The results of a ray tracing study into the effect of changing reflection and refraction of light on the capturing efficiency and on the uniformity of light distribution will be discussed in this paper.

Ray tracing, "following a path of a photon (or ray of light) as it bounces around the scene" (Glassner 1989), can be used to determine the path of light rays and the intensity at which sunlight enters the microalgal culture. The path of the focused sunlight inside a light guide of the GSC is visualized for a guide with a smooth or a rough, sandblasted distributor surface. A specific surface structure for the sandblasted light guide surface is assumed, leading to specific reflection and refraction patterns for focused rays of sunlight.

The ray tracing routine is explained in a separate model description. The model is validated by comparing results of simulations with measurements of the refraction of focused light out of real light guides. Refraction and reflection of light is then simulated for different situations and the efficiency of light capturing and the uniformity of light distribution into the Green Solar Collector is discussed.

Model description

Ray tracing

The ray tracing approach used in this research regards sunlight as a bundle of parallel rays. All reflections and refractions of light on the internal and external surfaces of the lens and light guide are calculated by Snell's law and Fresnel's formula. Average values are used for the refractive indices of the different materials involved in the ray tracing simulations, because only a minor change in refractive index occurs within the wavelength range studied (400 nm to 700 nm). These are: PMMA (lens and light guide): 1.49; water (algal suspension): 1.33; air: 1.00.

The calculation of the path of sunlight into the Green Solar Collector is split up in three parts, which are illustrated in Figure 1:

1. Focusing of direct sunlight through a lens and capturing of focused light into the light guide
2. Transport of captured light downwards through the rectangular top part of the light guide
3. Redistribution (refraction) of captured light out of the triangular bottom part of the light guide, i.e. the light distributor, into the algal suspension surrounding the triangular light distributor

Focusing and capturing of sunlight

Sunlight is focused on top of the light guide by refraction of sunlight through the prisms of the Fresnel lens. The lens is positioned perpendicular to the sun such that sunlight is focused in a line on top of the light guide (Zijffers et al. 2008). The width of this line is approximately 2 mm when focused perpendicularly on the light guide. At lower elevation angles of the sun the line widens to about 6 mm. Sunlight always strikes the lens perpendicular with respect to the width of the lens but not necessarily perpendicular with respect to the length of the lens.

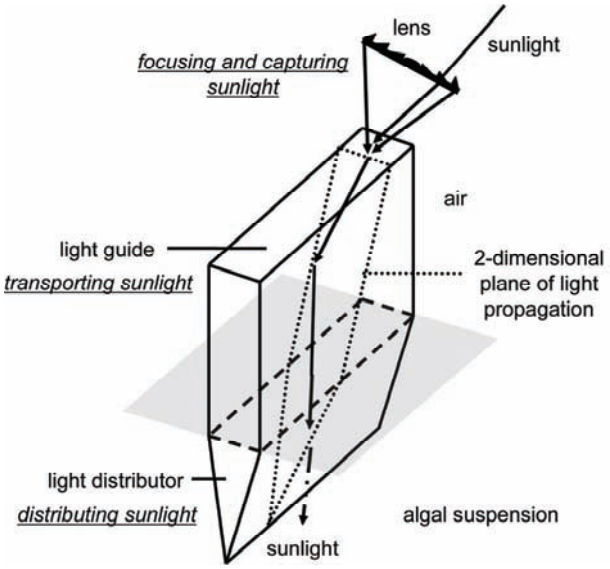

Figure 1. Focusing and capturing, transporting, and distributing sunlight into the algal suspension. The lens has a width of 52 mm and a focal point at 51 mm. The total height of the light guide is 110 m, which can be split up in a rectangular part of 70 mm and a triangular part of 40 mm. Width of the light guide was chosen to be 8 mm or 16 mm.

The specific lens used on the GSC focuses sunlight in a window of 55° (Figure 2). Since the ray tracing simulation requires a finite number of rays, each degree within the window of focus is considered to be a separate ray. A resolution per degree is chosen such that sufficient detail on the propagation of sunlight is obtained while maintaining reasonable computation times on a desktop computer. If desired, the model can be modified to use different windows of focus if other lens geometries are used on the GSC.

The intensity of each ray is calculated by correcting the radiant flux (Φ) of the direct sunlight for the incident angle (φ) of the sunlight with respect to the length of the lens and dividing it equally over 55 rays (Equation 1).

$$\phi_{ray} = \frac{\phi_{directnormal} * \cos(\varphi)}{55} \quad \text{(W)} \qquad \text{Equation 1}$$

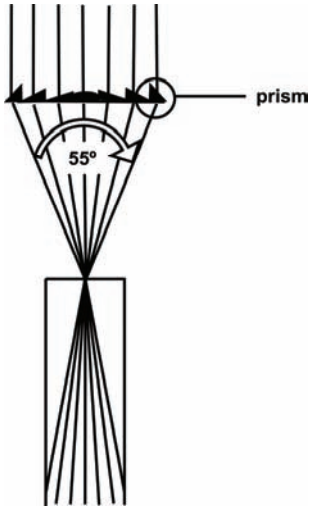

Figure 2. Focusing of light by a Fresnel lens and capturing into the light guide.

In passing the lens, light is reflected twice. Once on the air–PMMA interface entering the lens and once on the PMMA–air interface leaving the lens. The amount of reflection on the interfaces is calculated using the incident sunlight angle on the lens surface (φ). The amount of reflection on top of the light guide depends on the position of the lens with respect to the sun.

The sunlight rays are focused in a line on top of the light guide. The ray tracing results for a single 2-dimensional plane of light propagation, as shown in Figure 1, can thus be extrapolated for the entire length of the lens. However, the length of the light guide has to be much larger than the height to be allowed to neglect the different geometry at beginning and end of the light guide.

Transporting captured light

All captured light propagates by total internal reflection inside the rectangular top part of the guide as long as it is surrounded by air and the surface of the guide is perfectly smooth. The path of the refracted rays inside the light guide depends on the dimensions of the guide. All internal reflections on the light guide surface are perfect, i.e. no decrease in light intensity, and attenuation due to propagation in

PMMA is assumed to be negligible. In fact, the light energy content of the ray will decrease somewhat, but it will be less than 1% while propagating inside the short, transparent PMMA light guide before reaching the triangular light distributor surface. This number is based on the average attenuation of PMMA for visible light.

Redistributing captured light

Captured light must refract out of the light distributor surrounded by the algal suspension. Narrowing of the distributor towards the bottom causes rays to strike the distributor surface more perpendicularly and results in increased refraction of light out of the guide (Ries et al. 1997). The distributor can have a smooth surface, but since internal reflection is no longer desired the surface can also be roughened to further facilitate refraction of light out of the guide.

A. Refraction of light out of a smooth distributor

Snell's law and Fresnel's formula are used to calculate the fraction of the radiant flux that reflects on the smooth distributor surface surrounded by the algal suspension. The reflected radiant flux of a ray (Equation 2a) is traced until all light is refracted out of the guide. Obviously, light that does not reflect on the surface will be refracted out of the guide (Equation 2b) and penetrates into the algal culture. The location where light refracts out of the distributor is calculated and determined for all 55 rays. A distribution profile of refracted radiant flux over the distributor surface can thus be created depending on the specific position of the sun.

$$\phi_{reflectedray} = R * \phi_{ray} \quad \text{(W)} \quad \text{Equation 2a}$$

$$\phi_{refractedray} = (1 - R) * \phi_{ray} \quad \text{(W)} \quad \text{Equation 2b}$$

B. Refraction of light out of a sandblasted distributor

To trace the rays during reflection or refraction on a rough surface, the structure of the surface needs to be known. According to Csögör et al. (1999) an ideal rough surface can be considered to be a sphere emitter. The sandblasted distributor surface in the GSC is therefore assumed to be uniformly covered with infinitely small hemispherical dents. These hemispheres do not have any area; they are merely a tool to model the probable incident angles of a light ray on a sandblasted surface. The incident angles on the projection of the hemisphere on the 2-dimensional plane of light propagation (see Figure 1) are determined based on the incident angle of the ray on the distributor surface.

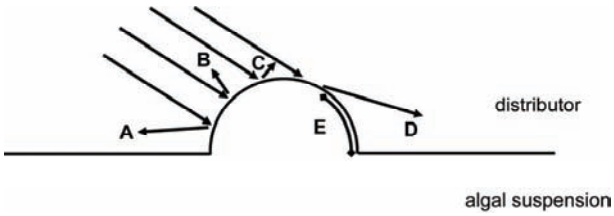

Figure 3. Incident angles on a hemisphere.

Figure 3 shows this 2-dimensional projection of a hemisphere with some possible incident angles. There is a certain part of the hemisphere where the sunlight cannot strike; i.e. the shadow side of the hemisphere, represented by E. The direction in which light can possibly reflect can be split up in two parts; the first one being reflections away from the surface, reflections B and C, the second being reflections towards the surface, reflections A and D. It is unclear which surface structure the light encounters that is reflected towards the surface on which the hemisphere is located, because, as explained before, the hemispheres are a tool to simulate the reflection on the sandblasted surface and have no actual area. In this study light that is reflected towards the surface is assumed to refract out of the sandblasted distributor surface.

To calculate the path of a ray after reflection, the angle of incidence on the sandblasted surface needs to be known. Figure 4 shows an enlarged hemisphere

on the light distributor and an enlarged ray represented by arrows R. The incident angle on the distributor surface is represented by angle δ. The number of possible incident angles on the imaginary hemisphere is thus angle δ plus 90°.

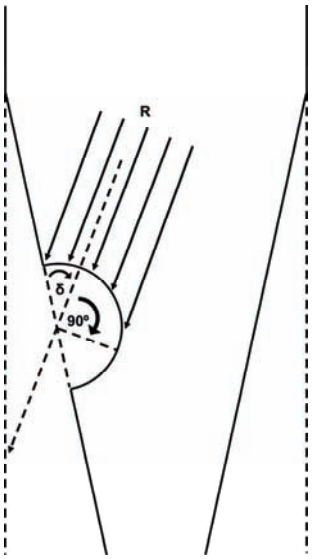

Figure 4. Incident angles on an enlarged hemisphere on the sandblasted surface of the distributor.

Each ray strikes a large part of the surface of the hemisphere and therefore the energy content of the ray has to be divided over several different incident angles on the 2-dimensional hemisphere. Again, a finite number of reflection and refraction events are required for the ray tracing simulation. Therefore these events are traced per whole degree on the hemisphere. The energy associated with a certain angle and the corresponding reflection-refraction event depends on the cosine of that specific incident angle on the hemisphere with regard to the sum of the cosine of all possible incident angles on the hemisphere (Equation 3).

$$\phi_{angle} = \cos(angle) * \frac{\phi_{ray}}{\cos(-\delta) + \cos(-\delta + 1^{\circ}) + ... + \cos(90^{\circ} - 1^{\circ}) + \cos(90^{\circ})} \quad \text{(W)}$$

$$\phi_{angle} = \cos(angle) * \frac{\phi_{ray}}{\sum_{-\delta}^{90} \cos(angle)} \quad \text{(W)}$$

Hence: $\sum_{-\delta}^{90} \phi_{angle} = \phi_{ray}$ (W)

Equation 3

After each reflection-refraction event the amount of refracted light is determined and used to calculate the light intensity on the distributor at that position. The reflected remaining radiant flux is considered to be a new ray and is traced to the next encounter with an imaginary hemisphere on the opposite surface of the distributor. Based on the location of the initial incident ray and the direction of reflected rays, the locations where the reflected rays strike the opposite surface are precisely calculated. As a result, the light intensity distribution over the distributor surface can be determined using the amount of refracted light energy at all locations on the light distributor.

The reflections away from the surface can be split up in two parts. Light can reflect downwards or upwards into the distributor. A part of the upwards reflection will not come in contact with the sandblasted surface on the opposite side of the distributor, because it reflects upwards out of the distributor. These rays will reflect internally within the light guide and will be lost and are therefore not traced any further.

Materials and Methods

Model validation

Perpendicular propagation of light focused by the lens and captured in the light guide was simulated using the Matlab software program and compared with the measured refraction of light out of real guides. Light was simulated to refract into

an 8 mm wide light guide with a rectangular top part of 70 mm height and a light distributor part of 40 mm height surrounded by air. The simulated results are compared to the light intensity measured on the distributor surface. A smooth as well as a sandblasted distributor surface was simulated.

Light measurements at the distributor surface

Light was focused on top of the light guide by a halogen lamp and ellipse-shaped reflector (Figure 5). The validation was performed in air, because small underwater light sensors were not available. Validation in air also validated the under water situation, because the simulation was adjusted for the refractive index of air or water. Light entered the light guide perpendicularly relative to the guide length so that it reflected within a vertical 2-dimensional plane within the guide.

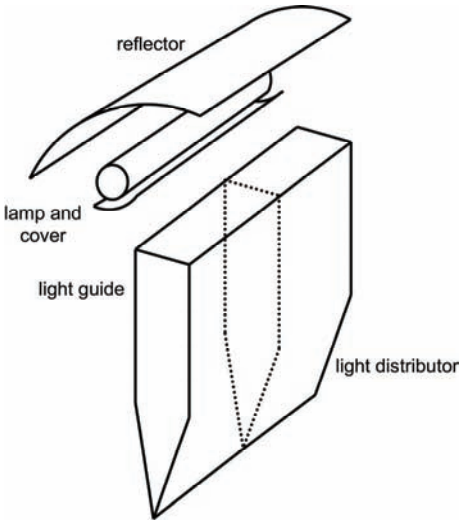

Figure 5. Halogen lamp and reflector that can rotate over the light guide to resemble focusing of sunlight by the Fresnel lens.

Based on the fact that an ellipse has two points of focus, an ellipsoid reflector was designed to focus light into a window of 55 degrees, as shown in Figure 6. A halogen lamp is placed in one point of focus and the top of the light guide in the other. The reflector is shaped such that the distance between the two points of

focus is equal to the focal distance of the lens. Direct light from the lamp to the light guide is blocked, to assure only light from the reflector enters the light guide. The simulation results are corrected for the angles of focus that are blocked by the lamp cover. The lamp and reflector assembly could rotate over the light guide to mimic the rotation of the lens.

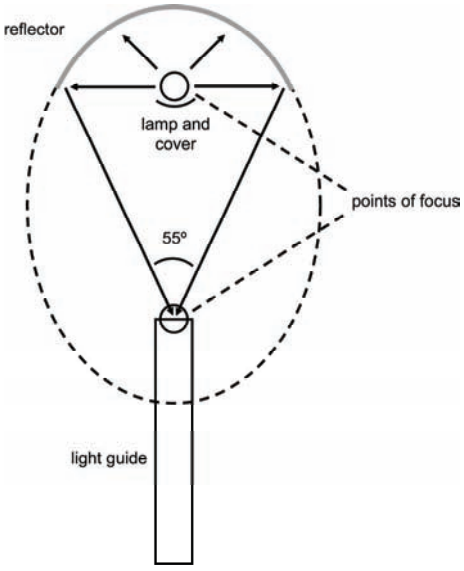

Figure 6. An ellipsoid reflector, focusing light in a window of 55°.

The light intensity was measured using three small 2-π photodiodes (Ø=1.4 cm) facing the distributor surface in a dark room and covering the photodiode from residual stray light of the lamp. Figure 7 shows the measuring positions on the distributor surface. Due to the size of the photodiode, measuring positions AL and AR (Figure 7) cover a fraction of the light guide. However, no light refracts out of the rectangular light guide and all measured light at positions AL and AR is attributed to the surface fraction of the triangular distributor. The intensity was measured at 3 positions over the length of the distributor at 3 different heights on both the left and right side of the distributor (Figure 7). It sums up to 18 measurements for one distributor to correct for deviations in the shapes of both light guide and distributor. In addition, five light guides – distributor combinations were used to validate the model to further reduce the effect of differences in shape

in these hand made guides. The small photodiodes were calibrated against a LI-190SA quantum sensor (LI-COR Biosciences, Lincoln, USA). A smooth as well as a sandblasted distributor surface was measured and evaluated.

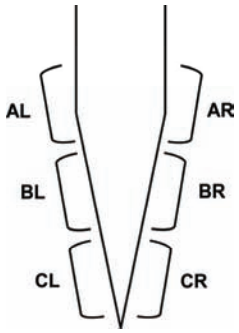

Figure 7. Light measuring positions on the light distributor.

Simulation of the distribution of refracted light out of the distributor

Two light guides, one with a width of 8 mm and one with a width of 16 mm, but having the same height of 70 mm for the rectangular top part and 40 mm for the distributor, were simulated. The reflection and refraction pattern inside the guide and distributor were calculated and the light intensity at the distributor surface was determined. These simulations were done for distributors with a smooth and a sandblasted surface assuming light enters the guide perpendicular with respect to the length of the light guide. However, during most of the day sunlight does not enter perpendicular to the length of the guide. The influence of the solar angle was simulated using the same model.

Results and Discussion

Simulated amount of light loss during capturing of light into the light guide

In focusing of light by the Fresnel lens, a fraction of light will reflect away on the lens surface and is lost. To calculate the total amount of reflection on the lens, the incident angle of sunlight on the lens (φ) and the specific angle on the prisms, as

shown in Figure 2, have to be combined. The influence of the prisms on the amount of reflection is small. The maximum amount of reflection of light perpendicular to the length and width of the lens surface was 8.0% in passing the prism, compared to 7.6% on the flat surface in the middle of the lens. Therefore, the lens was assumed to be flat and only the angle of the rays on the lens in the length direction was taken into account in calculating the percentage of reflection in passing the lens. The amount of reflection of light passing the lens, based on φ, is shown in Figure 8. The percentage of reflection has its minimum value of 7.6% over a broad range of incident angles. But, reflection increases steeply at increasing incident angles from the normal on the lens.

In refraction of focused light into the guide, the rays encounter one air-PMMA interface, resulting in additional reflection losses as shown in Figure 8. Since only one interface is passed, a lower percentage of reflection is obtained.

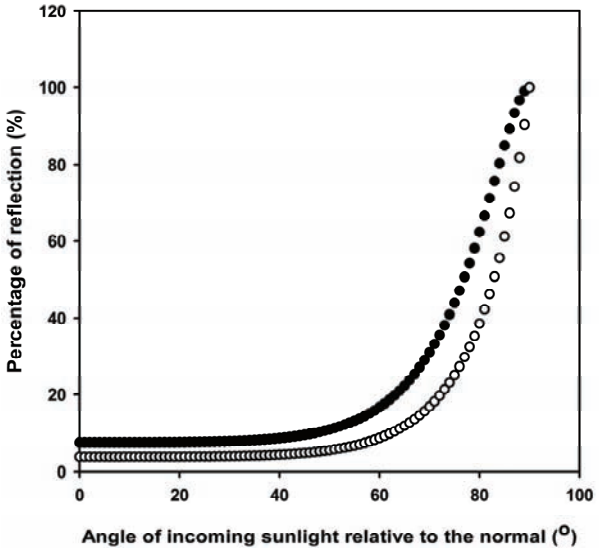

Figure 8. Percentage of light that reflects in passing the lens (closed symbols) and in refracting through the top of the light guide (open symbols) at different incoming angles.

Simulated reflection and refraction inside the light guide and distributor

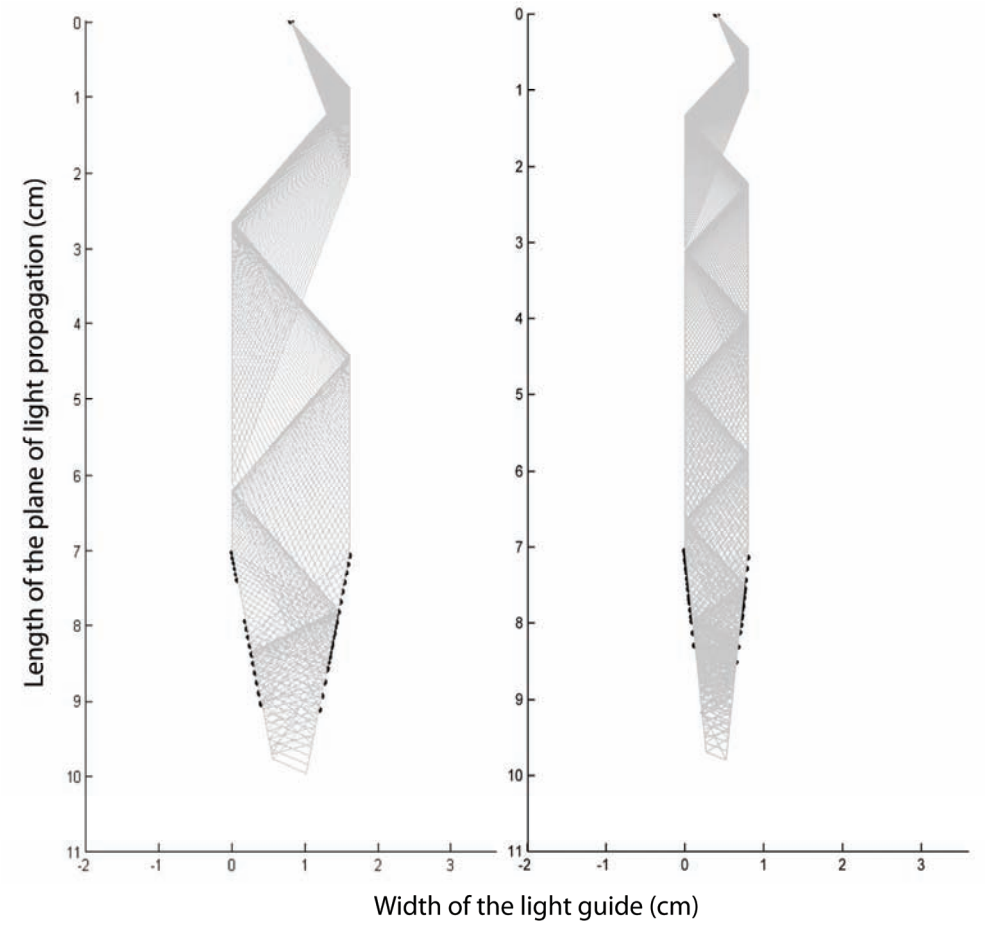

Figure 9. Simulated reflection into and refraction out of a 16 mm and 8 mm wide light guide with a smooth distributor surface. Light strikes the guide perpendicularly with respect to the length of the light guide. The light is focused by the lens at an angle of rotation of 60º.

The propagation of captured light is traced within the light guide and redistribution out of the distributor is determined. Figure 9 shows an example of a result of the ray tracing simulation in a 16 mm wide light guide and distributor. In the simulation, light is focused by a lens at an angle of rotation of 60º. Light strikes the top of the guide perpendicularly with respect to the length of the light guide. The

focused sunlight enters through the top of the light guide exactly in the middle. The angle of each specific ray inside the light guide is calculated using Equation 3 and Snell's law. A fraction of the radiant flux reflects from the light guide (see Figure 8), which is shown by the black mark on the point of entry. The 55 rays of sunlight, represented by the gray lines, propagate downward by internal reflection on the light guide – air interface. No light leaves the guide at this stage, hence the absence of the black marks on the outside of the rectangular part of the light guide. As soon as the light hits the surface of the triangular light distributor surrounded by the algal suspension, light leaves the light guide. Radiant flux refracts out of the distributor, shown by the black marks on the distributor surface. The grey lines propagate further downward until all radiant flux has refracted out of the distributor. The black marks are only shown when more than 1% of the radiant flux of the original ray refracts out of the distributor.

Model validation

The measured and simulated values for the light intensity distribution are compared in Figure 10 and 11. Figure 10 shows the measured and simulated results for the light intensity leaving the smooth light guide at the positions indicated in Figure 7. The focused light enters at different rotation angles of the lens or lamp; a small angle corresponds to a more perpendicular entry of focused light into the guide. The general pattern of the light intensity over the surface of the light guide fits the measured results well. However, deviations exist due to non perfect focusing of light by the ellipse shaped reflector and reflection of light from the small metal plate shielding the light guide from light directly from the lamp (Figure 5). Instead of the modeled perfect line of focus, the reflector produces a wider line of focus covering a large part of the upper surface of the light guide. A 12 mm diameter linear tungsten halogen lamp was used that showed a bright light radiating wire throughout the measurements. The diameter of this wire was approximately 1 mm. In case of perfect focus of this light, the line of focus on the light guide would also be approximately 1 mm.

This wide line is the cause that a fraction of the light is not focused on top of the light guide at large incoming angles. This explains the deviation between modeled and measured light intensities at the rotation angles of 60° and 75° where the modeled results are consistently higher than the measured light intensity (BR and BL in Figure 10). The line on top of the guide of sunlight focused by the lens on the actual GSC also has a width of 2 to 6 mm and will therefore show results in-between the results of the lamp and model. Stray light causes the measured results to deviate from the modeled results in case the light intensity calculated by the model is zero. Taking into account the fact that the model simulates a perfect situation, it gives a good approximation of local light intensities leaving the light guide.

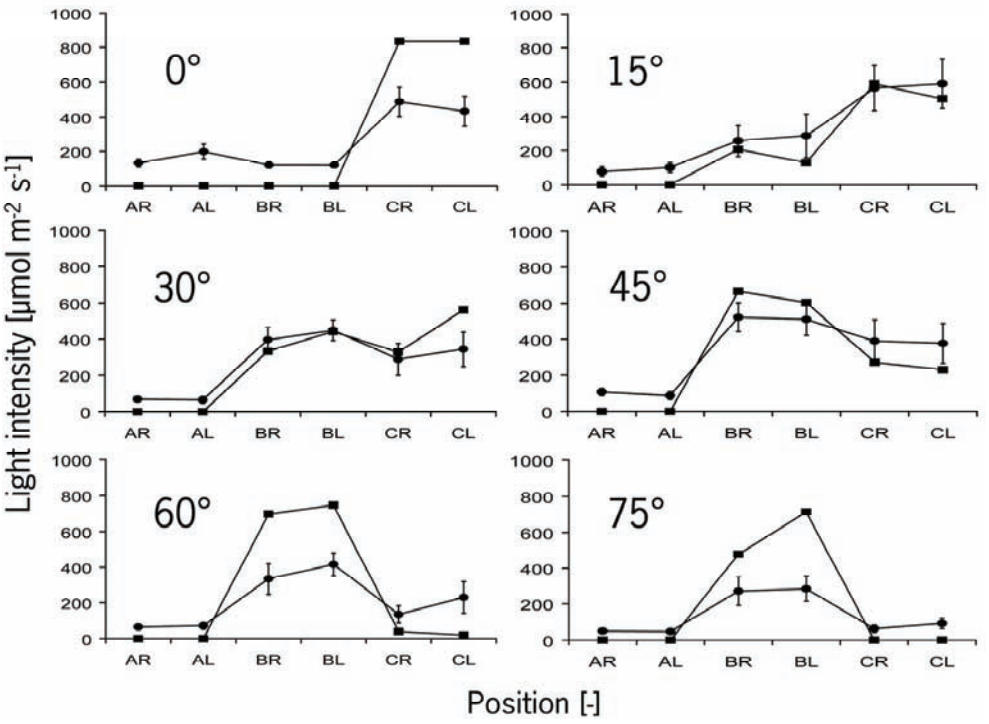

Figure 10. Light intensity leaving the smooth light guide at different rotation angles of the lens (simulated; square symbols) or rotation of the lamp (measured; round symbols).

The simulated results for the sandblasted light guide surface (Figure 11) show a similar trend to the measured results, taking into account the non perfect focusing by the ellipse reflector. The differences in the results, especially for positions CL and CR can be attributed to the underestimation of the reflection downwards due to the 2-dimensional representation of a 3 dimensional hemispherical dent, as explained in Appendix 1.

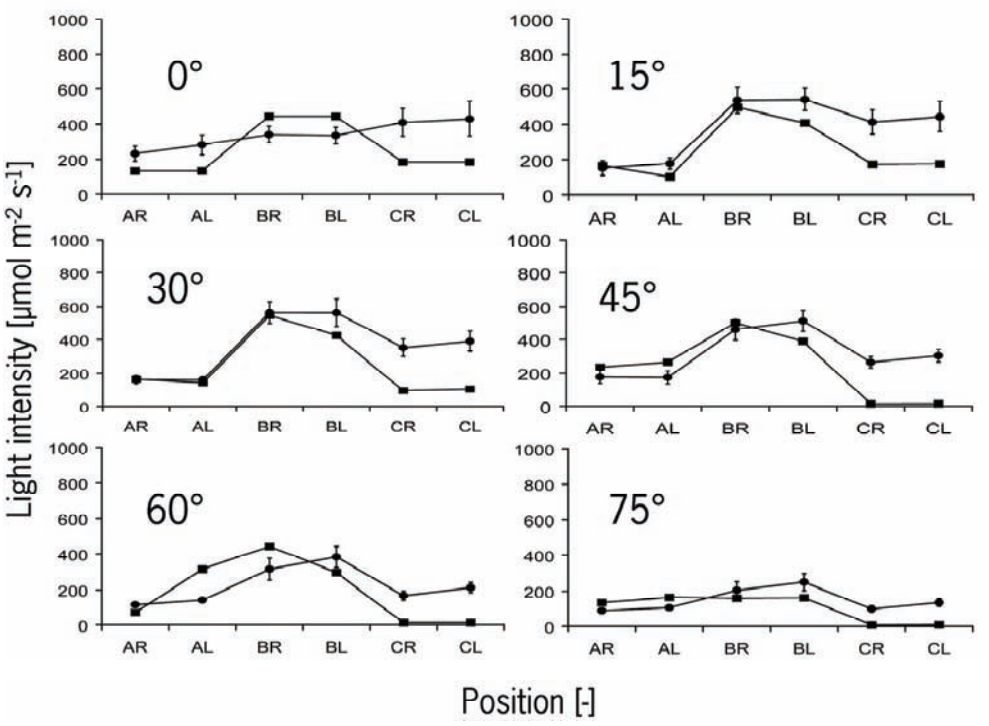

Figure 11. Light intensity leaving the sandblasted light guide at different rotation angles of the lens (simulated; square symbols) or rotation of the lamp (measured; round symbols).

The result of the 2-dimensional simulation underestimates the amount of light that reflects downward inside the distributor, especially at incident angles more perpendicular to the width of the light guide. The underestimation will be more apparent when the light guide is surrounded by air as can be seen in the results of the validation experiments (Figure 11). Apart from this weakness, the measured results for the smooth as well as the sandblasted distributor surface surrounded

by air (Figure 10 and 11) show the same trend as the modeled results. Therefore local light intensities on the distributor surface surrounded by the algal suspension can be estimated by the relatively simple 2-dimensional approach.

Simulated distribution of light refracted out of the guide submerged in the algal suspension: the effect of guide dimensions and surface structure

The validated model is used to do a more detailed investigation into the influence of changes in the dimensions of the guide and the influence of sandblasting the distributor surface on the light distribution out of the distributor.
If the surface of the distributor is smooth, most of the light will either completely refract out of the guide or completely reflect further into the guide on the first encounter of the rays with the interface of the distributor and algal suspension. At angles of 63° or larger from the normal on the smooth distributor-suspension interface the total ray will reflect on the interface. At smaller angles light will almost completely refract out of the guide. At an angle of 53°, for example, 97.5% of the light energy will refract out of the guide and only the remainder reflects internally. Gradual leakage of light from the guide into the algal suspension during the day is thus not possible due to the varying position of the sun in the sky.
Total internal reflection does not occur on the sandblasted surface, because the original ray on the distributor surface strikes the hemisphere at a multitude of angles, causing a large fraction of the radiant flux to refract into the algal suspension.

The dimensions of the light distributor part of the light guide are of influence on the amount of light leaving the guide and on the uniformity of light distribution. The reflection and refraction pattern in the light guide changes with the ratio of width to height of the distributor, because the angles of incidence of the rays on the distributor surface change.

A wider light guide causes a decrease in the incident angle of the incoming ray relative to the normal of the interface, causing light to refract out of the guide. It also causes the triangular bundle of focused rays to be more spread out over the

distributor surface in the wider light guide, especially at larger angles of rotation of the lens. This can be seen by comparing the propagation in the guides shown in Figure 9. This is also shown in Appendix 2, which shows the radiant flux distribution on the distributor surface for two distributors with different width and surface structure. Since light is more spread out over the surface of the wide distributor it causes a somewhat more uniform distribution of the radiant flux over its surface at rotation angles of the lens of 30º and larger. In a narrow distributor, at rotation angles of 15º and 30º, a large fraction of the rays will strike the smooth distributor-suspension interface at an angle larger than 63º from the normal and will therefore cause internal reflection. A larger fraction of the radiant flux will reflect internally and will therefore lead to a more uniform distribution over the distributor surface. However, at a rotation angle of 0º too much internal reflection occurs on the smooth surface causing again a decrease in uniformity of light distribution.

Sandblasting the surface does not result in a more uniform distribution of refracted light at larger rotation angles of the lens. In this case most of the rays will have a small angle of incidence relative to the normal on the hemispheres on the sandblasted surface, causing light to refract out of the guide. At rotation angles of the lens of 15º and 30º on the narrow light guide, sandblasting causes less uniform distribution, because the amount of internal reflection is diminished due to the hemispheres on the distributor surface. Reflection on the hemispheres causes less light to propagate downwards compared to internal reflection in the smooth distributor. However, the results shown in Appendix 2 underestimate the reflection downwards into the sandblasted distributor as explained in Appendix 1. But, no drastic improvement in the distribution can be expected, since the majority of the light will refract out of the distributor upon the first encounter with the hemisphere.

In the wider light guide the sandblasting of the distributor also causes less internal reflection at rotation angles of 15º and 30º and thus more reflection out of the top of the distributor. But, because the triangular bundle of focused rays is more

spread out over the distributor surface, the distribution is more uniform compared to the narrower light guide.

The distribution at a rotation angle of 30° is better on the smooth distributor surfaces, compared to the sandblasted surfaces and also the light intensity on the complete distributor surface is less than the solar intensity. However, in all other situations a wider sandblasted distributor is preferred.

Simulated reflection and refraction pattern based on the position of the sun

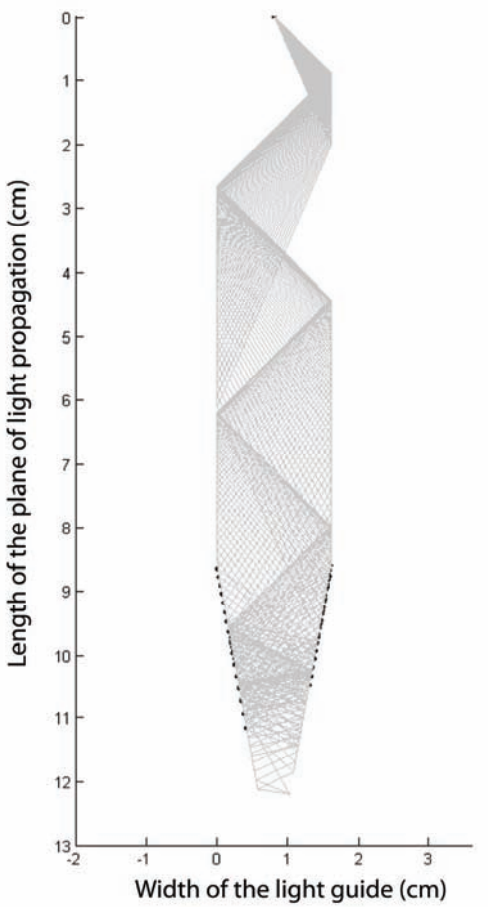

Figure 12. Simulated reflection in and refraction out of a 16 mm wide light guide with a smooth surface. Light strikes the guide at an angle of 60° with respect to the length of the light guide (also see Figure 1) the light is focused by the lens at an angle of rotation of 60°.

The previous discussion was based on results of simulations where light entered the guide perpendicular to the length of the guide with the lens rotating over the light guide. When the position of the sun is taken into account, the dimensions of the 2-dimensional plane of light propagation (illustrated in Figure 1) will change as can be deduced from Figure 12 when compared to Figure 9. The same simulation procedure is used to calculate the reflection and refraction pattern in the guide, taking into account its new dimensions. Figure 12 shows the pattern for light focused by the Fresnel lens that strikes the top of a smooth light guide at a rotation angle of 60º relative to the width and a 60º angle relative to the length. The plane in which the rays are traced is similar to the situation in Figure 9. Using Snell's law, the angle of refraction of the plane is calculated to be 35.5º relative to the length of the light guide (also see Figure 1). Therefore the plane increased in length by a factor of $\cos^{-1}(35.5º)$.

The refraction pattern inside the light guide changes when the orientation of the plane of light propagation within the light guide changes. This has no effect on the angle of incidence on the surface in the rectangular top part of the guide, where light still propagates through internal reflection. However, when the light distribution on the distributor surface for the 16 mm wide light guides in Figure 9 and 12 are compared, the gap on the upper left surface of the distributor in Figure 9, where light does not refract out of the guide, is gone in Figure 12. If light does not enter perpendicularly, the plane in which light rays are traced increases in length. The increase causes light to reflect at a different location in the guide changing the reflection and refraction pattern. The increase in length also has an influence on the imaginary dimensions of the distributor part in the 2-dimensional plane of light propagation. This part also becomes longer, creating a relatively narrower distributor and consequently changing the reflection and refraction pattern. A narrower distributor leads to a less uniform distribution of light over its surface when light enters less perpendicular with respect to the width of the guide. To have the best light capturing efficiency and most uniform distribution of light, a more perpendicular entry of light is desired.

Predicting the distribution of light out of the distributor at forehand based on the dimensions of the light guide and distributor is difficult because dimensions of the plane of light propagation change with changing position of the sun. It results in a continuously changing reflection pattern not only in the distributor, but also in the rectangular top part. Therefore, optimal dimensions of guide and distributor cannot be predicted based on the results of a few situations. Extensive ray tracing of sunlight is needed to know the light distribution on the distributor surface throughout the day. Based on the results for all angles of elevation and azimuth of the sun, a balanced choice for the dimensions of the light guide and distributor can be made to have the best distribution of light on the distributor surface.

Conclusions

Local light intensities at the surface of the distributor in the Green Solar Collector can be calculated trough ray tracing of focused direct sunlight. Results of simulations of refraction of light out of the distributor surface show the same trend as the measured results. The light capturing efficiency into the light guide is high and almost all captured light can be distributed into the algal suspension. However, from the results it also becomes clear that a uniform distribution of light over the entire surface of the distributor cannot be achieved during the entire day due to the large variation in incident angles of sunlight. At light entering at small angles from the normal, the uniformity of light distribution is much better. Scattering of light by the microalgae will further distribute the light throughout the algal suspension, especially at low biomass concentrations. The GSC, however, is designed for cultivating the algae at high biomass concentrations and in this situation light will be completely absorbed at several millimeters from the distributor surface. A uniform distribution is required to supply the correct light regime in this case.

A specific surface structure, other than the triangular shape and the sandblasted surface, might help to overcome the problems of non-uniform irradiation as mentioned by Gordon (2002). But, these tailor-made structures will only work with constant incoming angles of light, such that light always strikes the distributor

surface at the same position. However, the focused sunlight strikes the distributor surface at varying positions during the day and the tailor-made structures can therefore not be used in the Green Solar Collector.

During the day, however, the position of the sun in the sky changes, changing the incident angles on the lens and light guide. These angles determine the light capturing efficiency, which depends on location of the GSC, orientation with respect to the sun, and date and time. As can be seen in Figure 8, the reflection on the lens and light guide is at its minimum at an angle of 40º and less. The same applies for the loss on the light guide, which is also lowest at rotation angles of 45º and smaller. If Figure 8 and Appendix 2 are combined, it is clear that capturing of light at low elevation angles of the sun is poor. At elevation angles of 45º, the total capturing efficiency of direct sunlight into the light guides already is 80% and it increases up to 89% for a perpendicular focusing of sunlight. The GSC is therefore best suited for operation at locations at low latitudes, where the sun quickly rises to high elevation angles and the intensity of direct light is highest.

Our work clearly shows that the Green Solar Collector is most suited for operation at locations at low latitudes. At low latitudes, the sun rises and settles quickly and has a high elevation angle during most of the day. In this situation it is especially beneficial to reduce the (over-) saturating intensity of direct sunlight before illuminating the microalgae, since it results in an increased productivity compared to exposure to full sunlight as shown by Qiang et al.(1998a; 1998b). If the GSC is located such that the lens stretches from east to west the light distribution will be most uniform, because during the larger part of the day light enters at an angle of less than 30º from the normal. It results in an efficient capturing (Figure 8) and an increased uniformity of sunlight distribution out of the 16 mm wide sandblasted light guide at intensities which are about equal or less then the intensity of sunlight.

Appendix 1

Reflection and refraction on a 3-dimensional hemispherical dent

The ray of sunlight can strike at a number of locations on the hemisphere as previously explained in Figure 4. It was assumed that a ray of sunlight will always strike the hemisphere on the circular band formed by the projection of the hemisphere on the plane of light propagation (also see Figure 1). But, the ray can also strike the hemisphere at other locations as illustrated by the dotted arches in Figure 13.

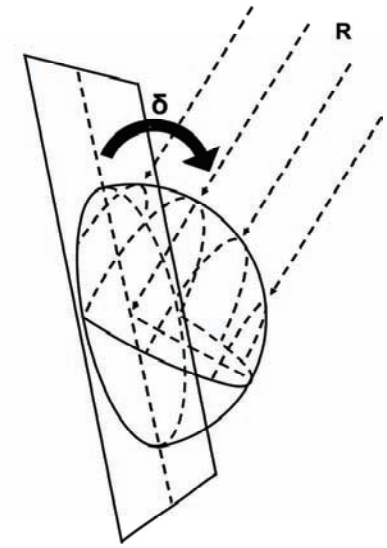

Figure 13. 3-Dimensional representation of a hemispherical dent on the sandblasted distributor surface.

The difference in incident angles on the hemisphere surface in this more realistic 3-dimensional situation compared to the 2-dimensional approach results in a change in reflection and refraction pattern. However, the difference is small enough to allow the use of the more simple 2-dimensional approach as explained below.

Figure 14 shows circular bands that correspond with equal incident angles (ε) when a vertical ray strikes the surface of the hemisphere. The vertical ray can be seen as an incident ray of light perpendicular on the distributor surface (δ = 90°, Figure 13). The amount of radiant flux associated with a certain incident angle on the hemisphere surface is calculated using Equation 4. It depends on the cosine of ε and the length of the circular band around the hemisphere at that angle, which changes with the sine of ε (Figure 14).

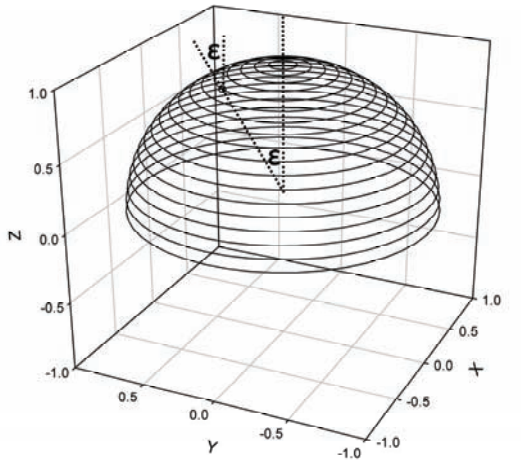

Figure 14. Circular bands on a hemisphere corresponding to equal incident angles when struck by a vertical ray (bands at a 5° incident angle interval).

$$\phi_{\varepsilon} = \cos(\varepsilon) * \sin(\varepsilon) * \frac{\phi_{ray}}{\sum_{0}^{90} \cos(\varepsilon) * \sin(\varepsilon)} \quad \text{(W)}$$

Hence: $\sum_{0}^{90} \phi_{\varepsilon} = \phi_{ray}$ (W) Equation 4

Figure 15 shows the percentage of the radiant flux that reflects away from the hypothetical 2- or the real 3-dimensional hemisphere, considering a ray which strikes the complete hemisphere surface. The percentage of reflection is calculated for the situation when the hemisphere is on the distributor – algal suspension

interface. The energy associated with each incident angle on the 2-dimensional hemisphere is calculated using Equation 3 (δ=0). The energy associated with each incident angle on the 3-dimensional hemisphere is calculated using Equation 4. The reflection at each incident angle is calculated using Snell's law and Fresnel's formula (Appendix 1). The smaller incident angles that incorporate most of the light energy will almost completely refract out of the distributor as can be seen from Figure 15. From an incident angle of around 55° on the hemisphere, reflection of light energy increases. Upon further increase in angle the amount of reflection decreases again due to the decrease in energy content associated with that angle.

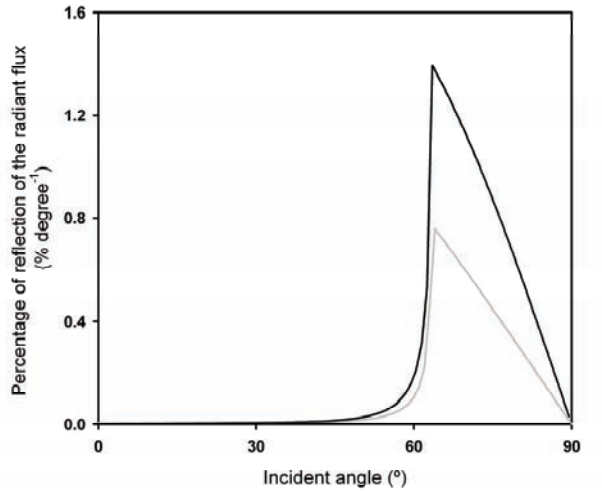

Figure 15. Percentage of reflection on a surface of a 2-dimensional hemisphere (gray) and on a 3-dimensional hemisphere (black) depending on the angle from the normal (90°-ε) on the surface.

If angle δ on the distributor surface (Figure 13) is 90°, 12% of the radiant flux reflects in the 2-dimensional case and 22% in the 3-dimensional case. The 10% difference is due the fact that in the 3-dimensional case there is a larger hemisphere surface fraction where light strikes at a large angle. If sunlight enters the light guide more perpendicularly with respect to the width of the guide, angle δ will be smaller and the ray can only strike on a fraction of the hemisphere surface. This fraction covers less surface area where light strikes at a large angle,

decreasing the total amount of reflection on the 2- as well as the 3- dimensional hemisphere surface (Figure 15).

If angle δ is more perpendicular however, the 2-dimensional representation coincides most with the real 3-dimensional situation, because the direction of the reflected light needs to be taken into account. In the 3-dimensional situation the reflected light at δ approaching 90° is more directed towards the surface of the distributor, because radiant flux reflects at angles larger than 45° (Figure 15) resulting in reflected light directed towards the distributor surface which refracts out of the distributor (also see Figure 3 and 13). In this case, in both the 2- and 3-dimensional representations all radiant flux will refract out of the guide, either by refraction at small incident angles or reflection towards the distributor surface.

When angle δ becomes smaller, the difference between the 2-dimensional representation and the real 3-dimensional situation is larger. Although less light will reflect on the hemisphere surface compared to the perpendicular case, the reflected light on the hemisphere is not directed towards the distributor surface, but is directed downwards into the distributor. Consequently, in the real 3-dimensional situation more light will reflect downwards into the distributor as compared to the 2-dimensional representation. The worst case scenario for difference between the 2-dimensional representation and the real 3-dimensional situation occurs when angle δ is 0°. In this situation the amount of reflection is the same as in case δ is 90°, but none of the reflected light is directed towards the distributor surface; it all reflects further downward into the distributor.

Reflection appears to be low anyhow since a minimum of 78% of the radiant flux will refract out of the distributor on the first encounter with the sandblasted surface in the 3-dimensional representation. In the 2-dimensional representation a minimum of 88% of the radiant flux refracts out of the distributor. Taking all the above into consideration, the more simple 2-dimensional approach provides a useful simulation of the real 3-dimensional sandblasted surface surrounded by the algal suspension.

Appendix 2

Table I. Simulated light distribution over the left and right vertical surface of the distributor in the algal suspension in two different light guides at various rotation angles of the lens.

Angle of rotation of the lens	Fraction of the light distributor surface	Smooth surface				Sandblasted surface			
		8 mm wide		16 mm wide		8 mm wide		16 mm wide	
		left	right	left	right	left	right	left	right
0°	1	0	0	568	568	1841	1841	1595	1595
	2	472	472	125	125	1715	1715	1620	1620
	3	1701	1701	919	919	1776	1776	1245	1245
	4	2482	2482	3071	3071	1079	1079	1302	1302
	5	2299	2299	2123	2123	431	431	991	991
	Refracted into the algal suspension	88.80		88.80		88.24		88.28	
	Loss on top of the guide	3.60		3.60		3.60		3.60	
	Reflection backwards	-		-		0.56		0.52	
15°	1	127	1139	781	240	1852	2561	1827	1136
	2	580	1396	125	1466	1707	2177	1619	1827
	3	1397	1286	429	1851	1117	1523	1217	1497
	4	2075	1626	1693	3734	856	1027	1276	1319
	5	2011	2155	2123	1132	431	431	991	566
	Refracted into the algal suspension	88.72		88.72		88.17		88.22	
	Loss on top of the guide	3.68		3.68		3.68		3.68	
	Reflection backwards	-		-		0.55		0.50	
30°	1	1565	1854	781	1444	2818	3255	931	2310
	2	1550	1926	1573	1466	2419	2159	2349	2082
	3	1398	1322	1255	1626	855	860	1712	1427
	4	1587	896	1673	2171	347	574	850	1032
	5	910	711	527	1001	294	63	600	162
	Refracted into the algal suspension	88.24		88.24		87.75		87.84	
	Loss on top of the guide	4.16		4.16		4.16		4.16	
	Reflection backwards	-		-		0.49		0.40	
45°	1	3319	3031	3055	1444	4070	3955	3170	1414
	2	2023	1946	1808	2325	2379	1904	2556	2248
	3	1152	1322	1016	1492	390	363	1640	981
	4	242	342	105	1906	80	97	92	813
	5	0	0	29	0	35	41	108	114
	Refracted into the algal suspension	86.04		86.04		85.64		85.75	
	Loss on top of the guide	6.36		6.36		6.36		6.36	
	Reflection backwards	-		-		0.40		0.29	
60°	1	3916	4506	2274	1510	3954	4476	2243	1479
	2	1563	1644	1689	4453	1415	1612	1634	4390
	3	217	39	1020	721	99	71	953	708
	4	0	1	37	6	74	68	89	27
	5	0	0	0	0	38	31	77	78
	Refracted into the algal suspension	76.45		76.45		76.14		76.24	
	Loss on top of the guide	15.95		15.95		15.95		15.95	
	Reflection backwards	-		-		0.31		0.21	
75°	1	3550	3439	2274	137	3482	3368	2242	138
	2	508	720	1689	3021	458	664	1631	2982
	3	0	0	970	19	37	42	942	7
	4	0	0	0	0	44	45	6	27
	5	0	0	0	0	26	22	23	78
	Refracted into the algal suspension	52.85		52.85		52.65		52.73	
	Loss on top of the guide	39.55		39.55		39.55		39.55	
	Reflection backwards	-		-		0.20		0.12	
90°	1	2348	1548	1345	137	2304	1519	1327	137
	2	473	208	6	3012	453	190	1	2980
	3	0	0	9	0	5	15	3	2
	4	0	0	0	0	16	33	6	5
	5	0	0	0	0	11	17	23	15
	Refracted into the algal suspension	29.44		29.44		29.35		29.38	
	Loss on top of the guide	62.96		62.96		62.96		62.96	
	Reflection backwards	-		-		0.09		0.06	

The lens focuses sunlight with an intensity of 2500 μmol photons m^{-2} s^{-1}. Values as shown in Table 1 represent the average light intensity in μmol photons m^{-2} s^{-1} over the different surface fractions of the distributor surface. It is divided into 5 equal fractions on the left and right surface. Fraction 1 is the top of the distributor surface and Fraction 5 is the bottom of the distributor surface. The lens is positioned towards the left side of the light guide. Percentage of the total sunlight that refracts into the algal suspension is presented as well as percentage of light loss on top of the light guide and percentage of reflection backwards due to sandblasting of the distributor surface. Light enters perpendicularly on the lens; reflection in passing the lens is thus constant at 7.6% (Figure 8). Reflection on top of the light guide causes light loss at all rotation angles. However at rotation angles of 63º and larger not all light can be focused on top op the light guide, resulting in an increased light loss on top of the guide.

Loss of light on top of the guide increases steeply at larger angles of rotation, similar to Figure 8. However, since the light is focused in a window of 55º, loss of light at rotation angles of 90º is less than 100%, even though a fraction of the focused sunlight is not being focused on top of the guide.

Acknowledgements

This work was financially supported by the EU/Energy Network project Solar-H (FP6 contract 516510).

References

An JY, Kim BW. 2000. Biological desulfurization in an optical-fiber photobioreactor using an automatic sunlight collection system. Journal of Biotechnology 80(1):35-44.

Csögör Z, Herrenbauer M, Perner I, Schmidt K, Posten C. 1999. Design of a photo-bioreactor for modelling purposes. Chemical Engineering and Processing 38(4-6):517-523.

Glassner AS. 1989. An Introduction to Ray Tracing. London: Academic Press. 329 p.

Gordon JM. 2002. Tailoring optical systems to optimized photobioreactors. International Journal of Hydrogen Energy 27(11-12):1175-1184.

Hirata S, Hayashitani M, Taya M, Tone S. 1996. Carbon dioxide fixation in batch culture of Chlorella sp using a photobioreactor with a sunlight-collection device. Journal of Fermentation and Bioengineering 81(5):470-472.

Perner-Nochta I, Posten C. 2007. Simulations of light intensity variation in photobioreactors. Journal of Biotechnology 131(3):276-285.

Pruvost J, Legrand J, Legentilhomme P, Muller-Feuga A. 2002. Simulation of microalgae growth in limiting light conditions: Flow effect. Aiche Journal 48(5):1109-1120.

Pulz O, Gerbsch N, Buchholz R. 1995. Light energy supply in plate-type and light diffusing optical-fiber bioreactors. Journal of Applied Phycology 7(2):145-149.

Qiang H, Faiman D, Richmond A. 1998a. Optimal tilt angles of enclosed reactors for growing photoautotrophic microorganisms outdoors. Journal of Fermentation and Bioengineering 85(2):230-236.

Qiang H, Zarmi Y, Richmond A. 1998b. Combined effects of light intensity, light-path and culture density on output rate of Spirulina platensis (Cyanobacteria). European Journal of Phycology 33(2):165-171.

Ries H, Segal A, Karni J. 1997. Extracting concentrated guided light. Applied Optics 36(13):2869-2874.

Zijffers JWF, Janssen M, Tramper J, Wijffels RH. 2008. Design process of an area-efficient photobioreactor. Marine Biotechnology 10(4):404-415.

Chapter 4

Photosynthetic yield of algae in panel photobioreactors: True yield and maintenance requirement

Abstract

The biomass yield on light energy of *Dunaliella tertiolecta* and *Chlorella sorokiniana* was investigated in a 1.25 cm and 2.15 cm light path panel photobioreactor at constant ingoing photon flux density (930 μmol photons m^{-2} s^{-1}) using the D-stat cultivation technique. Constant biomass yields of 0.65 ± 0.10 g mol $photons^{-1}$ for *D. tertiolecta* and 0.70 ± 0.10 g mol $photons^{-1}$ for *C. sorokiniana* were observed in both light path reactors over a broad range of biomass concentrations.

The observed biomass yield on light energy appeared to be based on a constant true biomass yield and a constant maintenance energy requirement per gram biomass. Using a simple model, a true biomass yield on light energy of 0.78 g mol $photons^{-1}$ and 0.75 g mol $photons^{-1}$ and a maintenance requirement of 0.0133 mol photons g^{-1} h^{-1} and 0.0068 mol photons g^{-1} h^{-1} were found for *D. tertiolecta* and *C. sorokiniana,* respectively. The steep decrease in observed yield at low light supply rates could thus be explained by the maintenance energy requirement of the large amount of biomass present at low dilution rates. The true biomass yield on light energy was assumed to differ from the theoretical maximal yield by a constant factor representing light energy losses.

Introduction

Microalgae represent a sustainable source for photoautotrophically produced compounds for the biofuel, food, feed, and pharmaceutical industry. Maximization of algal biomass production on sunlight is needed to make commercial bulk production of lower value products economically feasible. High volumetric productivities and high yields on sunlight are needed to decrease production system volumes and to lower production costs. This can be fulfilled by cultivating the microalgae at high light intensities in photobioreactors with a high reactor surface to volume ratio, i.e. a short optical path.

High photosynthetic efficiencies at high light intensities were obtained in dense cultures of the cyanobacterium *Arthrospira platensis* in short light path (1.3 cm and 2.8 cm) reactors that were turbulently mixed (Hu et al. 1996; Qiang et al. 1998a; Qiang and Richmond 1996; Qiang et al. 1998b). After recalculation of the presented data, the photosynthetic efficiency showed a maximum value of around 1.5 grams of biomass (dry matter) produced per mol of photons (g mol photons^{-1}) at incident light intensities up to 2000 μmol photons m^{-2} s^{-1}. This high efficiency was attributed to short exposure times to (over-) saturating light intensities at the reactor surface due to turbulent mixing. However, the same effect was not observed for the cyanobacterium *Anabaena siamensis* and the microalgae *Monodus subterraneus* grown under the same conditions (Hu et al. 1996). The maximum productivity obtained was 30% (*A. siamensis*) and 67% (*M. subterraneus*) of the productivity obtained with *A. platensis*. Other studies on microalgal cultivations in reactors with a short light path (between 1 cm and 3 cm) operated at high light intensities also showed lower photosynthetic efficiencies. Meiser et al. (2004) found a maximum yield of 0.5 g mol photons^{-1} for the diatom *Phaeodactylum tricornutum* at a light intensity of 1000 μmol photons m^{-2} s^{-1}. Hu et al. (1998) obtained a yield of 0.5 g mol photons^{-1} cultivating the microalga *Chlorococcum littorale* at a light intensity of 2000 μmol photons m^{-2} s^{-1}. Richmond et al. (2003) obtained a maximum yield of 0.6 g mol photons^{-1} cultivating the microalga *Nannochloropsis* sp. at a light intensity of 2000 μmol photons m^{-2} s^{-1}.

The biomass yield of *A. platensis* reported by Qiang and coworkers is close to the theoretical attainable maximum biomass yield on light energy. This can be calculated using the stoichiometric reaction equation for biomass formation on carbon dioxide, water and nitrate or urea (Appendix 1). Based on growth on nitrate a maximum yield of 1.5 g mol photons^{-1} can be achieved and on urea a maximum of 1.8 g mol photons^{-1}. The high yields reported by Qiang were remarkable, because such yields were generally only obtained at low light intensities. Under high light intensities, increased light saturation and possibly photoinhibition was usually observed.

In most cases, the yield values obtained for the photoautotrophic organisms mentioned before were recalculated from results obtained during batch cultivations or semi-continuous cultivations. The yield of biomass on light energy, however, is best investigated in chemostat cultivations where the organisms are acclimated to the conditions in the bioreactor with no biomass accumulation. In this case, the biomass yield can be directly related to a specific light availability. A disadvantage of chemostat cultures, on the other hand, is the number of conditions that can be determined in time. Achieving steady state conditions can take a considerable amount of time when large changes in dilution rates are made. By slowly changing the dilution rate in a photobioreactor using the A-stat method as described by Paalme et al. (1995), the microalgal productivity can be determined for a wide range of dilution rates in less time compared to performing a number of chemostat cultivations. The continuous rate of change of the dilution rate has to be chosen such that the microalgae are able to acclimate to the continuously changing conditions in the photobioreactor. In this way the system can be considered to be in a so called pseudo steady state and results represent a real steady state situation when corrected for biomass accumulation.

In this study, the yield of biomass on light energy at saturating light levels was investigated through cultivations of two different microalgae in flat-panel photobioreactors of a light path of 1.25 cm and 2.15 cm. An incident light intensity of approximately 930 µmol photons m^{-2} s^{-1} was used. The biomass yield on light energy was investigated through a reversed A-stat cultivation, i.e. a D-stat

cultivation as described by Hoekema et al. (2006). The marine microalga *Dunaliella tertiolecta* and the freshwater microalga *Chlorella sorokiniana*, were cultivated at decreasing dilution rates. Differences in biomass yield on light energy were expected, because of distinct differences between the microalgae. They differ in: cell wall composition, motility, reported maximum growth rate, and salinity of the cultivation medium. *D. tertiolecta* was used as a model for marine microalgae and was used before in a 3 cm light path A-stat cultivation (Barbosa et al. 2005), which will serve as a reference. The freshwater microalga *C. sorokiniana* was chosen because of its high growth rate, and hence high photosynthetic capacity. The maximum reported growth rate for *D. tertiolecta* was 0.11 h^{-1} (Barbosa et al. 2005) and for *C. sorokiniana* 0.27 h^{-1} (Sorokin 1959).

Materials and Methods

Microalgae and reactor startup

Table 1. Operational conditions of the different cultivations.

Alga	Incident light intensity (µmol photons m^{-2} s^{-1})	Illuminated surface area (m^2)	Light path (cm)	Aeration rate (L min^{-1})	Superficial gas velocity (m s^{-1})
D. tertiolecta	933	0.103	1.25	1.0	$6.67 \cdot 10^{-3}$
	990	0.103	2.15	2.0	$7.75 \cdot 10^{-3}$
C. sorokiniana	871	0.103	1.25	1.0	$6.67 \cdot 10^{-3}$
	940	0.103	2.15	2.0	$7.75 \cdot 10^{-3}$

Dunaliella tertiolecta CCAP 19/6B was maintained as a suspended culture in Erlenmeyer flasks containing artificial seawater medium. *Chlorella sorokiniana* CCAP 211/8k was maintained as a suspended culture in Erlenmeyer flasks containing M-8a medium. Prior to the D-stat experiments the algae were cultivated batch wise in the panel photobioreactor, until a sufficient biomass density was reached to withstand the maximum incident light intensity used in the experiments. After increasing the light intensity to the maximum value, chemostat

cultivation was started at 70% to 80% of the maximum growth rate. Table 1 shows the operational conditions of the different D-stat cultivations.

Medium

D. tertiolecta was cultivated in an enriched artificial seawater medium. The ratio between the salts, nutrient, and trace element concentrations were chosen according to the biomass composition determined by Ho et al. (2003). The *D. tertiolecta* medium was designed to support 100 grams of dry weight biomass. *C. sorokiniana* was cultivated on a concentrated M-8a medium, which was based on M-8 medium developed by Mandalam and Palsson (1998). The M-8a medium was estimated to support at least 50 grams of *C. sorokiniana* dry weight biomass. Sodium bicarbonate was added to both media after the pH was set. The medium used in the continuous cultivation experiments was kept under carbon dioxide atmosphere to prevent precipitation of salts. The following media composition was used (M):
D. tertiolecta: 0.42 NaCl, $5.6*10^{-3}$ $MgCl_2$, $3.6*10^{-4}$ $CaCl_2$, $5.3*10^{-3}$ Na_2SO_4, 0.10 KNO_3, $2.0*10^{-2}$ $NaHCO_3$, $6.3*10^{-3}$ NaH_2PO_4, $3.1*10^{-4}$ Na_2EDTA, $1.1*10^{-4}$ $FeCl_3$, $6.1*10^{-6}$ $CuSO_4$, $1.4*10^{-5}$ $ZnSO_4$, $9.5*10^{-8}$ $CoCl_2$, $1.5*10^{-5}$ $MnCl_2$, $1.0*10^{-7}$ Na_2MoO_4.
C. sorokiniana: $4.8*10^{-2}$ $CO(NH_2)_2$, $1.6*10^{-2}$ KH_2PO_4, $4.4*10^{-3}$ Na_2HPO_4., $4.9*10^{-3}$ $MgSO_4$, $2.7*10^{-4}$ $CaCl_2$, $9.5*10^{-4}$ EDTA ferric sodium salt, $3.0*10^{-4}$ Na_2EDTA, $3.0*10^{-6}$ H_3BO_3, $2.0*10^{-4}$ $MnCl_2$, $3.3*10^{-5}$ $ZnSO_4$, $2.2*10^{-5}$ $CuSO_4$, $5.0*10^{-3}$ $NaHCO_3$.

Reactor setup and control

Figure 1 shows a front and side view of the panel reactor. The reactor was built up by transparent polycarbonate sheets held together in a frame similar to the system used by Barbosa et al. (2005). The panel reactors had a width of 20 cm, a height of 60 cm, and a light path as shown in Figure 1 and Table 1.

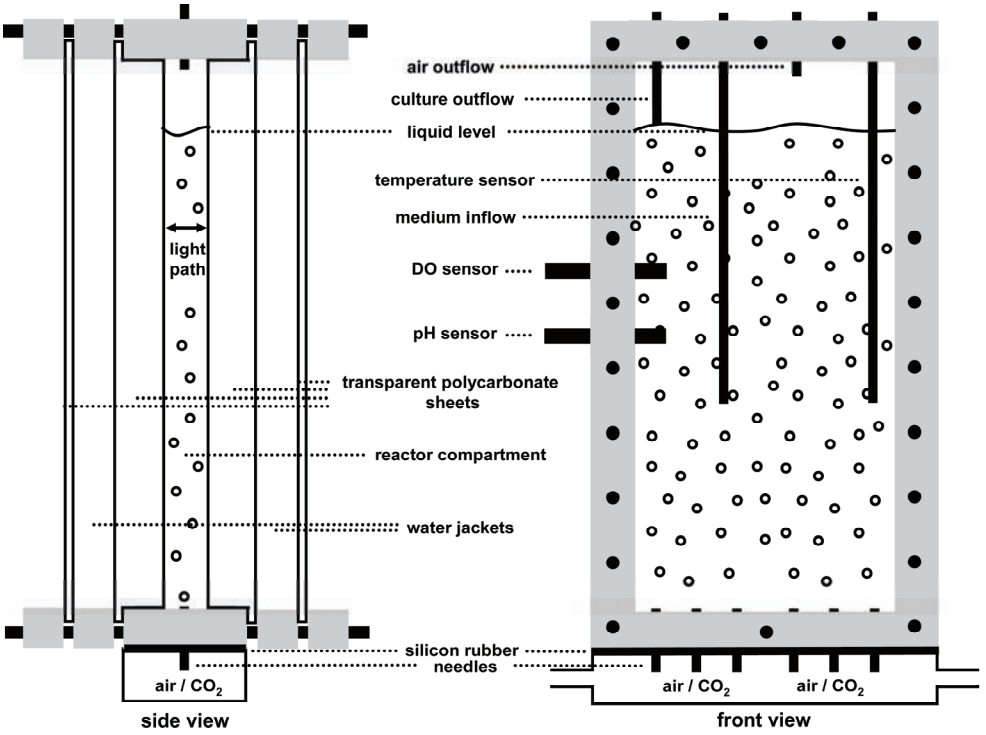

Figure 1. Front and side view of the flat-panel photobioreactor. The light path is determined by the thickness of the transparent polycarbonate sheets placed in the frame and was 1.25 cm or 2.15 cm.

The temperature inside the reactor was measured using a pt-100 and kept constant by an ADI 1030 Bio-controller (Applikon, Schiedam, the Netherlands) controlling the temperature of the cryostat connected to water jackets on both the front and back surface of the reactor. Temperature was maintained at 30 ºC and 37 ºC for *D. tertiolecta* and *C sorokiniana,* respectively. The reactor content was mixed by sparging of air through needles pierced through a piece of silicon rubber at the bottom of the reactor. At least 24 needles were used to prevent cell death due to high bubble formation speeds (Barbosa et al. 2004). The airflow through the needles was controlled by mass flow controllers (Brooks Instrument, Hatfield, USA). The pH was measured using pH gel sensors (Applisens, Schiedam, the Netherlands) connected to the ADI 1030 Bio-controller. The pH was maintained at 7.8 and 6.7

for *D. tertiolecta* and *C sorokiniana,* respectively, by addition of carbon dioxide to the air through mass flow controllers controlled by the ADI 1030 Bio-controller.

Illumination

The reactors were illuminated on one side using 10 compact fluorescent tubes (Lynx LE 55W, 535 mm, Sylvania, Danvers, USA). The PAR photon flux density on the reactor surface was measured several times throughout the experiment using a Li-190sa quantum sensor (LI-COR, USA). The light absorption and reflection in passing the first water jacket was determined in an empty reactor, and was corrected for in determining the photon flux density into the photobioreactor. The spectral composition of the light (Figure 2) was determined behind the water jacket (IRRAD 2000 fiber-optic spectroradiometer, TOP sensor systems, Eerbeek, the Netherlands).

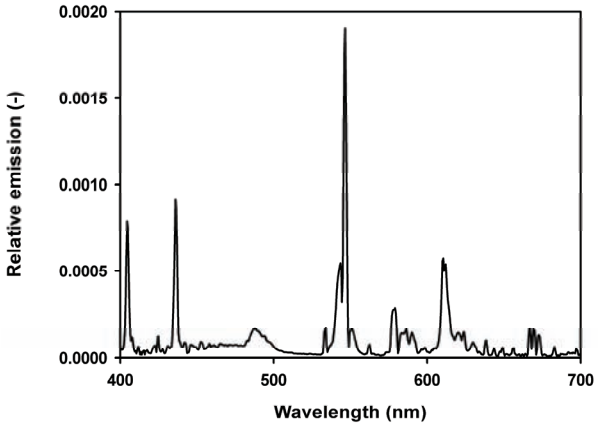

Figure 2. Spectral composition of the fluorescent tubes after passing the first water jacket (Lynx LE 55W, 535 mm, Sylvania, Danvers, USA). *The emission spectrum was normalized on a quantum basis.*

Continuous cultivation

The flow of fresh medium into the photobioreactor was programmed and controlled through BioXpert software (Applikon, Schiedam, the Netherlands), which determined the rotation speed of a peristaltic pump (Watson Marlow 205u, Cheltenham, UK). The actual dilution rate was determined from the decrease in weight of the medium vessel. The volume inside the reactor was kept constant by pumping excess algal suspension out through an overflow (Figure 1).

D. tertiolecta was cultivated using a linear decrease in dilution rate using a similar rate of change as Barbosa (2005). The dilution rate during the *D. tertiolecta* cultivations was calculated according to Equation 1.

$$D = D_0 - d * t \qquad (h^{-1}) \qquad \text{Equation 1}$$

Applying a constant deceleration rate, however, causes a rapid relative decrease in dilution rate at low dilution rates and larger deviations of the growth rate from the applied dilution rate. Because the relative change in dilution rate increases, the algae need to adapt more rapidly in order to maintain a situation representing steady state. *C. sorokiniana* was therefore cultivated using a proportional decrease in dilution rate according to Equation 2 and 3. Equation 2 will never reach zero, therefore an extra linear part was added to reach zero (Equation 3) in the final part of the experiment. The linear part starts at t_{linear}: a predefined time at which a smooth transition to a linear decrease in dilution was made.

If $t < t_{linear}$

$$D = D_0 * e^{-d_1 * t} \qquad (h^{-1}) \qquad \text{Equation 2}$$

Else

$$D = D_0 * e^{-d_1 * t_{linear}} - d_2 * \left(t - t_{linear}\right) \qquad (h^{-1}) \qquad \text{Equation 3}$$

Figure 3 shows the dilution rate development during the D-stat cultivations for the two algae. The proportional D-stat was designed to have the same duration as the

linear D-stat cultivations. The dilution rate shown was determined based on the actual fresh medium supply into the reactor, measured by the decrease in weight of the medium vessel. The points shown correspond to sampling times. Using these samples, the following parameters were analyzed: dry weight biomass concentration and spectrally averaged light absorption cross section.

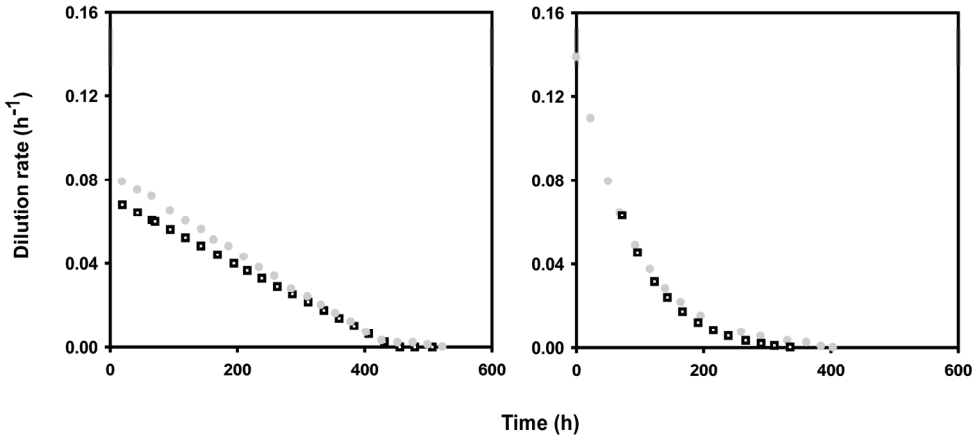

Figure 3. Dilution rate profiles during the D. tertiolecta (left) and C. sorokiniana (right) D-stat cultivations. □ 1.25 cm light path; ● 2.15 cm light path.

Dry weight

The biomass concentration was determined by a triplicate measurement of the dry weight of biomass in a reactor sample according to Zhu and Lee (1997). Glass microfiber filters (Whatman GF/F, Kent, UK) were used to filter the microalgae. The filter weight was determined on a 0.01 mg resolution balance (Sartorius ME 235P, Goettingen, Germany). Prior to filtration, the *D. tertiolecta* sample was diluted ten times using a 0.5 M ammonium formate solution to dissolve any possible salt depositions in the sample. Demineralized water was used to dilute the freshwater *C. Sorokiniana* sample. An additional volume of 50 ml of 0.5 M ammonium formate solution (*D. tertiolecta*) or demineralized water (*C. sorokiniana*) was filtered to further remove any small salt particles attached to the filter cake.

Absorption cross section

The spectrally averaged light absorption of the microalgae, a measure of the pigment content of the microalgae, was determined by measuring the wavelength dependent light absorption of the microalgae. The absorption was measured between 400 nm and 750 nm using an integrating sphere (Labsphere RSA-BE-65, North Sutton, USA) in a Beckman DU-640 spectrophotometer (Beckmann Coulter, Fullerton, USA). The results showed residual absorption of light above 720 nm. This was attributed to backward scattering and was subtracted from the absorbance measured at all wavelengths. The wavelength dependent specific coefficient combined with the spectral composition of the radiant flux entering the reactor (Figure 2) was used to calculate the spectrally averaged light absorption cross section according to Dubinsky et al. (1986). This spectrally averaged light absorption cross section is a measure for the specific light absorption, weighed for the light source used.

Specific growth rate

The specific growth rate of the organism in both the linear and the proportional D-stat cultivation was calculated from the dilution rate corrected for the biomass accumulation as shown in Equation 4 (Barbosa et al. 2005; Hoekema et al. 2006).

$$\mu_t = \frac{\left[\left(\frac{\left(C_{x,t} - C_{x,t+1}\right)}{\left(t_t - t_{t+1}\right) * C_{x,t}} + D_t\right) + \left(\frac{\left(C_{x,t} - C_{x,t-1}\right)}{\left(t_t - t_{t-1}\right) * C_{x,t}} + D_t\right)\right]}{2} \qquad (h^{-1}) \qquad \text{Equation 4}$$

Biomass yield on light energy

The biomass yield on light energy was calculated by Equation 5. The yield is based on the biomass production rate and light supply rate. The yield was not corrected for unused light passing through the flat-panel photobioreactor at very low biomass densities.

$$Y_{x,E} = \frac{C_x * \mu * V}{PFD_{in} * A * 3600 * 10^{-6}}$$ (g mol photons^{-1}) Equation 5

Specific light supply rate

The cultivation results were compared based on the specific light supply rate, calculated by Equation 6. The photon flux entering the panel photobioreactor was divided by the amount of biomass present in the reactor.

$$r_{E,x} = \frac{PFD_{in} * A}{C_x * V}$$ (µmol photons g^{-1} s^{-1}) Equation 6

Results

Biomass concentration

Figure 4 shows the biomass concentrations of *D. tertiolecta* and *C. sorokiniana* in the reactor during the continuous cultivations. Although the two microalgae differ in maximum growth rate and cultivation conditions, the biomass concentrations obtained during the D-stat were about equal for both algae in the 1.25 cm and 2.15 cm light path reactors. The two different microalgae were cultivated under controlled and optimal conditions. Concentrations of nutrients and trace elements were available in excess, pH and temperature were kept optimal, and produced oxygen was removed by aeration. Hence, the microalgae were cultivated under light limited conditions.

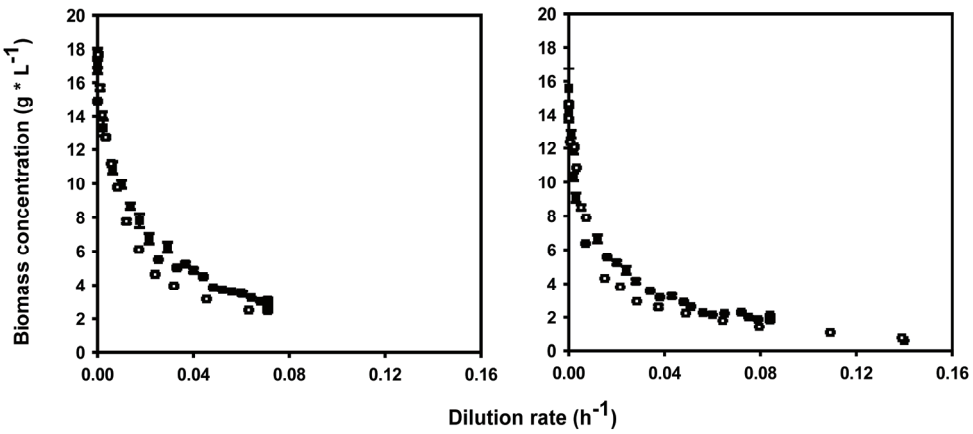

Figure 4. Biomass concentration of D.tertiolecta and C. sorokiniana during the D-stat cultivations. Left: 1.25 cm light path. Right: 2.15 cm light path. ■ D. tertiolecta biomass; □ C. sorokiniana biomass. Error bars represent standard errors from the mean.

Specific growth rate

The relation between the specific growth rate and applied dilution rate determines if the cultivation resembled steady state conditions. In Figure 5 the calculated growth rate and the applied dilution rate are compared. During all cultivations the growth rate was well able to keep up with the applied dilution rate. The growth rate of *D. tertiolecta* shows some deviation from the applied dilution rate at dilution rates lower than 0.015 h^{-1}. The linear decrease in dilution rate causes a fast relative decrease in dilution rate, leading to rapid biomass accumulation. The rapid biomass accumulation consequently causes a relative increase in growth rate compared to the dilution rate. This rapid accumulation also causes fast changes in light regime. The data obtained still give reliable information on the biomass yield achieved at these biomass densities and growth rates assuming biomass acclimation could keep up with these relative fast changes in light regime.

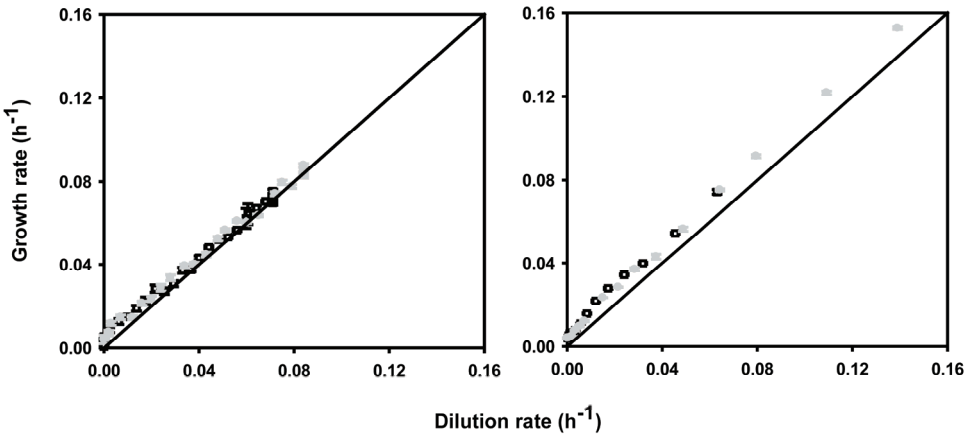

Figure 5. Growth rate development during the D. tertiolecta (left) and C. Sorokiniana (right) D-stat cultivations. □ 1.25 cm light path; ● 2.15 cm light path. Error bars represent standard errors from the mean.

Figure 5 (right) shows the comparison between the calculated growth rate and the applied dilution rate during the continuous *C. sorokiniana* cultivations, using the proportional change in dilution rate. The proportional change in dilution rate resulted in a growth rate at dilution rates below 0.01 h^{-1}, which was more similar to the applied dilution rate compared to the linear *D. tertiolecta* D-stat cultivations. At dilution rates above 0.01 h^{-1}, however, the growth rate differed more from the dilution rate compared to the *D. tertiolecta* cultivation. This is related to the larger absolute deceleration rates at high dilution rates in the *C. sorokiniana* cultivations compared to the *D. tertiolecta* cultivation. Nevertheless, when corrected for biomass accumulation these results will represent steady state conditions assuming biomass acclimation could keep up with the relative fast changes in light regime.

Biomass yield on light energy

Figure 6 and 7 show the biomass yield on light energy (Equation 5) during the *D. tertiolecta* and *C. sorokiniana* cultivations, respectively. Interestingly, an A-stat cultivation of *D. tertiolecta* in a 3 cm flat-panel reactor obtained by Barbosa et al. (2005) at similar conditions as in these experiments yielded similar results and

these are also shown in Figure 6 as a comparison. Apparently the light path length does not influence the yield of biomass on light energy in the range of 1 cm to 3 cm under the conditions investigated here.

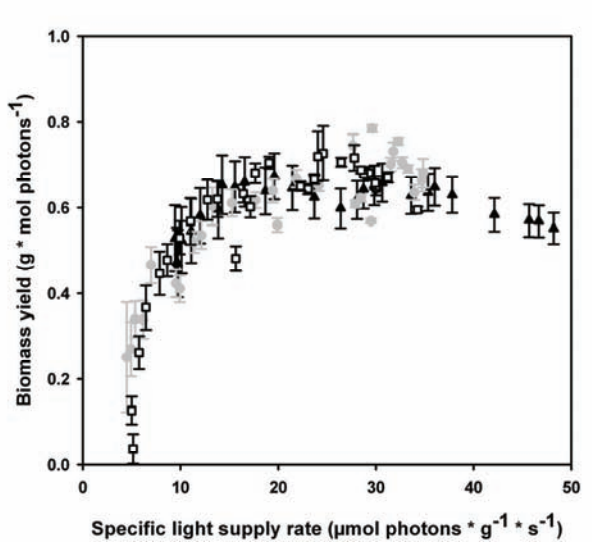

Figure 6. Biomass yield on light energy during the D. tertiolecta cultivations. □ 1.25 cm light path; ● 2.15 cm light path; ▲ 3 cm light path (Barbosa et al. 2005). Error bars represent standard errors from the mean.

The biomass yield for *D. tertiolecta* appeared not to be influenced by the reactor light path. A biomass yield of 0.65 ± 0.10 g mol photons^{-1} was obtained in all panel reactors at a wide range of biomass concentrations ranging from a light supply rate of 35 µmol photons g^{-1} s^{-1} down to 13 µmol photons g^{-1} s^{-1}. The light supply rate is inversely related to the biomass concentration since the photon flux density on the reactor surface is constant (Equation 6). The biomass yield was constant at biomass concentrations of 2.8 g L^{-1} to 6.8 g L^{-1} in a 1.25 cm reactor and 1.4 g L^{-1} to 3.8 g L^{-1} in a 2.15 cm reactor.

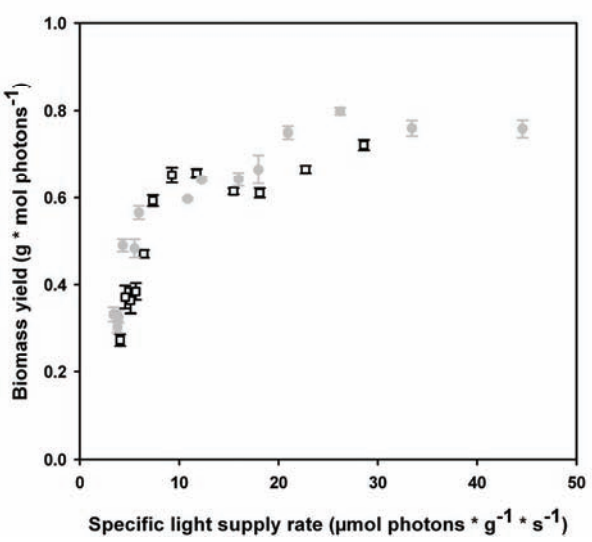

Figure 7. Biomass yield on light energy during the C. sorokiniana cultivations. □ 1.25 cm light path; ● 2.15 cm light path. Error bars represent standard errors from the mean.

The yields obtained during the *C. sorokiniana* cultivations were similar to the values obtained during the *D. tertiolecta* cultivations (Figure 7). Yields between 0.6 g mol photons^{-1} and 0.8 g mol photons^{-1} were obtained between light supply rates of 45 µmol photons g^{-1} s^{-1} down to 10 µmol photons g^{-1} s^{-1} during both *C. sorokiniana* cultivations. The biomass yield was constant at biomass concentrations from 2.5 g L^{-1} to 9.8 g L^{-1} in a 1.25 cm reactor and 0.7 g L^{-1} to 4.3 g L^{-1} in a 2.15 cm reactor.

Absorption cross section

The spectrally averaged light absorption cross sections change with the light availability as shown in Figure 8 and 9. During the D-stat cultivation the light supply rate decreases due to biomass accumulation. The light absorption cross section of *D. tertiolecta* (Figure 8) increased with this decreasing light supply rate, indicating a photo acclimation response generally observed for microalgae subjected to decreasing light availability. The cross section increases to a maximum value until it decreases slightly at the end of the D-stat cultivation.

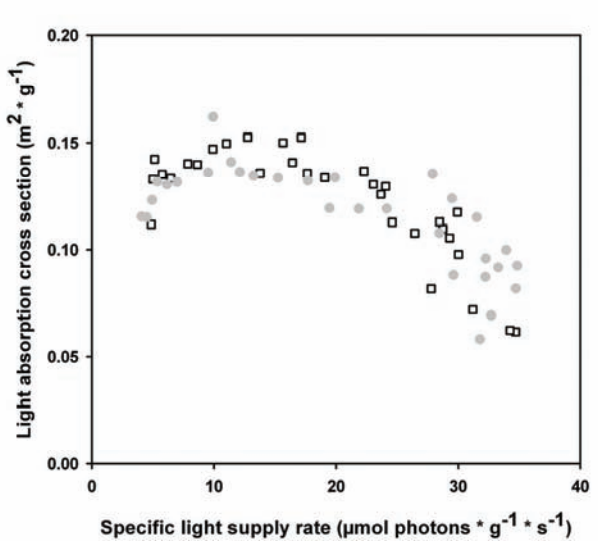

Figure 8. Spectrally averaged light absorption cross section of D. tertiolecta during the cultivations. □ 1.25 cm light path; ● 2.15 cm light path.

Figure 9 shows the light absorption cross section for *C. sorokiniana* during the two D-stat cultivations. A clear increase in absorption cross section with decreasing light supply rate was not obtained. However, a similar relation as *D. tertiolecta* for the light absorption cross section shows is expected, but only shifted to higher light supply rates. Unpublished results in a similar setup indeed show a smaller absorption cross section at higher light supply rates than the ones shown here. The decrease in absorption cross section at high biomass concentrations was more pronounced during the *C. sorokiniana* cultivation. It started at a higher light supply rate compared to *D. tertiolecta;* at 20 µmol photons g^{-1} s^{-1} instead of 10 µmol photons g^{-1} s^{-1}.

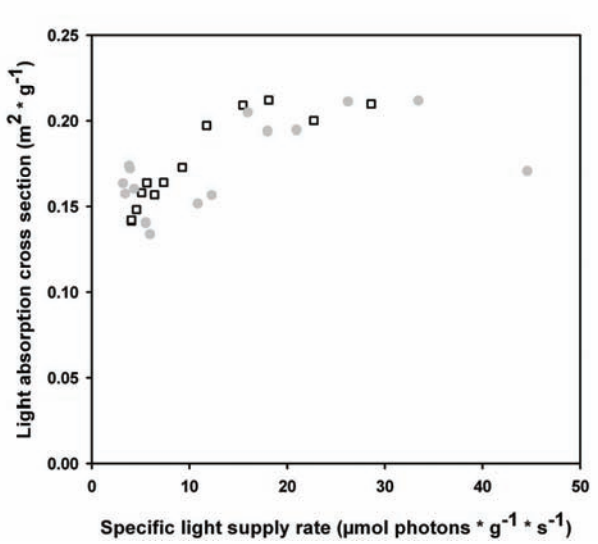

Figure 9. Spectrally averaged light absorption cross section of C. sorokiniana during the cultivations. □ 1.25 cm light path; ● 2.15 cm light path.

Discussion

During the panel reactor experiments the algae were exposed to the same photon flux density (PFD) at the reactor surface, which was about 930 µmol photons^{-1} m^{-2} s^{-1} (see Table 1). During the course of the D-stat cultivations biomass accumulated, changing the light regime in the reactors. The microalgae need to be able to acclimate to this changing light regime to obtain data on the biomass yield on light energy that is representative for a steady state situation. Figures 8 and 9 show the microalgae adapted to the changing light regime by changing the absorption cross section. The decreasing light supply rate caused an increase in the light absorption cross section until the maximum size was reached. Eventually, the light supply rate was insufficient to maintain the maximum absorption cross section causing the cross section to decrease.

Both the response in absorption cross section and the small difference in growth rate compared to the dilution rate showed that the microalgae were able to acclimate to the changing light regime. The results obtained during the D-stat were

therefore considered to be representative for a steady state situation. The relative decrease in yield at low light supply rates is much larger than the decrease in light absorbing cross section, indicating the decrease in yield was not due to this small decrease in light absorbing capacity. Furthermore, obtaining information on biomass yield on light energy at dilution rates of 0.02 h^{-1} and lower through D-stat cultivations is more feasible than through real steady states, taking into account the time it will take to reach a steady state and the higher risk of reactor fouling during long cultivations at high biomass concentrations.

The biomass yield on light energy of the acclimated microalgae is determined by the ability of the algae to use the supplied light energy for biomass formation. The light energy distribution in the reactor is characterized by a high PFD on the reactor surface, which decreases rapidly due to light absorption by the microalgae, creating a photic zone and a dark zone in the reactor. The photic zone is characterized by a strong light gradient with a PFD of about 930 μmol photons^{-1} m^{-2} s^{-1} at the surface that quickly decreases to a light intensity below the compensation point at the interface with the dark zone. The compensation point is the light intensity at which the photosynthesis and respiration compensate each other, i.e. net oxygen production is zero. Assuming a steady liquid flow, a decrease of the size of the photic zone will lead to a shorter exposure time to (over-) saturating light levels. Also, if panel width is reduced, the absolute residence time in the photic zone can be reduced, since at constant PFD a high biomass concentration and thus a smaller photic zone is obtained. Based on existing knowledge, such a reduction in exposure time to (over-) saturating light could lead to higher photosynthetic efficiencies, since less light induced damage will build up, and possibly also non-photochemical quenching (heat dissipation) of light energy will be less pronounced (Horton and Ruban 2005; Muller et al. 2001). Increased exposure times to (over-) saturating PFDs are therefore expected to lead to reduced photosynthetic efficiency and vice versa.

The strong decrease of biomass yield on light energy observed at low specific growth rates and high biomass densities in the panel reactors therefore does not seem to be related to the change in light regime, i.e. the decrease in size of the

photic zone. This strong decrease, however, can be explained assuming that a significant fraction of the light energy used is needed for cellular maintenance processes. It seems that at lower specific growth rates (high biomass concentration) an increasing fraction of the light energy is not used for biomass synthesis (anabolism) but is actually used to generate reductant to provide additional ATP from mitochondrial respiration. This assumption is strengthened by fitting a simple model (Pirt 1986), as shown by Equation 7, through the data obtained with both *C. sorokiniana* and *D. tertiolecta* for both the 1.25 cm and 2.15 cm light path panel reactors. The model relates the specific light supply rate ($r_{E,x}$; µmol photons g^{-1} s^{-1}) to the energy required for biomass production and cellular maintenance. The model assumes a constant efficiency in the conversion of available light energy into biomass, i.e. the true yield of biomass on supplied light energy ($Y_{x,E,(true)}$; g mol $photons^{-1}$) and a constant energy requirement for cellular maintenance processes ($m_{E,x}$; mol $photons^{-1}$ g^{-1} h^{-1}).

$$r_{E,x} * 0.0036 = \frac{\mu_t}{Y_{x,E(true)}} + m_{E,x} \qquad \text{(mol photons } g^{-1} h^{-1}\text{)} \qquad \text{Equation 7}$$

Plotting the left hand side of the equation as a function of the growth rate results in a straight line with the true yield as slope and the maintenance coefficient as offset. Since no clear influence of the light path on the observed biomass yield on light energy was observed, the data for the 1.25 cm and 2.15 cm reactors were taken together. Figure 10 shows the results for *D. tertiolecta* and *C. sorokiniana*. The following relations were found:

D. tertiolecta:

$$r_{E,x} * 0.0036 = \frac{\mu_t}{0.782} + 0.0133 \qquad R^2 = 0.977 \qquad \text{(mol photons } g^{-1} h^{-1}\text{)}$$

C. sorokiniana:

$$r_{E,x} * 0.0036 = \frac{\mu_t}{0.751} + 0.0068 \qquad R^2 = 0.988 \qquad \text{(mol photons } g^{-1} h^{-1}\text{)}$$

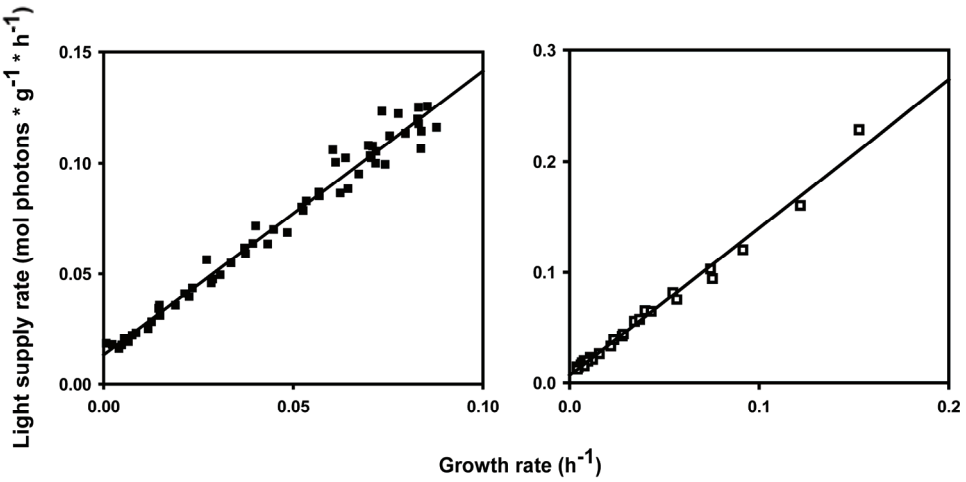

Figure 10. Specific light supply rate in the panel reactor as a function of the growth rate. ■ *D. tertiolecta;* □ *C. sorokiniana*

Both microalgae showed a constant true biomass yield and a constant maintenance factor during the D-stat cultivation. A true biomass yield on light energy of 0.78 g mol photons^{-1} and 0.75 g mol photons^{-1} was found for *D. tertiolecta* and *C. sorokiniana,* respectively. The yield differed from the theoretical maximum of 1.5 g mol photons^{-1} and 1.8 g mol photons^{-1} as calculated in Appendix 1. To explain the difference between theoretical and true yield it is assumed that a constant part of the absorbed light energy is not used for biomass formation, but is dissipated as heat. This took up a constant fraction of the absorbed light energy. In case of *D. tertiolecta* a calculated 48 % of the absorbed light energy was lost and in case of *C. sorokiniana* it increased to 58%. Figures 6 and 7 do not directly show a difference in observed biomass yield on light energy, but the microalgae do differ in the efficiency of light use. *D. tertiolecta* has a higher maintenance energy requirement, whereas *C. sorokiniana* has a lower true biomass yield on light energy. The higher maintenance energy requirement causes the yield of *D. tertiolecta* to decrease faster at higher biomass densities.

Conclusions

The D-stat cultivation technique is a tool for fast optimization of cultivation conditions to achieve optimal biomass yield on a limiting substrate such as light energy. Comparable values for biomass yield on supplied light energy were obtained for the two different species of microalgae. No beneficial effect of shorter exposure times to the (over-) saturating PFD at higher biomass concentrations was observed. Apparently, the absolute time spend in the photic zone throughout the different light regimes was such that light energy was absorbed with a constant efficiency.

These results were obtained at superficial gas velocities of $6.41*10^{-3}$ m s^{-1} and $7.75*10^{-3}$ m s^{-1}, typical values used in pneumatically agitated systems for microalgae production. From this work it is not possible to predict biomass yields at higher superficial gas velocities; increased levels of turbulence will also reduce exposure time to (over-) saturating light in the photic zone and could influence photosynthetic efficiency. Also, the occurrence of effects such as autoinhibition of algal growth at high biomass densities (Richmond et al. 2003) cannot be ruled out, although this work shows that maintenance requirements could be very important at high cell density cultivations.

Biomass productivity obtained in this study was constant during a wide range of specific light supply rates in both a 1.25 cm and 2.15 cm light path panel reactor for both *C. sorokiniana* and *D. tertiolecta*. The results of both microalgae corresponded to a simple model, indicating a constant true biomass yield on light energy and a constant biomass maintenance requirement. The steep decrease in observed yield at low light supply rates could be explained by the maintenance energy requirement of the large amount of biomass present at low dilution rates. The true biomass yield was assumed to differ from the theoretical maximum due to heat dissipation of a constant amount of the absorbed light energy in the photic zone.

Appendix 1

The theoretical biomass yield on light energy can be calculated based on the stoichiometric reaction equations for the formation of biomass on carbon dioxide, water, and the nitrogen source used in the cultivation.

For growth on nitrate:

$$CO_2(g) + 0.95 \cdot H_2O(l) + 0.12 \cdot NO_3^-(aq) \rightarrow CH_{1.78}O_{0.36}N_{0.12}(s) + 1.415 \cdot O_2(g) + 0.12 \cdot OH^-(aq)$$

For growth on urea:

$$0.94 \cdot CO_2(g) + 0.77 \cdot H_2O(l) + 0.06 \cdot CH_4ON_2(aq) \rightarrow CH_{1.78}O_{0.36}N_{0.12}(s) + 1.175 \cdot O_2(g)$$

The yield of the light reactions is assumed to be 0.1 mol of oxygen per mol of photons within the PAR spectrum. This value represents the maximal quantum yield as determined under low light by several independent researchers over the past decades. The theoretical maximal based on the Z-scheme of photosynthesis would be 0.125 mol of oxygen per mol of photons. The difference with 0.1 mol of oxygen per mol of photons is probably related to intrinsic inefficiencies of photosynthesis.

Assuming *D. tertiolecta* and *C sorokiniana* have the same elemental composition of $C_{1.78}O_{0.36}N_{0.12}$ as found for *Chlorella Spain* sp. (Duboc et al. 1999), the molecular mass of a C-mol biomass is 21.25 g mol^{-1}. To form one C-mol of biomass, 14.15 moles of photons or 11.75 moles of photons are needed to evolve the required amount of oxygen for growth on nitrate and urea, respectively, following the stoichiometric reaction equations. This leads to a theoretical biomass yield of 1.5 g mol photons^{-1} and 1.8 g mol photons^{-1} for growth on nitrate and urea, respectively.

Nomenclature

A	Illuminated reactor surface area (m^2)
C_x	Biomass concentration (g L^{-1})
D_0	Dilution rate; start of the D-stat (h^{-1})
D	Dilution rate (h^{-1})

d	Deceleration rate; linear D-stat (h^{-2})
d_1	Deceleration rate; proportional D-stat, proportional fraction (h^{-2})
d_2	Deceleration rate; proportional D-stat, linear fraction (h^{-2})
$m_{E,x}$	Biomass maintenance coefficient (mol photons^{-1} g^{-1} h^{-1})
PAR	Photosynthetic active radiation (µmol photons^{-1} m^{-2} s^{-1}, 400-700 nm)
PFD	Photon flux density (µmol photons^{-1} m^{-2} s^{-1})
$r_{E,x}$	Specific light supply rate (µmol photons g^{-1} s^{-1})
t	Time (h)
t_{linear}	Predefined time point at which linear part of the proportional D-stat starts (h)
μ	Growth rate (h^{-1})
V	Volume reactor content (L)
$Y_{x,E}$	Biomass yield on light energy (g mol photons^{-1})
$Y_{x,E(true)}$	True biomass yield on light energy (g mol photons^{-1})

Acknowledgements

This work was financially supported by the EU/Energy Network project SOLAR-H (FP6 contract 516510).

References

Barbosa MJ, Hadiyanto, Wijffels RH. 2004. Overcoming shear stress of microalgae cultures in sparged photobioreactors. Biotechnology and Bioengineering 85(1):78-85.

Barbosa MJ, Zijffers JW, Nisworo A, Vaes W, van Schoonhoven J, Wijffels RH. 2005. Optimization of biomass, vitamins, and carotenoid yield on light energy in a flat-panel reactor using the A-stat technique. Biotechnology and Bioengineering 89(2):233-242.

Dubinsky Z, Falkowski PG, Wyman K. 1986. Light Harvesting and Utilization by Phytoplankton. Plant and Cell Physiology 27(7):1335-1349.

Duboc P, Marison I, von Stockar U. 1999. Handbook of Thermal Analysis and Calorimetry. Kemp RB, editor: Elsevier. 267-365 p.

Ho TY, Quigg A, Finkel ZV, Milligan AJ, Wyman K, Falkowski PG, Morel FMM. 2003. The elemental composition of some marine phytoplankton. Journal of Phycology 39(6):1145-1159.

Hoekema S, Douma RD, Janssen M, Tramper J, Wijffels RH. 2006. Controlling light-use by Rhodobacter capsulatus continuous cultures in a flat-panel photobioreactor. Biotechnology and Bioengineering 95(4):613-626.

Horton P, Ruban A. 2005. Molecular design of the photosystem II light-harvesting antenna: photosynthesis and photoprotection. Journal of Experimental Botany 56(411):365-373.

Hu Q, Guterman H, Richmond A. 1996. A flat inclined modular photobioreactor for outdoor mass cultivation of photoautotrophs. Biotechnology and Bioengineering 51(1):51-60.

Hu Q, Kurano N, Kawachi M, Iwasaki I, Miyachi S. 1998. Ultrahigh-cell-density culture of a marine green alga Chlorococcum littorale in a flat-plate photobioreactor. Applied Microbiology and Biotechnology 49(6):655-662.

Mandalam RK, Palsson BO. 1998. Elemental balancing of biomass and medium composition enhances growth capacity in high-density Chlorella vulgaris cultures. Biotechnology and Bioengineering 59(5):605-611.

Meiser A, Schmid-Staiger U, Trosch W. 2004. Optimization of eicosapentaenoic acid production by Phaeodactylum tricornutum in the flat panel airlift (FPA) reactor. Journal of Applied Phycology 16(3):215-225.

Muller P, Li XP, Niyogi KK. 2001. Non-photochemical quenching. A response to excess light energy. Plant Physiology 125(4):1558-1566.

Paalme T, Kahru A, Elken R, Vanatalu K, Tiisma K, Vilu R. 1995. The computer-controlled continuous culture of Escherichia coli with smooth change of dilution rate (A-stat). Journal of Microbiological Methods 24(2):145-153.

Pirt SJ. 1986. Tansley Review No-4 - The Thermodynamic Efficiency (Quantum Demand) and Dynamics of Photosynthetic Growth. New Phytologist 102(1):3-37.

Qiang H, Faiman D, Richmond A. 1998a. Optimal tilt angles of enclosed reactors for growing photoautotrophic microorganisms outdoors. Journal of Fermentation and Bioengineering 85(2):230-236.

Qiang H, Richmond A. 1996. Productivity and photosynthetic efficiency of Spirulina platensis as affected by light intensity, algal density and rate of mixing in a flat plate photobioreactor. Journal of Applied Phycology 8(2):139-145.

Qiang H, Zarmi Y, Richmond A. 1998b. Combined effects of light intensity, light-path and culture density on output rate of Spirulina platensis (Cyanobacteria). European Journal of Phycology 33(2):165-171.

Richmond A, Zhang CW, Zarmi Y. 2003. Efficient use of strong light for high photosynthetic productivity: interrelationships between the optical path, the optimal population density and cell-growth inhibition. Biomolecular Engineering 20(4-6):229-236.

Sorokin C. 1959. Tabular Comparative Data for the Low-Temperature and High-Temperature Strains of Chlorella. Nature 184(4686):613-614.

Zhu CJ, Lee YK. 1997. Determination of biomass dry weight of marine microalgae. Journal of Applied Phycology 9(2):189-194.

Chapter 5

Photosynthetic yield of *Chlorella sorokiniana* at different levels of turbulence

Abstract

An increase in level of turbulence due to increased sparging of air in a panel photobioreactor was expected to influence the observed biomass yield of *Chlorella sorokiniana* on light energy. The maximum value of the observed yield was 0.75 ± 0.05 g mol photons^{-1}, but it did not increase as a result of increased mixing. Superficial gas velocities of 1.67*10^{-2} m s^{-1} and 4.00*10^{-2} m s^{-1} did not show any positive effect compared to the lowest velocity of 6.67*10^{-3} m s^{-1}. On the other hand, at a superficial gas velocity of 2.67*10^{-2} m s^{-1} this maximal yield could be maintained at higher biomass concentrations. Subtracting a constant biomass maintenance energy requirement from the absorbed light energy showed that the true yield of biomass on light energy could have increased at high biomass concentrations at a superficial gas velocity of 2.67*10^{-2} m s^{-1}. Increasing the turbulence thus could have a positive effect on the true yield, but high maintenance energy requirements did not allow for an increase of the observed yield.

Introduction

Discontinuous exposure of microalgae to (over-) saturating light intensities can result in increased photosynthetic efficiencies compared to a continuous exposure to these (over-) saturating light intensities. Phillips and Meyers (1954) found that the growth rate of *Chlorella* increased when it was exposed to flashing light of a high intensity instead of a continuous exposure. Furthermore, Kok (1956) and Terry (1986) found that oxygen quantum yields at high light intensities increased under specific flashing light conditions. The maximum benefit to be obtained from flashing light is full light integration. In this situation the biomass yield on light energy is equal to the yield under continuous light of intensity equal to the time averaged light intensity of the flashing light (Terry 1986). The fast circulation of the algae in short light path (SLP) high density photobioreactors is assumed to be able to expose the algae to such a light regime. However, conflicting observations have been made in such systems.

The cyanobacterium *Arthrospira platensis* showed increased biomass productivities at high levels of turbulence in SLP reactors at high biomass concentrations (Hu et al. 1996; Qiang et al. 1998a; Qiang and Richmond 1996; Qiang et al. 1998b). After recalculation of the presented data, the photosynthetic efficiency had a maximum value of around 1.5 grams of biomass (dry matter) produced per mol of photons (g mol photons^{-1}) at incident light intensities up to 2000 μmol photons m^{-2} s^{-1}. This is equal to the theoretical maximum for growth on nitrate as calculated in Appendix 1. However, the maximum efficiency obtained for the cyanobacterium *Anabaena siamensis* was 0.45 g mol photons^{-1} and 1.0 g mol photons^{-1} for the microalgae *Monodus subterraneus* grown under the same conditions (Hu et al. 1996). The green alga *Chlorococcum littorale* has also been cultivated in a panel reactor and after recalculation a yield of 0.53 g mol photons^{-1} was obtained (Hu et al. 1998). The cause of these differences in yield is unclear; it can be related to the cultivation conditions that do not match organism specific conditions required to obtain light integration. Further investigation into the biomass yield on light energy in photobioreactors is thus required.

In a previous study (Zijffers et al. manuscript submitted), *Chlorella sorokiniana* was cultivated in panel reactors of 1.25 cm and 2.15 cm optical path at a superficial gas velocity of $6.67*10^{-3}$ m s^{-1}. A relatively low maximum yield of 0.75 g mol photons^{-1} that decreased with increasing biomass concentration was observed during these cultivations. The low level of turbulence was expected to provide a light regime at which light integration could not be obtained. Increasing the level of turbulence in the panel reactor with the shortest light path is expected to positively influence the light regime. Possibly, the reactor conditions will be such that light integration as shown by an increase in biomass yield is obtained. *C. sorokiniana* was therefore cultivated in a 1.25 cm light path panel reactor at different levels of turbulence similar to the levels used by Hu et al. (1996). *C. sorokiniana* was cultivated using the D-stat cultivation technique subjecting the algae to a decreasing dilution rate and a changing light regime. All reactor conditions were optimal such that only the light availability determined productivity.

Materials and Methods

Microalgae and reactor start-up

Chlorella sorokiniana CCAP 211/8k was maintained as a suspended culture in Erlenmeyer flasks containing M-8 medium. Prior to the continuous cultivations the algae were cultivated batch wise in the panel photobioreactor at low light intensity, until a biomass density was reached to withstand the maximum incident light intensity used in the experiments (≈ 1000 μmol photons m^{-2} s^{-1}). After increasing the light intensity to the maximum value, chemostat cultivation was started at 70% to 80% of the maximum growth rate. Table 1 shows the operational properties of the different experiments. The superficial gas velocity is calculated by dividing the air flow rate by the horizontal cross sectional area of the panel reactors. The cultivation at a superficial gas velocity of $6.67*10^{-3}$ m s^{-1} was also presented in another manuscript (Zijffers et al. manuscript submitted) and is added here to compare four different superficial gas velocities.

Table 1. Operational properties of the different cultivations.

Alga	Incident light intensity (µmol photons m^{-2} s^{-1})	Illuminated surface area (m^2)	Aeration rate (L min^{-1})	Superficial gas velocity (m s^{-1})
C. sorokiniana	871	0.102	1.0	$6.67 \cdot 10^{-3}$
	1005	0.102	2.5	$1.67 \cdot 10^{-2}$
	848	0.100	4.0	$2.67 \cdot 10^{-2}$
	1041	0.100	6.0	$4.00 \cdot 10^{-2}$

Medium

C. sorokiniana was cultivated on a concentrated M-8a medium, which was based on M-8 medium developed by Mandalam and Palsson (1998). Sodium bicarbonate was added to the media after the pH was set. The medium used in the continuous cultivation experiments was kept under carbon dioxide atmosphere to prevent precipitation of salts. The following media composition was used (M): $4.8*10^{-2}$ $CO(NH_2)_2$, $1.6*10^{-2}$ KH_2PO_4, $4.4*10^{-3}$ Na_2HPO_4, $4.9*10^{-3}$ $MgSO_4$, $2.7*10^{-4}$ $CaCl_2$, $9.5*10^{-4}$ EDTA ferric sodium salt, $3.0*10^{-4}$ Na_2EDTA, $3.0*10^{-6}$ H_3BO_3, $2.0*10^{-4}$ $MnCl_2$, $3.3*10^{-5}$ $ZnSO_4$, $2.2*10^{-5}$ $CuSO_4$, $5.0*10^{-3}$ $NaHCO_3$.

Reactor setup and control

The panel reactors were built up by transparent polycarbonate sheets held together in a frame equal to the reactor used by Zijffers et al. (manuscript submitted) and similar to the system used by Barbosa et al. (2005). The panel reactors had a width of 20 cm, a height of 60 cm, and a light path of 1.25 cm. The temperature inside the reactor was measured using a pt-100 and was kept constant at 37 ºC by an ADI 1030 Bio-controller (Applikon, Schiedam, the Netherlands) controlling the temperature of the cryostat connected to water jackets on both the front and back surface of the reactor. The reactor content was mixed by sparging of air through needles (internal diameter 0.5 mm) pierced through a piece of silicon rubber at the bottom of the reactor. At least 28 needles were used to prevent cell death due to high bubble formation speeds (Barbosa et al. 2004). The airflow through the

needles was controlled by a mass flow controller (Brooks Instrument, Hatfield, USA). The pH was measured using pH gel sensors (Applisens, Schiedam, the Netherlands) connected to the ADI 1030 Bio-controller. The pH was maintained at 6.7 by addition of carbon dioxide to the air through another mass flow controller controlled by the ADI 1030 Bio-controller.

Illumination

The reactors were illuminated on one side using 10 fluorescent tubes (Lynx LE 55W, 535 mm, Sylvania, Danvers, USA). The PAR photon flux density on the reactor surface was measured several times throughout the experiment using a Li-190sa quantum sensor (LI-COR, USA). The light absorption and reflection in passing the first polycarbonate plates and the water in the first water jacket was determined in an empty reactor and was corrected for in determining the photon flux density into the photobioreactor. The spectral composition of the light was determined behind the water jacket (IRRAD 2000 fiber-optic spectroradiometer, TOP sensor systems, Eerbeek, the Netherlands).

Continuous cultivation

During the continuous cultivations, the biomass concentration was changed by gradually changing the rate of medium refreshment using the D-stat cultivation technique. The D-stat is similar to the A-stat cultivation technique as developed by Paalme et al (1995), but a slow continuing decrease instead of increase in dilution rate is applied (Hoekema et al. 2006). Furthermore, a proportional change in dilution rate was applied to subject the microalgae to a constant relative decrease in applied dilution rate to allow the cells to acclimate to the changing light regime also at low dilution rates. The flow of fresh medium into the photobioreactor was programmed and controlled through BioXpert software (Applikon, Schiedam, the Netherlands), which determined the rotation speed of a peristaltic pump (Watson Marlow 205u, Cheltenham, UK). The actual dilution rate was determined from the decrease in weight of the medium vessel. The volume inside the reactor was kept constant by pumping excess algal suspension out through an overflow.

A proportional decrease in dilution rate was applied to have a constant relative decrease in dilution rate to maintain a pseudo steady state situation (Equation 1). At low dilution rates, a shift to a linear decrease had to be made to reach a dilution rate of zero (Equation 2).

If $t < t_{linear}$

$$D = D_0 * e^{-d_1 * t} \quad (h^{-1}) \quad \text{Equation 1}$$

Else

$$D = D_0 * e^{-d_1 * t_{linear}} - d_2 * \left(t - t_{linear}\right) \quad (h^{-1}) \quad \text{Equation 2}$$

Figure 1 shows the dilution rate development during the D-stat cultivations. The points shown correspond to sampling times. The following parameters were analyzed: dry weight biomass concentration and spectrally averaged light absorption cross section.

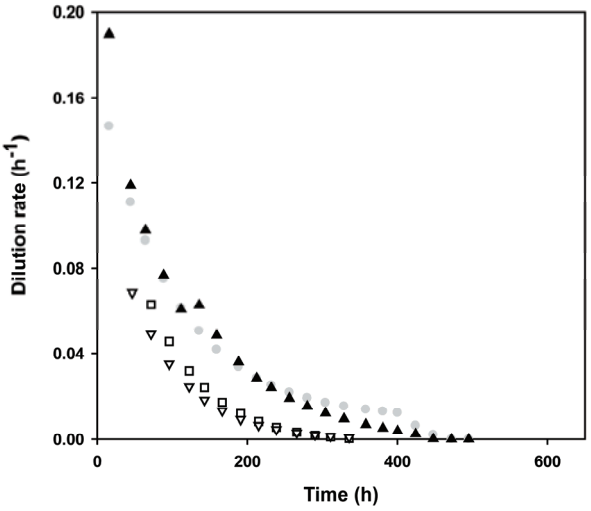

*Figure 1. Dilution rate profiles during the continuous C. sorokiniana cultivations at different superficial gas velocities. □ 6.67*10-3 m s-1 (Zijffers et al. manuscript submitted); ● 1.67*10-2 m s-1; ▲ 2.67*10-2 m s-1; ▽ 4.00*10-2 m s-1.*

Dry weight

The biomass concentration was determined by measuring the dry weight of biomass in a reactor sample according to Zhu and Lee (1997). Glass microfiber filters (Whatman GF/F, Kent, UK) were used to filter the microalgae. The filter weight was determined on a 0.01 mg resolution balance (Sartorius ME 235P, Goettingen, Germany). Prior to filtration, the *C. Sorokiniana* sample was diluted ten times using demineralized water. After filtration of the diluted sample, an additional 50 ml of demineralized water was filtered to remove any salt particles attached to the filter cake.

Absorption cross section

The spectrally averaged light absorption cross section of the microalgae, a measure of the pigment content, was determined by measuring the wavelength dependent light absorption of the microalgae. The absorption was measured between 400 nm and 750 nm using an integrating sphere (Labsphere RSA-BE-65, North Sutton, USA) in a Beckman DU-640 spectrophotometer (Beckmann Coulter, Fullerton, USA). The results showed residual absorption of light above 720 nm. This was attributed to backward scattering and was subtracted from the absorbance measured at other wavelengths. The wavelength dependent specific coefficient combined with the spectral composition of the fluorescent light source used was used to calculate the spectrally averaged light absorption cross section according to Dubinsky et al. (1986). This spectrally averaged light absorption cross section is a measure for the absorption, weighed for the light source used.

Specific growth rate

The specific growth rate of the organism was calculated from the dilution rate corrected for the biomass accumulation as shown in Equation 3 (Barbosa et al. 2005; Hoekema et al. 2006).

$$\mu_t = \frac{\left[\left(\frac{\left(C_{x,t} - C_{x,t+1}\right)}{\left(t_t - t_{t+1}\right) * C_{x,t}} + D_t\right) + \left(\frac{\left(C_{x,t} - C_{x,t-1}\right)}{\left(t_t - t_{t-1}\right) * C_{x,t}} + D_t\right)\right]}{2} \qquad (h^{-1}) \qquad \text{Equation 3}$$

Biomass yield on light energy

The biomass yield on light energy was calculated by Equation 4. This will be referred to as observed yield to distinguish from the true yield as mentioned in the introduction. The observed yield was not corrected for unused light passing through the flat-panel photobioreactor at low biomass densities.

$$Y_{x,E(obs)} = \frac{C_x * \mu * V}{PFD_{in} * A * 3600 * 10^{-6}} \qquad (\text{g mol photons}^{-1}) \qquad \text{Equation 4}$$

Specific light supply rate

The cultivation results were compared based on the specific light supply rate calculated using Equation 5. The photon flux entering the panel photobioreactor was divided by the amount of biomass present in the reactor.

$$r_{E,x} = \frac{PFD_{in} * A}{C_x * V} \qquad (\mu\text{mol photons g}^{-1}\ \text{s}^{-1}) \qquad \text{Equation 5}$$

Results and Discussion

During the course of a D-stat experiment the dilution rate of the panel reactors decreased, increasing the residence time of the algae. As a result biomass accumulates as a function of time decreasing the specific light supply rate and decreasing the penetration depth of the light in the reactor, i.e. the photic zone. Since the reactor is illuminated from one side, a dark zone is present beyond the penetration depth of the light.

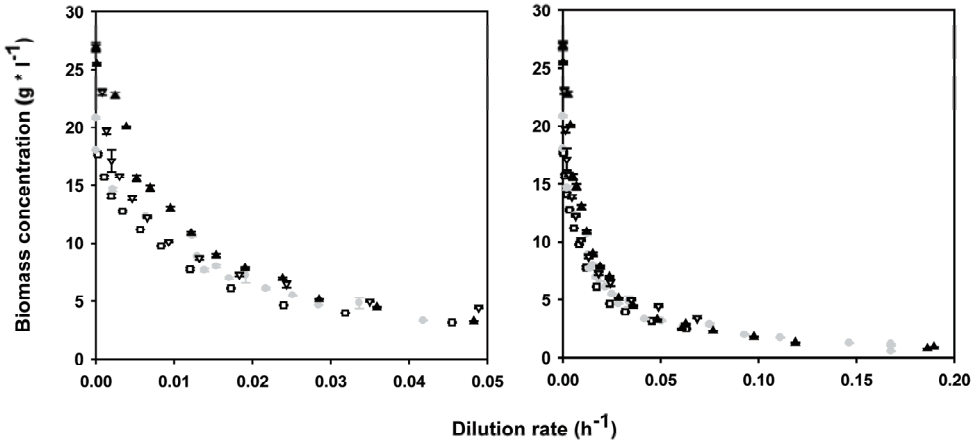

*Figure 2. Biomass concentration during the D-stat cultivations at different superficial gas velocities. □ 6.67*10^{-3} m s^{-1} (Zijffers et al. manuscript submitted); ● 1.67*10^{-2} m s^{-1}; ▲ 2.67*10^{-2} m s^{-1}; ▽ 4.00*10^{-2} m s^{-1}. The graph on the left side zooms in on the low light supply rates as shown in the complete graph on the right. Error bars represent standard errors from the mean.*

Figure 2 shows the biomass concentration obtained during the D-stat cultivations. Small differences in biomass concentration were obtained between the different cultivations. The cultivation at a superficial gas velocity (U_g) of 2.67*10^{-2} m s^{-1} showed the highest biomass concentration at low dilution rates. Based on the increase in biomass concentration during the D-stat, the growth rate was calculated according to Equation 3. The relation between the specific growth rate and applied dilution rate, as shown in Figure 3, determines if the cultivation resembled steady state conditions. As can be seen, the growth rate of *C. sorokiniana* was able to adjust to the applied dilution rate. The growth rate was higher than the dilution rate, but this will always occur during a D-stat cultivation in which biomass accumulates.

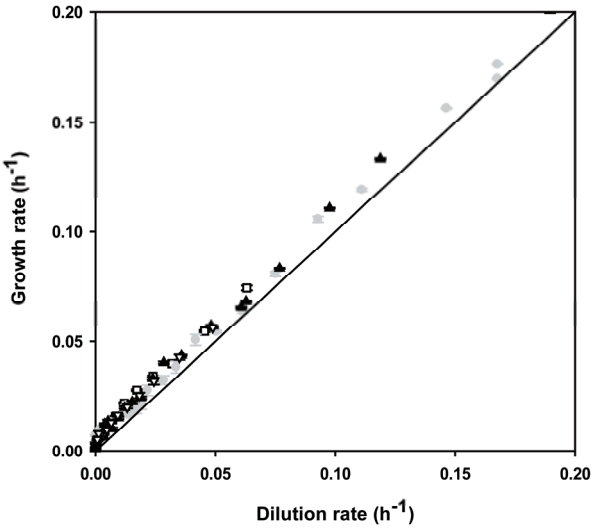

*Figure 3. Calculated growth rate during the D-stat cultivations at different superficial gas velocities. □ 6.67*10^{-3} m s^{-1} (Zijffers et al. manuscript submitted); ● 1.67*10^{-2} m s^{-1}; ▲ 2.67*10^{-2} m s^{-1}; ▽ 4.00*10^{-2} m s^{-1}. Error bars represent standard errors from the mean.*

Light absorption cross section

The light absorption cross section of *C. sorokiniana*, as shown in Figure 4, adapted to the changing light supply rates during the D-stat cultivation. At high light supply rates the absorption cross section was smallest, but it increased with decreasing light supply rates to its maximum value. At even lower light supply rates the amount of absorbed light energy seemed to be insufficient to maintain the absorption cross section and it decreased. Small differences in absorption cross section were obtained for the different airflow rates at the same light supply rate, showing a slight influence of the airflow rate on the light regime.

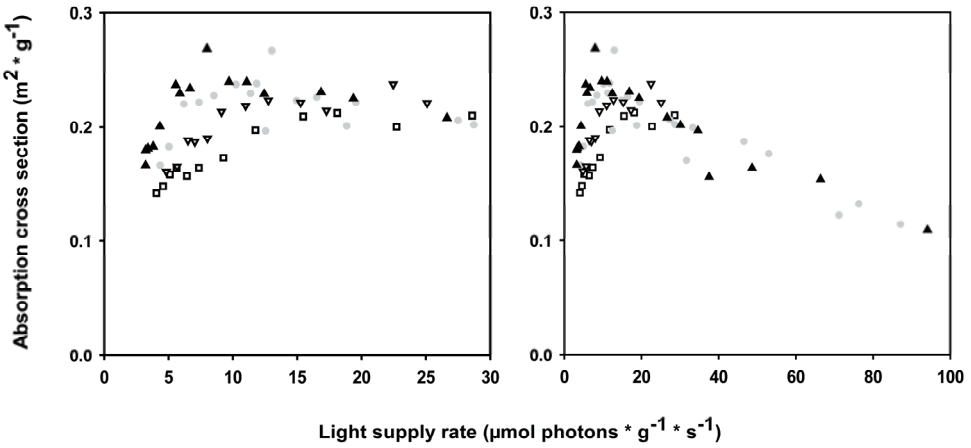

*Figure 4. Light absorption cross section during the D-stat cultivations at different superficial gas velocities. □ 6.67*10^{-3} m s^{-1} (Zijffers et al. manuscript submitted); ● 1.67*10^{-2} m s^{-1}; ▲ 2.67*10^{-2} m s^{-1}; ▽ 4.00*10^{-2} m s^{-1}. The graph on the left side zooms in on the low light supply rates as shown in the complete graph on the right.*

Biomass yield on light energy

Figure 5 shows the observed yield on light energy obtained during the D-stat cultivations, calculated using Equation 4. During the D-stat cultivation the biomass concentration increased, decreasing the light supply rate. A change in turbulence was expected to influence the biomass yield on light energy. However, the maximum observed yield did not change significantly from 0.75 g mol photons^{-1} as found at a superficial gas velocity (U_g) of 6.67*10^{-3} m s^{-1} (Zijffers et al. manuscript submitted). During the cultivation at a U_g of 1.67*10^{-2} m s^{-1} the yield decreased between a light supply rate of 30 µmol photons g^{-1} s^{-1} and 10 µmol photons g^{-1} s^{-1} when compared to U_g of 6.67*10^{-3} m s^{-1}. During the cultivation at a U_g of 4.00*10^{-2} m s^{-1} lower biomass yields were observed throughout the cultivation. A positive effect of an increase in turbulence is shown by the increased biomass yield at a U_g of 2.67*10^{-2} m s^{-1} at low light supply rates (= high biomass concentrations) compared to the yield at low light supply rates during the other cultivations. Obtaining the maximum yield at high biomass concentrations is

beneficial because less volume of growth media is required and less water needs to be removed in downstream processing of the biomass.

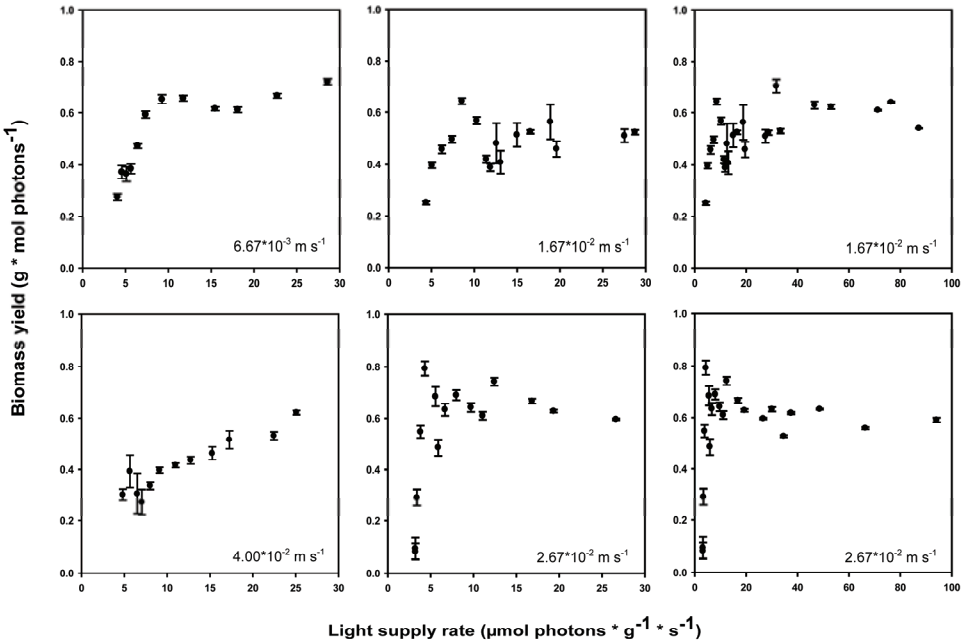

*Figure 5. Biomass yield on light energy during the D-stat cultivations at different superficial gas velocities. The graphs in the middle zoom in on the low light supply rates of the complete graphs of the cultivations at a U_g of 1.67*10^{-2} m s^{-1} and 2.67*10^{-2} m s^{-1} shown to the right. Error bars represent standard errors from the mean. Cultivation at a U_g of 6.67*10^{-3} m s^{-1} was performed by Zijffers et al. (manuscript submitted).*

Higher biomass yields were obtained by Hu Qiang, Richmond, and coworkers (see introduction) at high biomass concentrations of the cyanobacterium *Arthrospira platensis* in turbulently mixed panel reactors. Their high yields were obtained at biomass concentrations up to 14 g L^{-1}. However, the biomass needed to be filtered daily and suspended in fresh medium to remove growth inhibiting compounds that were excreted by the cyanobacterium. Significantly lower productivities were obtained if the growth medium was not refreshed (Richmond et al. 2003).

The decrease in yield at higher biomass concentrations in our experiments might therefore also be caused by growth inhibition. However, conflicting results have

been obtained on autoinhibition of growth in *Chlorella* cultures. Pratt et al. (1945) showed the formation of growth inhibiting compounds during batch cultivation. Scutt (1964) only found inhibiting compounds in filtered cell extracts after 4 days to 7 days of storage and no growth inhibition was found in growing cultures. Mandalam and Palsson (1995) also did not observe autoinhibition during growth. Balancing the medium composition has shown to increase the *Chlorella vulgaris* biomass concentration obtained during batch growth (Mandalam and Palsson 1998). The same balanced medium was used during this study to prevent growth inhibition. The occurrence of growth inhibition thus cannot be entirely excluded at low growth rates during the final stages of the D-stat cultivations. However, the decrease in observed yield can be well explained by an increase in maintenance energy requirement due to the high biomass concentrations.

In a previous study we showed that the biomass accumulation at a U_g of $6.67*10^{-3}$ m s^{-1} could be described by assuming a constant true yield and biomass maintenance requirement as discussed by Pirt (1965; 1986) and shown by Equation 6 (Zijffers et al. manuscript submitted).

$$r_{E,x} * 0.0036 = \frac{\mu_t}{Y_{x,E(true)}} + m_{E,x} \qquad \text{(mol photons } g^{-1}\ h^{-1}\text{)} \qquad \text{Equation 6}$$

A true yield ($Y_{x,E(true)}$) of 0.768 g mol $photons^{-1}$ and a maintenance requirement ($m_{E,x}$) of 0.0088 mol photons g^{-1} h^{-1} were obtained for the 1.25 cm *C. sorokiniana* cultivation at a U_g of $6.67*10^{-3}$ m s^{-1}. Figure 6 shows the light supply rate as a function of the growth rate obtained. The influence of turbulence on the true yield and maintenance is best shown by displaying the results relative to the results obtained during the cultivation at a U_g of $6.67*10^{-3}$ m s^{-1}, which is plotted as a solid line in the graphs of the other levels of turbulence in Figure 6.

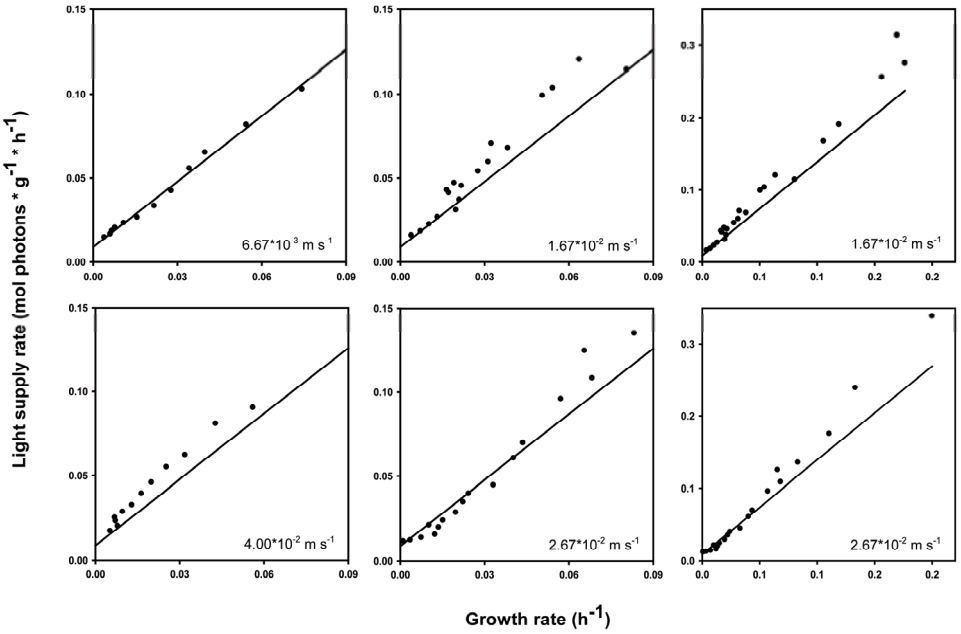

*Figure 6. Light supply rate as a function of the growth rate during the D-stat cultivations at different superficial gas velocities. The graphs in the middle zoom in on the low light supply rates of the complete graphs of the cultivations at a U_g of 1.67*10^{-2} m s^{-1} and 2.67*10^{-2} m s^{-1} shown to the right. The solid line represents the relation found at a U_g of 6.67*10^{-3} m s^{-1}. Cultivation at a U_g of 6.67*10^{-3} m s^{-1} was performed by Zijffers et al. (manuscript submitted).*

At light supply rates above 0.11 mol photons g^{-1} h^{-1} (30 µmol photons g^{-1} s^{-1}) the difference between the relation found at a U_g of 6.67*10^{-3} m s^{-1} and the results obtained at higher superficial gas velocities increased due to light which was not absorbed. No dark zone was present in the reactor in this situation. Due to low biomass concentrations and small light absorption cross sections of the microalgae, light passed through the panel reactor. The results below 0.11 mol photons g^{-1} h^{-1} show the light supply rates at which all light was absorbed by the microalgae.

An increase in turbulence in most cases resulted in a decrease in growth rate obtained at a certain light supply rate, displaying a negative effect of the increase in turbulence. Increased shear forces due to the increased superficial gas velocity

is expected to have caused this decrease in growth rate. The increase in airflow rate caused an increase in number of bubble ruptures at the liquid surface, causing an increased number of algae to be swung out of the algal suspension. This was shown by the deposition of a thick biofilm on the interior reactor surface above the suspension, i.e. the headspace.

During the cultivations at a U_g of $2.67*10^{-2}$ m s^{-1} a higher growth rate was obtained at light supply rates below 0.07 mol photons g^{-1} h^{-1} as indicated by the points below the solid line in Figure 6. However, the observed yield, as shown in Figure 5, only showed a slight improvement at these low light supply rates. Apart from the observed yield, it is interesting to see how the true yield (Equation 6) changed with changing level of turbulence. This was determined based on two assumptions. First, the data points were representative of real steady states to be able to calculate the true yield for each point separately using Equation 6. Second, the constant maintenance energy requirement ($m_{E,x}$) of 0.0088 mol photons g^{-1} h^{-1} as obtained at a U_g of $6.67*10^{-3}$ m s^{-1} was also applied to the other cultivations. The calculated value for the true biomass yield on light energy for all cultivations is plotted in Figure 7. The solid line represents the true yield found at a U_g of $6.67*10^{-3}$ m s^{-1}.

When the maintenance requirement is subtracted from the observed yield, fluctuations of the true yield around a relatively constant value are shown. The true yield is generally lower than the true yield of 0.768 g mol photons^{-1}, except for the cultivation at a U_g of $2.67*10^{-2}$ m s^{-1} where a positive effect of an increase in turbulence is shown. The calculated true yield increased up to 1.82 g mol photons^{-1}, which is equal to the theoretical maximum as calculated in Appendix 1.

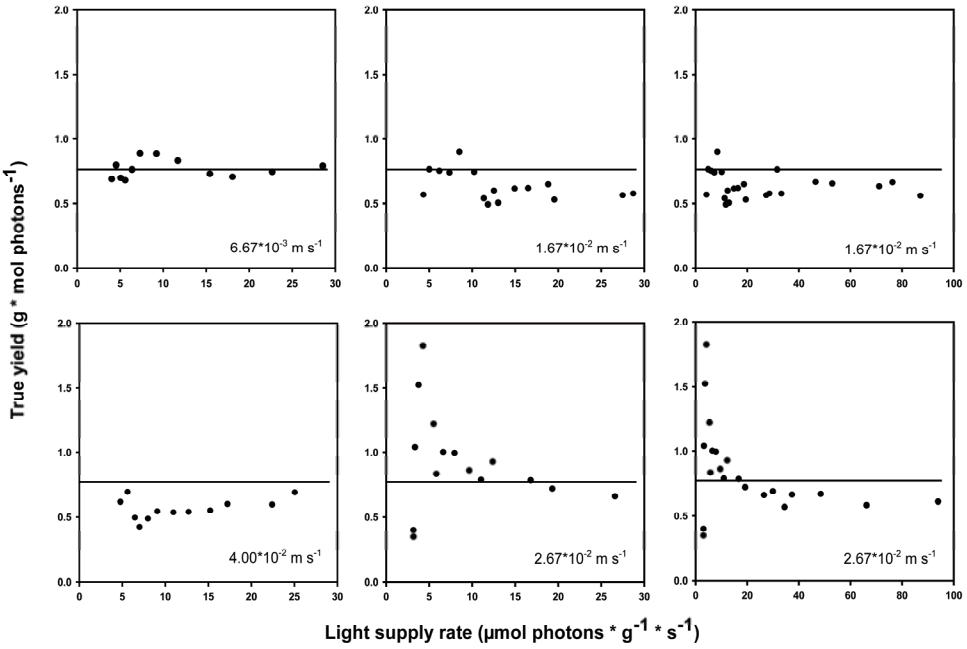

*Figure 7. Calculated true biomass yield on light energy. The graphs in the middle zoom in on the low light supply rates of the complete graphs of the cultivations at a U_g of 1.67*10^{-2} m s^{-1} and 2.67*10^{-2} m s^{-1} shown to the right. The solid line represents the true yield found at a U_g of 6.67*10^{-3} m s^{-1}. Cultivation at a U_g of 6.67*10^{-3} m s^{-1} was performed by Zijffers et al. (manuscript submitted).*

Conclusions

An increase in turbulence had a small effect on the observed yield of *C. sorokiniana* in a panel photobioreactor. At a superficial gas velocity (U_g) of 1.67*10^{-2} m s^{-1} and 4.00*10^{-2} m s^{-1} no increase in observed biomass yield was obtained compared to a U_g of 6.67*10^{-3} m s^{-1}. An increase in the calculated true biomass yield was observed at high biomass concentrations at a U_g of 2.67*10^{-2} m s^{-1}. However, biomass maintenance requirements appeared to consume an increasing fraction of the absorbed light energy and the increase in true yield did not result in an increase in observed yield. However, the maximum value for the observed yield was obtained at a higher biomass density.

Appendix 1

The theoretical biomass yield on light energy can be calculated based on the stoichiometric reaction equations for the formation of biomass on carbon dioxide, water, and the nitrogen source used in the cultivation.

For growth on nitrate:

$$CO_2(g) + 0.95 \cdot H_2O(l) + 0.12 \cdot NO_3^-(aq) \rightarrow CH_{1.78}O_{0.36}N_{0.12}(s) + 1.415 \cdot O_2(g) + 0.12 \cdot OH^-(aq)$$

For growth on urea:

$$0.94 \cdot CO_2(g) + 0.77 \cdot H_2O(l) + 0.06 \cdot CH_4ON_2(aq) \rightarrow CH_{1.78}O_{0.36}N_{0.12}(s) + 1.175 \cdot O_2(g)$$

The yield of the light reactions is assumed to be 0.1 mol of oxygen per mol of photons within the PAR spectrum. This value represents the maximal quantum yield as determined under low light by several independent researchers over the past decades.

Assuming *A. platensis* and *C sorokiniana* have the same elemental composition of $C_{1.78}O_{0.36}N_{0.12}$ as found for *Chlorella Spain* sp. (Duboc et al. 1999), the molecular mass of a C-mol biomass is 21.25 g mol^{-1}. Following the stoichiometric reaction equations, 11.75 moles of photons are needed to evolve the required amount of oxygen to form one C-mol of biomass using urea as nitrogen source and 14.15 moles of photons using nitrate. A theoretical maximal biomass yield of 1.8 g mol photons^{-1} for growth on urea and 1.5 g mol photons^{-1} for growth on nitrate is obtained.

Nomenclature

A	Illuminated reactor surface area (m^2)
C_x	Biomass concentration (g L^{-1})
D_0	Dilution rate; start of the D-stat (h^{-1})
D	Dilution rate (h^{-1})
d_1	Deceleration rate; proportional D-stat, proportional fraction (h^{-2})

d_2 Deceleration rate; proportional D-stat, linear fraction (h^{-2})

$m_{E,x}$ Biomass maintenance coefficient (mol photons^{-1} g^{-1} h^{-1})

PAR Photosynthetic active radiation (µmol photons^{-1} m^{-2} s^{-1}, 400-700 nm)

PFD Photon flux density (µmol photons^{-1} m^{-2} s^{-1})

$r_{E,x}$ Specific light supply rate (µmol photons g^{-1} s^{-1})

t Time (h)

t_{linear} Predefined time point at which linear part of the proportional D-stat starts (h)

µ Growth rate (h^{-1})

U_g Superficial gas velocity (m s^{-1})

V Volume reactor content (L)

$Y_{x,E(obs)}$ Observed biomass yield on light energy (g mol photons^{-1})

$Y_{x,E(true)}$ True biomass yield on light energy (g mol photons^{-1})

Acknowledgements

This work was financially supported by the EU/Energy Network project SOLAR-H (FP6 contract 516510).

References

Barbosa MJ, Hadiyanto, Wijffels RH. 2004. Overcoming shear stress of microalgae cultures in sparged photobioreactors. Biotechnology and Bioengineering 85(1):78-85.

Barbosa MJ, Zijffers JW, Nisworo A, Vaes W, van Schoonhoven J, Wijffels RH. 2005. Optimization of biomass, vitamins, and carotenoid yield on light energy in a flat-panel reactor using the A-stat technique. Biotechnology and Bioengineering 89(2):233-242.

Dubinsky Z, Falkowski PG, Wyman K. 1986. Light Harvesting and Utilization by Phytoplankton. Plant and Cell Physiology 27(7):1335-1349.

Duboc P, Marison I, von Stockar U. 1999. Handbook of Thermal Analysis and Calorimetry. Kemp RB, editor: Elsevier. 267-365 p.

Hoekema S, Douma RD, Janssen M, Tramper J, Wijffels RH. 2006. Controlling light-use by Rhodobacter capsulatus continuous cultures in a flat-panel photobioreactor. Biotechnology and Bioengineering 95(4):613-626.

Hu Q, Guterman H, Richmond A. 1996. A flat inclined modular photobioreactor for outdoor mass cultivation of photoautotrophs. Biotechnology and Bioengineering 51(1):51-60.

Hu Q, Kurano N, Kawachi M, Iwasaki I, Miyachi S. 1998. Ultrahigh-cell-density culture of a marine green alga Chlorococcum littorale in a flat-plate photobioreactor. Applied Microbiology and Biotechnology 49(6):655-662.

Kok B. 1956. Photosynthesis In Flashing Light. Biochimica Et Biophysica Acta 21(2):245-258.

Mandalam RK, Palsson BO. 1995. Chlorella-Vulgaris (Chlorellaceae) Does Not Secrete Autoinhibitors at High Cell Densities. American Journal of Botany 82(8):955-963.

Mandalam RK, Palsson BO. 1998. Elemental balancing of biomass and medium composition enhances growth capacity in high-density Chlorella vulgaris cultures. Biotechnology and Bioengineering 59(5):605-611.

Paalme T, Kahru A, Elken R, Vanatalu K, Tiisma K, Vilu R. 1995. The computer-controlled continuous culture of Escherichia coli with smooth change of dilution rate (A-stat). Journal of Microbiological Methods 24(2):145-153.

Phillips JN, Myers J. 1954. Growth Rate Of Chlorella In Flashing Light. Plant Physiology 29(2):152-161.

Pirt SJ. 1965. Maintenance Energy of Bacteria in Growing Cultures. Proceedings of the Royal Society of London Series B-Biological Sciences 163(991):224-&.

Pirt SJ. 1986. Tansley Review No-4 - The Thermodynamic Efficiency (Quantum Demand) And Dynamics Of Photosynthetic Growth. New Phytologist 102(1):3-37.

Pratt R, Oneto JF, Pratt J. 1945. Studies on Chlorella-Vulgaris .10. Influence of the Age of the Culture on the Accumulation of Chlorellin. American Journal of Botany 32(7):405-408.

Qiang H, Faiman D, Richmond A. 1998a. Optimal tilt angles of enclosed reactors for growing photoautotrophic microorganisms outdoors. Journal of Fermentation and Bioengineering 85(2):230-236.

Qiang H, Richmond A. 1996. Productivity and photosynthetic efficiency of Spirulina platensis as affected by light intensity, algal density and rate of mixing in a flat plate photobioreactor. Journal of Applied Phycology 8(2):139-145.

Qiang H, Zarmi Y, Richmond A. 1998b. Combined effects of light intensity, light-path and culture density on output rate of Spirulina platensis (Cyanobacteria). European Journal of Phycology 33(2):165-171.

Richmond A, Zhang CW, Zarmi Y. 2003. Efficient use of strong light for high photosynthetic productivity: interrelationships between the optical path, the optimal population density and cell-growth inhibition. Biomolecular Engineering 20(4-6):229-236.

Scutt JE. 1964. Autoinhibitor Production by Chlorella Vulgaris. American Journal of Botany 51(6P1):581-&.

Terry KL. 1986. Photosynthesis In Modulated Light - Quantitative Dependence Of Photosynthetic Enhancement On Flashing Rate. Biotechnology and Bioengineering 28(7):988-995.

Zhu CJ, Lee YK. 1997. Determination of biomass dry weight of marine microalgae. Journal of Applied Phycology 9(2):189-194.

Zijffers JWF, Schippers K, Zheng K, Janssen M, Tramper J, Wijffels RH. manuscript submitted. Photosynthetic yield of algae in panel photobioreactors: True yield and maintenance requirement.

Chapter 6

General Discussion

Abstract

To obtain high areal productivities of microalgae for production of bulk chemicals and biofuels the efficiency of sunlight utilization has to be maximized. This can be realized by reducing the photon flux density at the light exposed surface by optical engineering. Specific reactor design and use of sun tracking devices is needed to obtain a high capturing efficiency of direct sunlight. Efficient coupling of light capturing elements to specifically designed light distributing elements will reduce the light intensity and enhance uniformity of light distribution inside the algal suspension. A transparent reactor top surface is still needed to allow diffuse light, which cannot be focused, to penetrate into the algal suspension. This reduction of sunlight intensity can result in high yields when the corresponding biomass concentration and light path is further optimized. A too low biomass concentration will result in large cultivation volumes. High biomass densities are therefore preferred. However, when high biomass concentrations are combined with a long light path, the average light intensity inside the photobioreactor is too low. This will lead to a low specific growth rate and hence the maintenance requirement for light energy will significantly reduce reactor productivity. Continuous cultures at high dilution rate are required and at high biomass densities, which can only be realized at a sufficiently short light path.

Introduction

Microalgae are considered to be an attractive source of biobased, renewable fuels, and chemicals because of the very high areal productivity in comparison with agricultural crops (Apt and Behrens 1999; Chisti 2007; Spolaore et al. 2006). Chisti (2008) assumed that with microalgae an annual oil production of almost 100 m^3 ha^{-1} $year^{-1}$ could be obtained. Taking the estimated 30% oil content this would mean that at locations with the highest solar irradiance microalgae grow with 20% efficiency of PAR irradiance energy captured into biomass. The efficiency of 20% is equal to the theoretical maximum that can be obtained as explained in Textbox 1. So far, such efficiencies have not been obtained at high solar irradiance levels.

Textbox 1. Theoretical maximum biomass yield.

The theoretical biomass yield on light energy can be calculated based on the stoichiometric reaction equations for the formation of biomass on carbon dioxide, water, and the nitrogen source used in the cultivation.

For growth on nitrate:

$$CO_2(g) + 0.95 \cdot H_2O(l) + 0.12 \cdot NO_3^-(aq) \rightarrow CH_{1.78}O_{0.36}N_{0.12}(s) + 1.415 \cdot O_2(g) + 0.12 \cdot OH^-(aq)$$

For growth on ammonium:

$$CO_2(g) + 0.71 \cdot H_2O(l) + 0.12 \cdot NH_4^+(aq) \rightarrow CH_{1.78}O_{0.36}N_{0.12}(s) + 1.175 \cdot O_2(g) + 0.12 \cdot H^+(aq)$$

For growth on urea:

$$0.94 \cdot CO_2(g) + 0.77 \cdot H_2O(l) + 0.06 \cdot CH_4ON_2(aq) \rightarrow CH_{1.78}O_{0.36}N_{0.12}(s) + 1.175 \cdot O_2(g)$$

The yield of the light reactions is assumed to be 0.1 mol of oxygen per mol of photons within the PAR spectrum. This value represents the maximal quantum yield as determined under low light by several independent researchers over the past decades. The photosynthetic active region (PAR) represents light of wavelengths within the range of 400 nm to 700 nm that can be used by the microalgae. These wavelengths contain 43% - 45% of the energy of the full sunlight spectrum.

Assuming *D. tertiolecta* and *C sorokiniana* have the same elemental composition of $C_{1.78}O_{0.36}N_{0.12}$ as found for *Chlorella Spain* sp. (Duboc et al. 1999), the molecular mass of a C-mol biomass is 21.25 g mol^{-1}. To form one C-mol of biomass, 14.15 moles of photons or 11.75 moles of photons are needed to evolve the required amount of oxygen for growth on nitrate and urea or ammonium, respectively, following the stoichiometric reaction equations. This leads to a theoretical biomass yield of 1.5 g mol $photons^{-1}$ and 1.8 g mol $photons^{-1}$ for growth on nitrate and urea or ammonium, respectively. To calculate the percentage of light energy captured into biomass, the heat of combustion of a gram of biomass is divided by the energy content of a mol of photons of the light source used. In case of sunlight the energy content is 2.2 $*10^2$ kJ mol $photons^{-1}$. The caloric content of a gram of microalgae is estimated to be between 20 kJ g^{-1} and 25 kJ g^{-1} (Grima et al. 1997; Morita et al. 2000).

Table 1 shows the efficiencies obtained during cultivations focused on maximizing outdoor biomass productivity. The efficiencies of light use presented in Table 1 are published as such, or recalculated from the presented data. The yield is based on the amount of light entering the reactor (volumetric) or on the amount of light

radiating on the ground surface occupied by the reactor (areal). A volumetric yield of a single reactor unit cannot directly be translated to an areal yield of multiple reactor units, due to mutual shading of reactors in a multiple unit production system, as further explained in Textbox 2.

Textbox 2. Volumetric and areal yield.

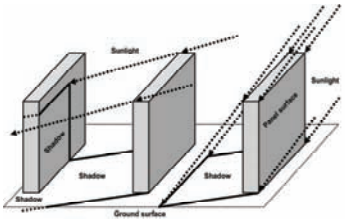

The volumetric yield is defined as the productivity of a reactor unit divided by the light input through the reactor surface of that unit. The areal yield is defined as the productivity divided by the light energy irradiating the ground surface occupied by the reactor and the total shaded ground area during the day. The volumetric yield of a single reactor is not representative for the areal yield of multiple reactors, because the shadow produced by the reactor and the effect it can have on neighboring reactor units is disregarded. Areal yield is best determined by dividing the productivity of all reactor units in a larger setup by the irradiance on the ground surface occupied by all reactor units.

Table 1. Efficiencies of (PAR) light use obtained in outdoor microalgal and cyanobacterial cultivations.

Reactor	Efficiency		Reference
Tubular	6.6%	areal	Torzillo et al. 1993
	5.9% (a)	volumetric	Grima et al. 1994
	6.2% - 10.9%	volumetric	Zittelli et al. 1996
	5.6%	volumetric	Tredici and Zittelli 1998
	3.4% - 11.8%	volumetric	Fernandez et al. 1998
	5.3% - 8.1%	volumetric	Zittelli et al. 1999
	5.4% - 6.2% (a)	areal	Fernandez et al. 2001 Molina et al. 2001
Helical coil	6.6%	volumetric	Tredici and Zittelli 1998
	4.0% - 9.5%	areal	Morita et al. 2002
Column	9.1% - 11.4%	areal	Zittelli et al. 2006
Panel	5.0% - 9.5%	volumetric	Tredici et al. 1991
	8.0% - 20.0%	volumetric	Qiang et al. 1998

(a) Light intensities on the reactor surface were not reported in theses studies. The solar irradiance at the production location was taken from the S@tel-Light database[1] and used to calculate the efficiency of light use based on the reported productivities.

[1] *www.satel-light.com*

Table 1 shows that a large variation in efficiencies of light use were obtained in different reactor types. In general the efficiency obtained ranges from 4% to 11%. The higher efficiencies were obtained during cultivations at lower light intensities (during winter) or in reactors that captured less light energy at high direct sunlight intensities. A high efficiency of 20% based on the volumetric PAR light energy input and biomass output of the cyanobacterium *Arthrospira platensis*, was obtained by Qiang et al. (1998) in a panel reactor. Lower efficiencies were obtained in panel reactors that captured more light energy.

Photoautotrophic microalgal productivity is a function of the incident light intensity, specific surface area, and the mixing regime in the cultivation system (Richmond 2004; Torzillo et al. 2003). Outdoor photobioreactors suffer from a number of limitations when biomass yield on an areal basis is determined. A low yield is either caused by suboptimal circumstances in the reactor, limiting biological efficiency, or by a suboptimal design of the reactor, limiting light supply to the algae. Maximal areal microalgal productivity will therefore require cultivation systems that provide optimal cultivation conditions, efficiently capture all sunlight, and supply captured light energy at optimal intensities. This review discusses the potential for areal efficient and energy efficient microalgal cultivations based on:

1. Efficiency of light capture and distribution into the cultivation system.
2. Efficiency of light use in microalgal cultivation.

Light capture and distribution

The first step in areal efficient cultivation is the efficient capture and delivery of light to the microalgae. Loss of light through reflection from the reactor surface has to be minimized and preferably reactors should fully cover the ground surface to prevent light from striking the ground surface. Ponds and horizontal tubular systems can fully cover large areas and capture sunlight well, but (over-) saturating sunlight intensities at the reactor surface limit the productivity of these systems. Two different strategies can be identified to supply algae with lower and more suitable sunlight intensities:

1. Distributing and lowering the intensity of direct sunlight over the reactor surfaces through specific reactor shapes, through mutual shading of reactors, and through diffusion of light by reflection on whitened ground surfaces.
2. Capturing sunlight into light guides and transporting captured sunlight into the bioreactor, followed by redistribution at lower light intensities.

Vertical column or panel reactors use the first strategy to decrease the (over-) saturating sunlight intensities at high solar elevation angles. During the middle of the day when the sunlight intensity is highest, light strikes the vertical reactor surface at a small angle and the sunlight is distributed over a larger area decreasing the (over-) saturating intensity. In larger scale cultivation systems light will reflect between multiple photobioreactors. Reactors on the outside of the cultivation system intercept (over-) saturating sunlight intensities, shielding the reactors in the middle. This strategy is most often applied in production systems consisting of horizontal tubes placed close together on vertical racks as also illustrated in Chisti (2007; 2008), but could also be applied to rows of vertical panel reactors (Qiang et al. 1998). By reflection of sunlight on reactor surfaces and on whitened ground surfaces the light is diffused and can be redirected to otherwise shaded reactor parts. As such, the algae are exposed to lower light intensities (Carlozzi 2003; Pulz et al. 1995). The actual light intensity at the reactor surfaces in large scale (multiple units) column, panel, or tubular cultivation systems depends on the orientation and areal density of the individual units.

The variation in the intensity of direct light inside a vertical panel reactor (corrected for reflection on the surface) is illustrated in Figure 1 (also see Textbox 2), which shows the direct normal light intensity and the light intensity on a vertical panel facing south or east in Huelva, Spain (latitude: 37.214º; longitude -7.064º). As a reference also the direct light intensity on a horizontal surface is included. Figure 1 shows that the orientation of a vertical panel greatly influences the direct light intensity in the panel reactor. This light intensity will further change during the year due to the changing position of the sun on the horizon. The intensity was

recalculated from irradiance data obtained from the Photovoltaic Geographical Information System (PVGIS)[2] database.

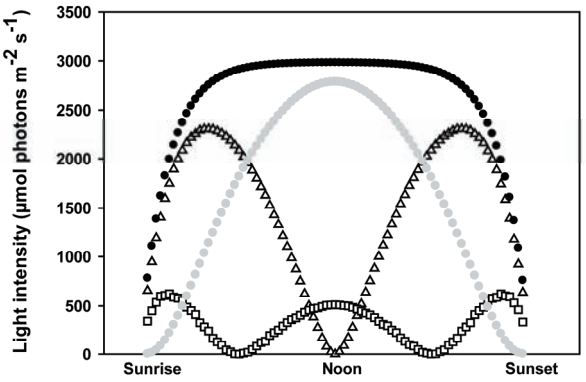

Figure 1.The available direct normal sunlight intensity (●) and the direct light intensity inside a vertical panel facing south (□) and east (Δ) in Huelva, Spain during the 21st of June. As a reference also a horizontal reactor surface is included (●).

Light that reaches the ground surface in between the panels will diffusely reflect and approximately 64% of this reflected light will still enter the panels. The 64% is based on 80% efficiency of reflection of a whitened concrete surface and a uniform diffuse reflection from the ground surface in all directions that again results in some reflection of light on the panel surface. As shown in Figure 1, in most situations the intensity inside the panel is less than the direct sunlight intensity, increasing the potential for efficient cultivation. Especially a vertical surface facing south will be exposed to much lower light intensities. This means that less light can be captured by a single reactor unit and, consequently, more units have to be placed on the same ground area. Since the position of the sun will change during the day and year a tedious optimization has to be done to find the optimal spacing of the reactor units at which overall light capture is maximal and intensity at the reactor surface is minimal, taking into account shading effects throughout the day (see Textbox 2).

[2] http://re.jrc.ec.europa.eu/pvgis/index.htm

In the second strategy to supply sunlight at a lower and more suitable intensity, sunlight is captured into light guides or optical fibers and is emitted from the lateral surface of the guides or fibers at lower intensities (Hirata et al. 1996; Ogbonna et al. 1999; Pulz et al. 1995). Using internal illumination through light guides and optical fibers, large conventional (stainless steel) tanks could be used to grow photoautotrophic microorganisms under controlled conditions as illustrated in Figure 2. A short light path is maintained in the tank by dense distribution of light radiating optical fibers. The major advantage of using optical fibers is creating a higher illuminated surface to volume ratio in large volume reactor vessels (An and Kim 2000; Matsunaga et al. 1991). The saturating solar irradiance was divided over multiple optical fibers and delivered into the photobioreactor through the surface of the fiber, which in total provides a larger illuminated surface compared to the transparent reactor surface. However, large numbers of fibers are required limiting the applicability.

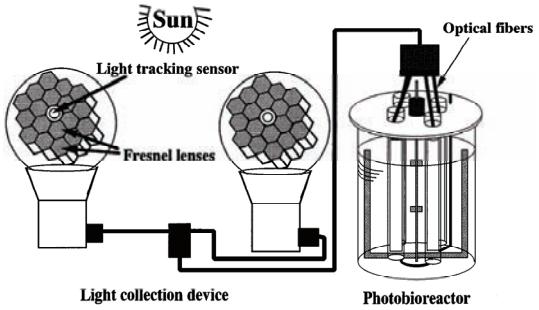

Figure 2. Internally illuminated optical fiber photobioreactor (Ogbonna et al. 1999).

Reactors supplying light through optical fibers were not used commercially due to low efficiencies in the delivery of captured light into the photobioreactor (An and Kim 2000; Gordon 2002; Ogbonna et al. 1999). The delivery problem was solved by direct focus of sunlight on short light transporting and distributing elements as used in the Green Solar Collector (GSC) (Zijffers et al. 2008a) as shown in Figure 3. It uses moveable linear Fresnel lenses to focus sunlight onto light guides that direct the light downwards into the algal suspension.

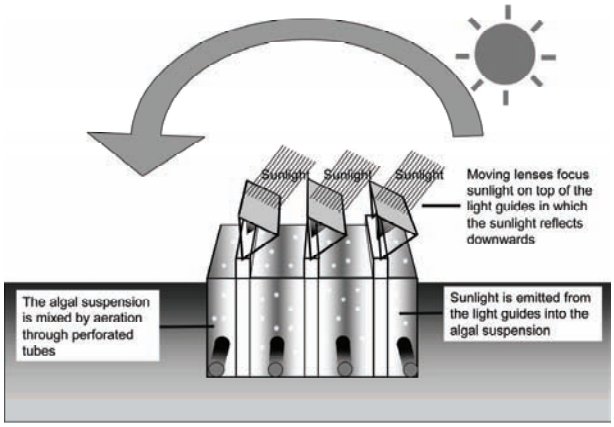

Figure 3. The Green Solar Collector.

Apart from an efficient capture, the captured light should also be uniformly delivered from the lateral surfaces of optical fibers and light guide like structures to the microalgae, which has proven to be difficult (An and Kim 2000; Hirata et al. 1996; Pulz et al. 1995). Csogor (1999) managed to overcome this lateral distribution problem to a large extent by roughening the surface of the illuminating surface of the guide. A specific surface structure might further help to obtain a uniform distribution of light (Gordon 2002). However, this specific surface structure is tailored to specific constant incoming angles of captured light into the optical fiber or light guide. The incoming angles of captured light into the light guide in the GSC change during the day due to the moving sun and a specific light guide surface structure could therefore not be applied (Zijffers et al. 2008b). Roughening the surface through sandblasting was used to enhance the uniformity of light distribution from the distributor surface.

Solar fiber-optic mini-dish concentrators as illustrated in Figure 4 and described by Feuermann et al. (2002) are able to efficiently capture sunlight into optical fibers. If these fibers are coupled to specifically designed light extractors (illustrated in Figure 5) sunlight can be uniformly extracted into the algal suspension (Gordon 2002). The shape and distribution of the light extractors can be designed to match the desired cultivation conditions. Based on these principles, a reactor can be

designed in which sunlight can be delivered to the algae at either a high or a low intensity, tailored to the microalgae.

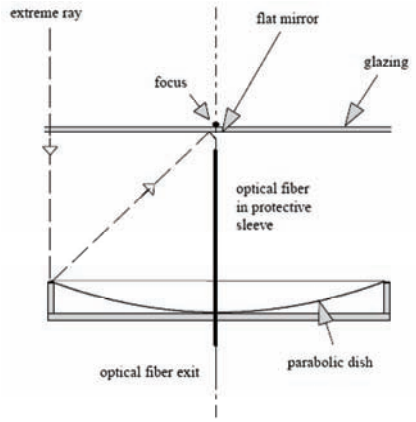

Figure 4. Schematic drawing of a solar fiber-optic mini-dish concentrator (Gordon 2002).

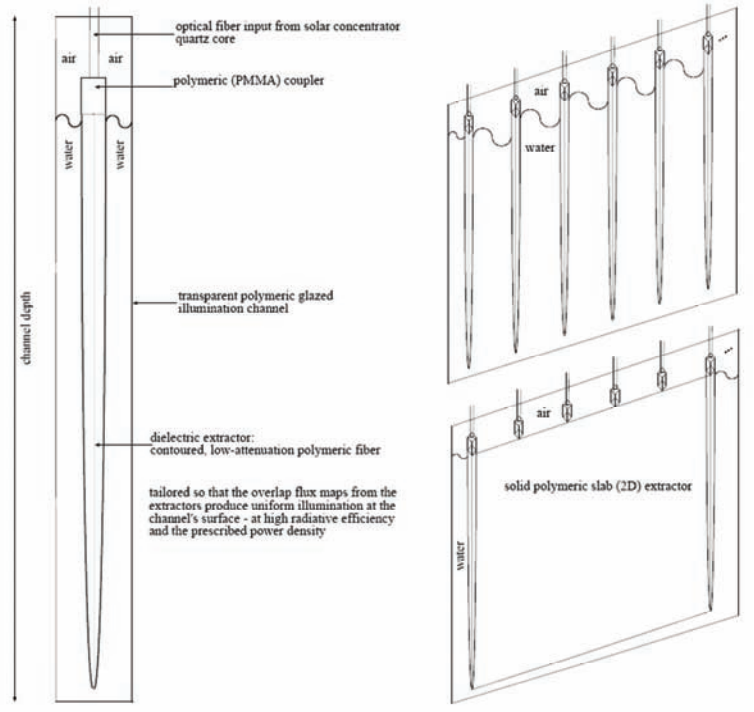

Figure 5. An example of a light extractor (Gordon 2002).

Photovoltaic panels that are able to precisely follow the azimuth and elevation of the sun by rotating around a vertical and a horizontal axis, i.e. dual-axis tracking of the sun, have shown an considerable increase in energy production per panel through reduction of reflection of light from the panel surface (Aiuchi et al. 2006; Bakos 2006). The direct light capturing efficiency of a dual-axis tracking module, the GSC and a horizontal panel is shown in Table 2. Reflection losses in passing the cover of the panels prevent a 100% capturing of available light energy.

Table 2. Light capturing efficiency of a panel that is perpendicular to the sun, a mini-dish concentrator, a Green Solar Collector and a horizontal reactor cover on the 21st of June in Huelva, Spain.

	Percentage of light captured
Perpendicular panel (dual-axis tracking)	92%
Mini-dish concentrator (dual-axis tracking) (Feuermann et al. 2002)	89%
Green Solar Collector (dual-axis tracking)	75%
Horizontal reactor cover (no tracking)	62%

Dual-axis movement thus increases the amount of captured light energy. Reflection of light on the lenses and light guide prevents the full capture of all direct sunlight in the GSC (Zijffers et al. 2008a; Zijffers et al. 2008b). Reflection losses are less when light is captured in optical fibers, using the dual-axis moveable mini-dishes as described by Feuermann et al. (2002). Furthermore, dual-axis movement of sunlight capturing elements connected to light guides or optical fibers is required to focus sunlight on a specific spot to be able to capture sunlight into the light guides and fibers. Single axis moving elements or fixed elements are unable to focus sunlight on a specific spot and can therefore not be used to capture light into light guides or optical fibers.

Direct light can be focused, transported, and distributed, whereas diffuse light, i.e. light coming from all directions, cannot be focused. Although direct light is the major fraction (approximately 75%) of the clear sky areal irradiance, diffuse light should be taken into consideration in designing a production system. On cloudy days, sunlight is completely diffuse and no direct light is present. Since in this

situation the microalgae completely rely on diffuse light, the cultivation system needs to be able to capture diffuse light well. A transparent reactor cover is therefore required.

Efficiency of light use in microalgal cultivation

Textbox 3. PI-curve.

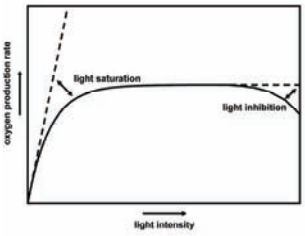

The Photosynthetic activity – Irradiance curve (PI-curve) shows the oxygen production rate, i.e. the photosynthetic activity, of a diluted microalgal culture as a function of the light intensity experienced by the algae. At low light intensities the oxygen production increases linearly with the light intensity. In this situation the photosynthetic efficiency, i.e. the oxygen produced per quanta light energy, is highest. At the end of the linear increase the photosynthetic activity is maximal at maximum efficiency. Light saturation (a decrease in photosynthetic efficiency) starts at continuous illumination of low light intensities. The photosystems become saturated and light energy is dissipated as heat. With increasing light intensity the photosynthetic activity increases to its maximum until light inhibition occurs. At this point the light intensity is such that it becomes damaging, causing the oxygen production to decrease.

Maintaining algae in an efficient growth phase is difficult, since the photosynthetic efficiency is maximal in only a small range of low light intensities. The photosynthetic efficiency as a function of experienced light intensity is visualized by a Photosynthetic activity - Irradiance curve (PI-curve) as illustrated in Textbox 3. The intensity of sunlight can reach up to 2000 µmol photons m^{-2} s^{-1} depending on season and latitude, limiting the efficiency of microalgal cultivation at continuous solar illumination. As a comparison, light saturation usually occurs between 100 µmol photons m^{-2} s^{-1} and 200 µmol photons m^{-2} s^{-1} (MacIntyre et al. 2002).

This saturation effect is also the rationale behind the optical engineering approach to reduce light intensity (= increase light exposed reactor surface) discussed in the previous section. Besides this purely technical solution, it has also been hypothised that by decreasing light path (=reactor depth) and increasing biomass density and mixing rate photosaturation could be reduced or even completely circumvented (Gordon and Polle 2007). Under these conditions a steep light gradient will develop and algae will only be exposed to (over-) saturating light when they are in the so-called photic zone close to the reactor surface. Depending on reactor design this photic zone could be as small as 1 mm (Gitelson et al. 1996).

Because of this light gradient combined with fast mixing of the suspension microalgae will experience an intermittent or fluctuating light regime.

It has been found in dedicated laboratory studies that discontinuous exposure to the (over-) saturating light intensities can increase the efficiency of light utilization (Kok 1956; Phillips and Myers 1954). This effect is also called light integration and full light integration implies that the photosynthetic activity under intermittent light is equal to the activity under continuous light of an intensity equal to the time-averaged intensity under intermittent light (Nedbal et al. 1996; Terry 1986). (Over-) Saturating sunlight intensities could thus be efficiently used when supplied at the right frequency with sufficiently long dark periods. It has been suggested that such high frequency intermittent light exposure can be mimicked in high density algal cultures in short light path photobioreactors at a high mixing rate (Gordon and Polle 2007).

Short reactor depths, high biomass concentrations, and turbulent mixing, however, did appear not to be a guarantee for light integration and high biomass yields. In our laboratory maximum efficiencies of about 8% were observed during *Dunaliella tertiolecta* and *Chlorella sorokiniana* cultivations in 1.25 cm and 2.15 cm panel reactors (Zijffers et al. manuscript submitted-a). The maximum efficiency obtained with some other microalgae in panel reactors was 10% for the microalga *Monodus subterraneus* (Hu et al. 1996) and 5.5% for the microalga *Chlorococcum littorale* (Hu et al. 1998). These results are in the same efficiency range as the results shown in Table 1.

The fact that maximal efficiency was not reached could be related to the fact that growth inhibition occurs at high cell densities, but this is unlikely in the experiments with *D. tertiolecta* and *C. sorokiniana* (Zijffers et al. manuscript submitted-a; Zijffers et al. manuscript submitted-b). In light path reactors of 1.25 cm or higher it might therefore not be possible to reach full light integration. On the other hand, the observed yield during the cultivations could be well described by assuming a constant true yield of biomass on light energy and a constant biomass maintenance requirement as shown by Equation 1 (Pirt 1965; Pirt 1986).

According to this relation the light energy needed for maintenance could well explain the reduction in biomass yield on light energy (photosynthetic efficiency) at high biomass density and low specific growth rate.

$$r_{E,x} * 0.0036 = \frac{\mu_t}{Y_{x,E(true)}} + m_{E,x} \qquad \text{(mol photons } g^{-1}\ h^{-1}\text{)} \qquad \text{Equation 1}$$

Equation 1 relates the specific light supply rate ($r_{E,x}$; µmol photons g^{-1} s^{-1}) to the energy required for biomass production, i.e. the true yield of biomass on supplied light energy ($Y_{x,E,(true)}$; g mol $photons^{-1}$) and the energy requirement for cellular maintenance processes ($m_{E,x}$; mol $photons^{-1}$ g^{-1} h^{-1}).

The optimal situation from a light use efficiency point of view will be a situation in which the microalgae are exposed to a light intensity such that maximum photosynthetic activity and efficiency is obtained. The easiest method to obtain a high observed yield will be continuous cultures at low light intensities and low biomass concentrations. On the other hand, the light intensity must still be sufficiently high to support specific growth rates higher than half of the maximal specific growth rate. In this way, the fraction of the absorbed light energy needed to fulfill the maintenance energy requirement will be relatively small and the biomass yield can be maximized (see Textbox 4).

Increasing the volumetric light input by decreasing the reactor depth (the light path) has shown that the yield remains constant, but that it is obtained at increased biomass concentrations. (Zijffers et al. manuscript submitted-a). Decreasing the light path further will increase the volumetric productivity and possibly also the observed yield if light integration can be obtained at shorter light path lengths. The decrease in light path length and subsequent increase in volumetric productivity can cause other problems: for example sufficient gas exchange can become a problem. Decreasing the light path and decreasing the incident light intensity can result in higher biomass densities at high true yields, because the lower incident light intensity results in a decrease in light energy lost due to light saturation. The volumetric light input remains high and thus the

potential for high biomass concentrations as well. The growth rate needs to be high to keep the total maintenance energy requirement low.

Textbox 4. Maximum yield.

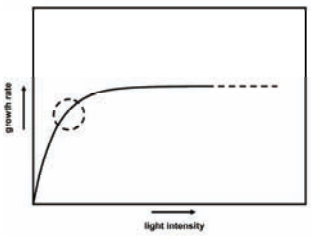

The growth rate versus irradiance curve of microalgae as shown on the right is similar to the PI-curve. During conditions at which light integration is obtained, the microalgae in a concentrated microalgal culture are discontinuously exposed to an (over-) saturating light intensity such that the culture behaves as if exposed to continuous light of a low intensity equal to the time averaged exposure. To optimally benefit from light integration, conditions need to be obtained such that the photosynthetic efficiency is maximal, but biomass maintenance energy requirement is minimal. The time averaged light intensity has to be such that the growth rate is as high as possible. In this case the biomass concentration is low and maintenance requirements are minimal. The maximum growth rate can, however, not be obtained at maximum efficiency. An optimum (as shown by the dashed circles) can be found depending on the biomass maintenance requirement and the photosynthetic efficiency obtained at the time averaged light intensity. At lower time averaged light intensities the yield decreases due to increased maintenance requirements (in case of an increase in biomass) or due to a lowering of the photosynthetic activity and growth rate (in case of a change in mixing). At higher time averaged light intensities the yield decreases due to increased light saturation.

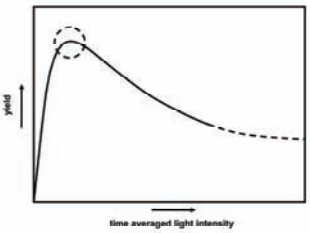

Perspectives

Commercial cultivation of microalgae should be done in areas with highest yearly direct irradiance levels, providing a potential for high areal productivities. The sunlight should be efficiently captured and distributed at reduced intensities. Systems designed for mass cultivation of microalgae should therefore cover complete ground surfaces in order to maximize capture of direct and diffuse sunlight, in other words, all sunlight should be captured. The cultivation system also has to be fully transparent to also facilitate the penetration of diffuse light into the cultivation system. Between the tropic of Cancer and Capricorn high direct irradiance levels are obtained at high elevation angles of the sun. In this situation sunlight can be captured by fiber-optic mini-dishes on top of a reactor without much mutual shading. The reactor conditions need to be such that efficient use of captured light can be obtained. Internally illuminated reactors can combine a high efficiency of light capture and fully controlled reactor compartments providing suitable conditions for high efficiencies of light use.

Using low light intensities high efficiencies of light use can be achieved, but low biomass concentrations will be obtained in systems with larger light paths. Increased energy inputs are required to circulate large volumes of growth medium through the larger light path cultivation system and to remove water in downstream processing, which limits the energetic yield. In theory, high yields can also be obtained at high biomass concentrations, either by obtaining light integration at high light intensities and high growth rates or by a decrease in optical path and a subsequent decrease in light intensity. A tenfold decrease in light path will in theory allow a tenfold decrease in light intensity, because the volumetric light input remains constant. Similar biomass concentrations can thus in theory be obtained, but in the shorter light path reactor high yields will be more easily obtained because light saturation is more easily prevented. The reduction in light path length will, however, provide new challenges for pneumatically agitated reactors.

To obtain high biomass yields, a high level of control over the captured light energy and the cultivation conditions is required independent of the desired biomass concentration. Internally illuminated photobioreactors can distribute the captured light energy such that equal conditions are obtained in the photobioreactor. Reactor conditions such as turbulence and dilution rate can be adjusted to match the light intensity present to obtain maximal efficiency of light use.

Acknowledgements

This work was financially supported by the EU/Energy Network project SOLAR-H (FP6 contract 516510).

References

Aiuchi K, Yoshida K, Onozaki M, Katayama Y, Nakamura M, Nakamura K. 2006. Sensor-controlled heliostat with an equatorial mount. Solar Energy 80(9):1089-1097.

An JY, Kim BW. 2000. Biological desulfurization in an optical-fiber photobioreactor using an automatic sunlight collection system. Journal of Biotechnology 80(1):35-44.

Apt KE, Behrens PW. 1999. Commercial developments in microalgal biotechnology. Journal of Phycology 35(2):215-226.

Bakos GC. 2006. Design and construction of a two-axis Sun tracking system for parabolic trough collector (PTC) efficiency improvement. Renewable Energy 31(15):2411-2421.

Carlozzi P. 2003. Dilution of solar radiation through "culture" lamination in photobioreactor rows facing South-North: A way to improve the efficiency of light utilization by cyanobacteria (Arthrospira platensis). Biotechnology And Bioengineering 81(3):305-315.

Chisti Y. 2007. Biodiesel from microalgae. Biotechnology Advances 25(3):294-306.

Chisti Y. 2008. Biodiesel from microalgae beats bioethanol. Trends in Biotechnology 26(3):126-131.

Csögör Z, Herrenbauer M, Perner I, Schmidt K, Posten C. 1999. Design of a photo-bioreactor for modelling purposes. Chemical Engineering and Processing 38(4-6):517-523.

Fernandez FGA, Camacho FG, Perez JAS, Sevilla JMF, Grima EM. 1998. Modeling of biomass productivity in tubular photobioreactors for microalgal cultures: Effects of dilution rate, tube diameter, and solar irradiance. Biotechnology and Bioengineering 58(6):605-616.

Fernandez FGA, Sevilla JMF, Perez JAS, Grima EM, Chisti Y. 2001. Airlift-driven external-loop tubular photobioreactors for outdoor production of microalgae: assessment of design and performance. Chemical Engineering Science 56(8):2721-2732.

Feuermann D, Gordon JM, Huleihil M. 2002. Solar fiber-optic mini-dish-concentrators: First experimental results and field experience. Solar Energy 72(6):459-472.

Gitelson A, Qiuang H, Richmond A. 1996. Photic volume in photobioreactors supporting ultrahigh population densities of the photoautotroph Spirulina platensis. Applied and Environmental Microbiology 62(5):1570-1573.

Gordon JM. 2002. Tailoring optical systems to optimized photobioreactors. International Journal of Hydrogen Energy 27(11-12):1175-1184.

Gordon JM, Polle JEW. 2007. Ultrahigh bioproductivity from algae. Applied Microbiology and Biotechnology 76(5):969-975.

Grima EM, Camacho FG, Perez JAS, Cardona JU, Fernandez FGA, Sevilla JMF. 1994. Outdoor Chemostat Culture of Phaeodactylum-Tricornutum Utex-640 in a Tubular Photobioreactor for the Production of Eicosapentaenoic Acid. Biotechnology and Applied Biochemistry 20:279-290.

Grima EM, Camacho FG, Perez JAS, Fernandez FGA, Sevilla JMF. 1997. Evaluation of photosynthetic efficiency in microalgal cultures using averaged irradiance. Enzyme and Microbial Technology 21(5):375-381.

Hirata S, Hayashitani M, Taya M, Tone S. 1996. Carbon dioxide fixation in batch culture of Chlorella sp using a photobioreactor with a sunlight-collection device. Journal of Fermentation and Bioengineering 81(5):470-472.

Hu Q, Guterman H, Richmond A. 1996. A flat inclined modular photobioreactor for outdoor mass cultivation of photoautotrophs. Biotechnology and Bioengineering 51(1):51-60.

Hu Q, Kurano N, Kawachi M, Iwasaki I, Miyachi S. 1998. Ultrahigh-cell-density culture of a marine green alga Chlorococcum littorale in a flat-plate photobioreactor. Applied Microbiology and Biotechnology 49(6):655-662.

Kok B. 1956. Photosynthesis In Flashing Light. Biochimica Et Biophysica Acta 21(2):245-258.

MacIntyre HL, Kana TM, Anning T, Geider RJ. 2002. Photoacclimation of photosynthesis irradiance response curves and photosynthetic pigments in microalgae and cyanobacteria. Journal Of Phycology 38(1):17-38.

Matsunaga T, Takeyama H, Sudo H, Oyama N, Ariura S, Takano H, Hirano M, Burgess JG, Sode K, Nakamura N. 1991. Glutamate Production from Co2 by Marine Cyanobacterium Synechococcus Sp using a novel Biosolar Reactor employing Light-Diffusing Optical Fibers. Applied Biochemistry and Biotechnology 28-9:157-167.

Molina E, Fernandez J, Acien FG, Chisti Y. 2001. Tubular photobioreactor design for algal cultures. Journal of Biotechnology 92(2):113-131.

Morita M, Watanabe Y, Saiki H. 2000. Investigation of photobioreactor design for enhancing the photosynthetic productivity of microalgae. Biotechnology and Bioengineering 69(6):693-698.

Morita M, Watanabe Y, Saiki H. 2002. Photosynthetic productivity of conical helical tubular photobioreactor incorporating Chlorella sorokiniana under field conditions. Biotechnology and Bioengineering 77(2):155-162.

Nedbal L, Tichy V, Xiong FH, Grobbelaar JU. 1996. Microscopic green algae and cyanobacteria in high-frequency intermittent light. Journal of Applied Phycology 8(4-5):325-333.

Ogbonna JC, Soejima T, Tanaka H. 1999. An integrated solar and artificial light system for internal illumination of photobioreactors. Journal of Biotechnology 70(1-3):289-297.

Phillips JN, Myers J. 1954. Growth Rate Of Chlorella In Flashing Light. Plant Physiology 29(2):152-161.

Pirt SJ. 1965. Maintenance Energy of Bacteria in Growing Cultures. Proceedings of the Royal Society of London Series B-Biological Sciences 163(991):224-&.

Pirt SJ. 1986. Tansley Review No-4 - The Thermodynamic Efficiency (Quantum Demand) and Dynamics of Photosynthetic Growth. New Phytologist 102(1):3-37.

Pulz O, Gerbsch N, Buchholz R. 1995. Light energy supply in plate-type and light diffusing optical-fiber bioreactors. Journal of Applied Phycology 7(2):145-149.

Qiang H, Faiman D, Richmond A. 1998. Optimal tilt angles of enclosed reactors for growing photoautotrophic microorganisms outdoors. Journal of Fermentation and Bioengineering 85(2):230-236.

Richmond A. 2004. Principles for attaining maximal microalgal productivity in photobioreactors: an overview. Hydrobiologia 512(1-3):33-37.

Spolaore P, Joannis-Cassan C, Duran E, Isambert A. 2006. Commercial applications of microalgae. Journal of Bioscience and Bioengineering 101(2):87-96.

Terry KL. 1986. Photosynthesis In Modulated Light - Quantitative Dependence Of Photosynthetic Enhancement On Flashing Rate. Biotechnology and Bioengineering 28(7):988-995.

Torzillo G, Carlozzi P, Pushparaj B, Montaini E, Materassi R. 1993. A 2-Plane Tubular Photobioreactor for Outdoor Culture of Spirulina. Biotechnology and Bioengineering 42(7):891-898.

Torzillo G, Pushparaj B, Masojidek J, Vonshak A. 2003. Biological constraints in algal biotechnology. Biotechnology and Bioprocess Engineering 8(6):338-348.

Tredici MR, Carlozzi P, Zittelli GC, Materassi R. 1991. A Vertical Alveolar Panel (Vap) for Outdoor Mass Cultivation of Microalgae and Cyanobacteria. Bioresource Technology 38(2-3):153-159.

Tredici MR, Zittelli GC. 1998. Efficiency of sunlight utilization: Tubular versus flat photobioreactors. Biotechnology and Bioengineering 57(2):187-197.

Zijffers JWF, Janssen M, Tramper J, Wijffels RH. 2008a. Design process of an area-efficient photobioreactor. Marine Biotechnology 10(4):404-415.

Zijffers JWF, Salim S, Janssen M, Tramper J, Wijffels RH. 2008b. Capturing sunlight into a photobioreactor: Ray tracing simulations of the propagation of light from capture to distribution into the reactor. Chemical Engineering Journal 145(2):316-327.

Zijffers JWF, Schippers KJ, Zheng K, Janssen M, Tramper J, Wijffels RH. manuscript submitted-a. Photosynthetic yield of algae in panel photobioreactors: True yield and maintenance requirement.

Zijffers JWF, Zheng K, Janssen M, Tramper J, Wijffels RH. manuscript submitted-b. Photosynthetic yield of Chlorella sorokiniana at different levels of turbulence. .

Zittelli GC, Lavista F, Bastianini A, Rodolfi L, Vincenzini M, Tredici MR. 1999. Production of eicosapentaenoic acid by Nannochloropsis sp cultures in outdoor tubular photobioreactors. Journal of Biotechnology 70(1-3):299-312.

Zittelli GC, Rodolfi L, Biondi N, Tredici MR. 2006. Productivity and photosynthetic efficiency of outdoor cultures of Tetraselmis suecica in annular columns. Aquaculture 261(3):932-943.

Zittelli GC, Tomasello V, Pinzani E, Tredici MR. 1996. Outdoor cultivation of Arthrospira platensis during autumn and winter in temperate climates. Journal of Applied Phycology 8(4-5):293-301.

Summary

Areal efficient microalgal cultivation is required to fully exploit sunlight areal irradiance for production of microalgae for biofuel components and products, such as vitamins, carotenoids, and polyunsaturated fatty acids. The Green Solar Collector (GSC), an area efficient photobioreactor for the outdoor cultivation of microalgae is therefore designed. The GSC is a photobioreactor that delivers all incident sunlight on the area covered by the reactor to the algae at such intensities that the light energy can be efficiently used for biomass formation. This results in a design in which sunlight is captured into vertical plastic light guides. Sunlight reflects internally in the guide and eventually scatters out of the light guide into flat-panel photobioreactor compartments. Sunlight is focused on top of the light guides by dual-axis positioning of linear Fresnel lenses. The shape and material of the light guide is such that light is maintained in the guides when surrounded by air. The bottom part of a light guide, the distributor, is sandblasted to obtain a more uniform distribution of light inside the bioreactor compartment and is triangular shaped to ensure the efflux of all light out of the guide. The dimensions of the guide are such that light enters the flat-panel photobioreactor compartment at intensities that can be efficiently used by the biomass present. The integration of light capturing, transportation, distribution, and usage is such that high biomass productivities per area can be achieved.

The path of the focused rays of light in the GSC is calculated using ray tracing to determine local light intensities on the distributor surface. Reflection and refraction of the propagating rays of sunlight from point of focus to refraction into the photobioreactor is calculated. Refraction out of smooth and sandblasted distributor surfaces is simulated. For the sandblasted surface a specific structure is assumed and corresponding reflection and refraction patterns are described by a 2-dimensional modeling approach. Results of the simulations are validated by measurements on real light guide surfaces. The validated model is used to determine the influence of the solar angle on the uniformity and efficiency of light

distribution over the light distributor surface. The simulations show that efficient capturing of sunlight and redistribution inside the algal biomass can be achieved in the Green Solar Collector at higher elevation angles of the sun, making the Green Solar Collector suitable for operation at low latitudes with a high level of direct irradiance.

Microalgal cultivation experiments under controlled conditions were performed to investigate the efficiency of light use at constant light intensity and varying biomass concentration. The biomass yield on light energy of *Dunaliella tertiolecta* and *Chlorella sorokiniana* was investigated in a 1.25 cm and 2.15 cm light path panel photobioreactor at constant ingoing photon flux density (930 µmol photons m^{-2} s^{-1}) using the D-stat cultivation technique. Constant biomass yields of 0.65 ± 0.10 g mol $photons^{-1}$ for *D. tertiolecta* and 0.70 ± 0.10 g mol $photons^{-1}$ for *C. sorokiniana* were observed in both light path reactors over a broad range of biomass concentrations. The yield decreased at high biomass densities and low dilution rates.

The observed biomass yield on light energy could be described by a constant true biomass yield and a constant maintenance energy requirement per gram biomass. Using a simple model, a true biomass yield on light energy of 0.78 g mol $photons^{-1}$ and 0.75 g mol $photons^{-1}$ and a maintenance requirement of 0.0133 mol photons g^{-1} h^{-1} and 0.0068 mol photons g^{-1} h^{-1} were found for *D. tertiolecta* and *C. sorokiniana,* respectively. The steep decrease in observed yield at low light supply rates could thus be explained by the maintenance energy requirement of the large amount of biomass present at low dilution rates. The true biomass yield on light energy was assumed to differ from the theoretical maximal yield by a constant factor representing light energy losses.

An increase in level of turbulence due to increased sparging of air in a panel photobioreactor was expected to influence the observed biomass yield of *Chlorella sorokiniana* on light energy. The maximum value of the observed yield was 0.75 ± 0.05 g mol $photons^{-1}$, but it did not increase as a result of increased mixing. Superficial gas velocities of $1.67*10^{-2}$ m s^{-1} and $4.00*10^{-2}$ m s^{-1} did not show any

positive effect compared to the lowest velocity of $6.67*10^{-3}$ m s^{-1}. On the other hand, at a superficial gas velocity of $2.67*10^{-2}$ m s^{-1} this maximal yield could be maintained at higher biomass concentrations. Subtracting a constant biomass maintenance energy requirement from the absorbed light energy showed that the true yield of biomass on light energy could have increased at high biomass concentrations at a superficial gas velocity of $2.67*10^{-2}$ m s^{-1}. Increasing the turbulence thus could have a positive effect on the true yield, but high maintenance energy requirements will not allow for an increase of the observed yield.

The efficiency of sunlight utilization can be maximized by reducing the photon flux density at the light exposed reactor surface. Specific reactor design and use of sun tracking devices is needed to obtain a high capturing efficiency of direct sunlight. Efficient coupling of light capturing elements to specifically designed light distributing elements will reduce the light intensity and enhance uniformity of light distribution inside the algal suspension. A transparent reactor top surface is still needed to allow diffuse light, which cannot be focused, to penetrate into the algal suspension. The reduction of sunlight intensity can result in high yields when the corresponding biomass concentration and light path is further optimized. A too low biomass concentration will result in large cultivation volumes. High biomass densities are therefore preferred. However, when high biomass concentrations are combined with a long light path the average light intensity inside the photobioreactor is too low. This will lead to a low specific growth rate and hence the maintenance requirement for light energy will significantly reduce reactor productivity. Continuous cultures at high dilution rate are required and at high biomass densities this can only be realized at a sufficiently short light path.

Samenvatting

Het kweken van microalgen op zonlicht dient efficiënt te gebeuren om het grondgebruik voor de productie van microalgen voor biobrandstof componenten en producten zoals vitamines, carotenoïden en meervoudig onverzadigde vetzuren beperkt te houden. De Groene Zonnecollector (GZC), een oppervlakte efficiënte fotobioreactor voor het kweken van microalgen is daarom ontworpen. Het is een fotobioreactor waarin al het zonlicht dat op het oppervlak van de reactor invalt aan de algen wordt aangeboden op een dusdanige intensiteit dat het licht efficiënt kan worden gebruikt voor de vorming van biomassa. Dit resulteert in een ontwerp waarin het zonlicht wordt opgevangen in verticale plastic platen zogenaamde "light guides". Zonlicht weerspiegelt intern in de platen totdat het licht uit de platen breekt en verstrooid wordt in vlakke plaat fotobioreactor compartimenten. Zonlicht wordt gefocust op de bovenkant van de "light guides" door lineaire Fresnel lenzen. De lineaire Fresnel lenzen zijn zo geplaatst dat ze over twee assen kunnen bewegen waardoor de zon gedurende de gehele dag gevolgd kan worden. De vorm en materiaal van de "light guides" is zodanig dat het licht intern reflecteert in de "guides" zolang deze omringd zijn door lucht. Het onderste deel van een "guide", de lichtdistributeur, is driehoekig gevormd om al het licht uit de "guide" te laten breken. Het oppervlak van de distributeur is gezandstraald om een meer uniforme verdeling van het licht in de bioreactor te verkrijgen. De afmetingen van de "guide" zijn zodanig dat de lichtintensiteit in de fotobioreactor dusdanig is dat het licht efficiënt kan worden gebruikt door de microalgen. De hoge efficiëntie van lichtinvang, transport en distributie gecombineerd met de potentie tot efficiënt gebruik van het licht resulteren in een systeem waarbij hoge biomassaproductiviteiten per eenheid oppervlak kunnen worden bereikt.

De voortplanting van de lichtstralen in de Groene Zonnecollector en lokale lichtintensiteiten op het oppervlak van de distributeur is berekend door middel van "ray tracing" simulaties. Terugkaatsing en breking van de zich voortplantende zonlichtstralen is berekend vanaf het focussen door een lens tot aan de breking uit

de lichtdistributeur in het reactor compartiment. De breking van het licht op de gladde en de gezandstraalde oppervlaktes van de distributeur is gesimuleerd. Voor het gezandstraalde oppervlak is een specifieke structuur aangenomen en de bijbehorende reflectie en brekingskarakteristieken zijn beschreven door middel van een 2-dimensionaal model. Resultaten van simulaties zijn gevalideerd met lichtintensiteitmetingen aan het oppervlak van echte lichtdistributeurs. Het gevalideerde model wordt gebruikt voor het bepalen van de invloed van de invalshoek van de zon op de uniformiteit en efficiëntie van de breking van licht uit de lichtdistributeur. De simulaties laten zien dat een efficiënte invang van zonlicht en een uniforme verdeling binnen de algenbiomassa kan worden bereikt in de Groene Zonnecollector bij hogere invalshoeken van de zon, waardoor de Groene Zonnecollector geschikt is voor gebruik op locaties op lage breedtegraden met een hoog niveau van direct zonlicht.

Hoe efficiënt de microalgen licht gebruiken is onderzocht in groei experimenten onder gecontroleerde omstandigheden bij een constante lichtintensiteit en bij uiteenlopende biomassaconcentraties. De biomassa opbrengt op lichtenergie van de microalgen *Dunaliella tertiolecta* en *Chlorella sorokiniana* is onderzocht in een vlakke plaat fotobioreactor. De algen werden gekweekt in reactoren van 1,25 cm en 2,15 cm dikte (lichtweg) bij een constante lichtintensiteit (930 µmol fotonen m^{-2} s^{-1}) met behulp van de D-stat cultivatie techniek. De microalgen hadden een constante biomassa opbrengst op lichtenergie van 0,65 ± 0,10 g mol $fotonen^{-1}$ voor *D. tertiolecta* en 0,70 ± 0,10 g mol $fotonen^{-1}$ voor *C. sorokiniana* voor beide lichtwegen en over een breed gebied van biomassaconcentraties. De opbrengst nam af bij hoge biomassaconcentraties en lage verdunningssnelheden. De waargenomen biomassaopbrengst op lichtenergie kon beschreven worden door een constante echte biomassa opbrengst en een constant energie benodigdheid voor onderhoud van de microalg. Met behulp van een eenvoudig model is een echte biomassa opbrengt van respectievelijk 0,78 g mol $fotonen^{-1}$ en 0,75 g mol $fotonen^{-1}$ en een onderhoudsbehoefte van respectievelijk 0,0133 mol fotonen g^{-1} h^{-1} en 0,0068 mol fotonen g^{-1} h^{-1} gevonden voor *D. tertiolecta* en *C. sorokiniana*. De scherpe daling van de opbrengst bij lage lichttoevoer per hoeveelheid biomassa zou dus verklaard kunnen worden door de hoeveelheid energie die nodig is voor onderhoud van de

grote hoeveelheid biomassa aanwezig bij lage verdunningssnelheden. Het werkelijke rendement van de biomassa opbrengst op lichtenergie wijkt van de theoretische maximale opbrengst met een constante factor, veroorzaakt door lichtenergieverliezen.

De verwachting was dat de waargenomen biomassa opbrengst van *C. sorokiniana* op lichtenergie beïnvloed wordt door een verhoging van de mate van turbulentie ten gevolge van een toegenomen inbreng van de lucht in een vlakke plaat fotobioreactor. De maximale waarde van de opbrengst was 0,75 ± 0,05 g mol fotonen^{-1} en deze werd niet verhoogd door een verhoging van de turbulentie. Superficiële gassnelheden van 1,67 * 10^{-2} m s^{-1} en 4,00 * 10^{-2} m s^{-1} hadden geen positief effect in vergelijking tot de laagste gassnelheid van 6,67 * 10^{-3} m s^{-1}. Echter, bij een superficiële gassnelheid van 2,67 * 10^{-2} m s^{-1} kon de maximale opbrengst bereikt worden bij hogere biomassaconcentraties.
De werkelijke biomassa productie efficiëntie op lichtenergie lijkt toegenomen bij hoge biomassa concentraties bij een superficiële gassnelheid van 2,67 * 10^{-2} m s^{-1} als de constante energiebehoefte voor onderhoud van de biomassa afgetrokken wordt van de geabsorbeerde hoeveelheid lichtenergie. Het verhogen van de turbulentie kan dus een positief effect hebben op de efficiëntie van biomassa productie, maar door de grote energiebehoefte voor onderhoud zal een verhoging van de opbrengst niet waargenomen worden.

De efficiëntie van zonlichtgebruik kan gemaximaliseerd worden door een vermindering van de fotonflux dichtheid op het aan het licht blootgesteld reactor oppervlak. Specifiek reactor ontwerp en het volgen van de zon is nodig voor het verkrijgen van een hoge efficiëntie van het vastleggen van direct zonlicht. Efficiënte koppeling van licht invangende elementen aan specifiek ontworpen licht distributie elementen resulteert in een vermindering van de lichtintensiteit en verbetering van de uniformiteit van het licht binnenin de algen suspensie. Een transparant reactor oppervlak is nodig om diffuus licht, dat niet gefocust kan worden, door te laten dringen in de algen suspensie.
De vermindering van de intensiteit van zonlicht kan resulteren in hogere opbrengsten, als de bijbehorende biomassa concentratie en lichtweg verder is

geoptimaliseerd. Een te lage biomassa concentratie zal leiden tot grote reactorvolumes. Hoge biomassa dichtheden hebben dan ook de voorkeur. Echter, wanneer hoge biomassa concentraties worden gecombineerd met een grote lichtweg, dan is de gemiddelde lichtintensiteit in de photobioreactor te laag. Dit zal leiden tot een geringe specifieke groeisnelheid en door de energiebehoefte voor onderhoud zal dit resulteren in een aanzienlijke verlaging van de productiviteit. Continu doorstroomde culturen bij hoge verdunning zijn een vereiste en bij hoge biomassa dichtheden kan dit alleen worden gerealiseerd bij een voldoende korte lichtweg.

Dankwoord

Het proefschrift is af na vijf mooie jaren werken aan een nog mooier onderwerp! Een verandering in mentaliteit, van “wie weet gaat het me lukken” en “als het me niet lukt dan heb ik gewoon lekker vier jaar een baan”, tot daadwerkelijk een proefschrift en een verdediging.

In dit traject zijn een aantal mensen erg belangrijk geweest en die ik hier dan ook graag wil bedanken. René, ik wil je bedanken voor je vertrouwen in mij. Na mijn eerste afstudeeropdracht gaf je aan van mij meer te verwachten en dat ik dat in mijn volgende afstudeeropdracht moest laten zien. Na een succesvolle tweede afstudeeropdracht en een fijn vakantiebaantje als student-assistent nam je me in dienst op het project “de Groene Zonnecollector” en gaf je me de mogelijkheid om op dit onderwerp te promoveren. Als ik het even minder zag zitten, wist jij met een paar rake opmerkingen me weer met volle energie aan de slag te laten gaan. Marcel, jouw begeleiding is onmisbaar geweest in het tot stand komen van dit proefschrift. Met een kritische, maar vooral positieve blik voorzag jij mijn artikelen keer op keer weer van duidelijk en zeer nuttig commentaar. Jouw hulp is essentieel geweest in het tot stand komen van correcte en hopelijk interessante artikelen. Hans, jouw input op mijn artikelen gaf een frisse kijk op het geheel en heeft geleid tot beter leesbare stukken.

Maria en Tim, mijn paranimfen, ik ben blij dat jullie tijdens mijn verdediging op het op het podium bij mij zijn. Maria “Sweety!!!”, jij hebt me plezier gegeven in het doen van onderzoek en mij op het pad gezet dat uiteindelijk naar vandaag geleid heeft. Ik wilde nooit promoveren, maar door jou ben ik gaan twijfelen; heel erg bedankt daarvoor. Tim, als jij weer enorm op de vakgroep “zat te pieken”, kon ik moeilijk niets zitten doen. Jouw inzet en toewijding zijn een inspiratie geweest en hebben ervoor gezorgd dat ik (hopelijk) geen “banaan” of “perenplukker” ben geworden.

Verder op de universiteit. Mijn andere oud-kamergenoten, Cynthia, Eduard en Sebastiaan, samen hebben we er iedere dag weer een gezellige boel van gemaakt. Hetzelfde kan ik zeggen van mijn "nieuwe" kamergenoten, Tamara, Klaske en Niels. Werk is belangrijk, maar een goed gesprek ook. De studenten die ik heb mogen begeleiden: Harmen, Carla, Klaske, Sina, Hans, Ruben, Benjamin en Ke. You all contributed and I learned something of every one of you. Alonso, I hope I have been of some help to you and I really enjoyed our trip to China. Rouke, dankzij jouw hulp is de opstelling op het dak zo snel tot stand gekomen en je bent altijd behulpzaam geweest bij het goed laten verlopen van de experimenten op het 2e bordes. Fred, bedankt voor de hulp met het aansluiten van allerlei sensoren, regelaars, analyse en data-acquisitie apparatuur. Sebastiaan, als je op het 2e bordes wat klemmetjes, ventielen, slangenkoppelingen, etcetera mist, kijk dan eens op het algenlab. De mensen van de werkplaats voor het klaarstaan en meedenken over allerlei praktische, ontwerptechnische en elektronische vragen. Verder wil ik iedereen op de vakgroep bedanken voor de gezellige pauzes, labuitjes, sinterkerstdiners en borrels!

Mijn ouders, ik wil jullie bedanken voor jullie steun en vertrouwen en het feit dat jullie me gestimuleerd hebben om te gaan studeren. Dit proefschrift is voor jullie hopelijk net zo'n bekroning als voor mij. Jos en Tineke, bedankt dat ik vele weekenden bij jullie de computer bezet mocht houden en voor jullie steun en interesse

Gelukkig heb ik naast mijn proefschrift aan mijn promotieonderzoek nog wat tastbaars overgehouden; een leuke, lieve en prachtige vriendin, mijn toekomstige vrouw. Maartje, dankzij jou is dit proefschrift af. Jij wist mij te motiveren en te inspireren en als dat niet lukte mij gewoon aan het werk te zetten. Bedankt! Samen kunnen wij ver komen!

Jan-Willem

Publications

Barbosa MJ, Zijffers JW, Nisworo A, Vaes W, van Schoonhoven J, Wijffels RH. 2005. Optimization of biomass, vitamins, and carotenoid yield on light energy in a flat-panel reactor using the A-stat technique. Biotechnology and Bioengineering 89(2):233-242.

Zijffers JWF, Janssen M, Tramper J, Wijffels RH. 2008. Design process of an area efficient photobioreactor. Marine Biotechnology 10(4):404-415.

Zijffers JWF, Salim S, Janssen M, Tramper J, Wijffels RH. 2008. Capturing sunlight into a photobioreactor: Ray tracing simulations of the propagation of light from capture to distribution into the reactor. Chemical Engineering Journal 145(2):316-327.

Zijffers JWF, Schippers KJ, Zheng K, Janssen M, Tramper J, Wijffels RH. 2008. Photosynthetic yield of algae in panel photobioreactors: True yield and maintenance requirement, *manuscript submitted for publication*

Zijffers JWF, Zheng K, Janssen M, Tramper J, Wijffels RH. 2008. Photosynthetic yield of Chlorella sorokiniana at different levels of turbulence, *manuscript submitted for publication*

Zijffers JWF, Janssen M, Tramper J, Wijffels RH. 2008. Microalgal photobioreactors: obtaining maximal areal yield, *manuscript in preparation*

Training Activities

Discipline specific activities

Courses

Bioreactor Design and Operation (VLAG, 2006)
Advanced Course on Applied Genomics of Industrial Fermentation (BODL, 2006)

Meetings

The 10th International Conference on Applied Phycology (2005)
Netherlands Process Technology Symposium (2005)
BSDL symposium (2006, 2007)
Solar-H workshop (2005, 2006, 2007)
7th European workshop European Society of Microalgal Biotechnology (2007)
10th International Conference on Shellfish Restoration (2007)

General courses

Workshop introduction to problem-directed education for tutors (OWU, 2005)
PhD introduction week (VLAG, 2005)
Discussion techniques (OWU, 2005)
PhD Presentation Skills (Centa, 2006)
Information Literacy (WGS, 2006)
PhD Scientific Writing (Centa, 2007)
Career Perspectives (VLAG, 2008)

Optionals

Preparing PhD research proposal (2004)
PhD study tour Denmark and Sweden (2006)

Curriculum Vitae

Jan-Willem Feye Zijffers was born in Zwolle (the Netherlands) on the 29th of July 1978. In 1990 he started his secondary education in Zwolle at the Carolus Clusius College, where he received his diploma in 1996. In the same year, he started studying bioprocess technology at Wageningen University where he specialized in bioreactor engineering. His MSc theses focused on the feasibility of sponge cultivation for the production of bioactive compounds and on the optimization of the yield of *Dunaliella tertiolecta* biomass, vitamins, and carotenoids on light energy. He obtained his MSc degree in 2003 and started as a junior researcher at the department of Food and Bioprocess Engineering of Wageningen University focusing on the design of the Green Solar Collector, an outdoor photobioreactor for areal efficient microalgal cultivation. In 2004, the project was transformed into a PhD study. The results of this study are written in this thesis. On the 29th of September 2008, he started working as a Process Technologist Bacteriological Processing at Intervet/Schering-Plough Animal Health.

Jan-Willem Feye Zijffers werd geboren in Zwolle op 29 juli 1978. In 1990 begon hij aan het Atheneum op het Carolus Clusius College in Zwolle, waar hij in 1996 zijn diploma behaalde. In datzelfde jaar begon hij met de studie bioprocestechnologie aan de Wageningen Universiteit met als specialisatie bioreactorkunde. Zijn afstudeerscripties hadden als onderwerp de haalbaarheid van sponsenteelt voor de productie van biologisch actieve verbindingen en de optimalisatie van de opbrengst van biomassa, vitaminen en carotenoïden op lichtenergie geproduceerd door de alg *Dunaliella tertiolecta*. Na zijn afstuderen in 2003 begon hij als junior onderzoeker binnen de vakgroep levensmiddelen- en bioprocestechnologie van de Wageningen Universiteit met het ontwerpen van de Groene Zonnecollector, een fotobioreactor voor oppervlakte efficiënte teelt van microalgen. In 2004 werd het project omgevormd tot een promotiestudie. De resultaten van deze studie staan beschreven in dit proefschrift. Sinds 29 september 2008, is hij werkzaam als Procestechnoloog Bacteriological Processing bij Intervet/Schering-Plough Animal Health.